AN ELECTRON SPIN RESONANCE STUDY OF NORMAL AND NEOPLASTIC BIOLOGICAL MATERIAL

by

Daniel W. Nebert, B.A.

THESIS
Presented to the Department of Biochemistry
and the Graduate Division of the University of Oregon Medical School
in partial fulfillment of
the requirements for the degree of
Master of Science

June 1964

APPROVED:

[redacted]

(Professor in Charge of Thesis)

[redacted]

(Chairman, Graduate Council)

ACKNOWLEDGMENTS

I wish to acknowledge with thanks the help and advice of Dr. B. T. Allen, Dr. D. Ghanekar, Dr. Y. Hashimoto, Dr. T. Yamano and every other member of our laboratory. My thanks go especially to my senior instructor Professor Howard S. Mason who gave me his confidence, patience and help, making this work possible.

The kind cooperation of Dr. T. Kakefuda, City of Hope Research Center, Duarte, California, and Dr. H. P. Morris, National Cancer Institute, Bethesda, Maryland, must also be acknowledged.

This study was supported by grants from the American Cancer Society and the United States Public Health Service, to whom we are indebted.

* * *

ABBREVIATIONS

ADP	Adenosine diphosphate
ATP	Adenosine triphosphate
DNA	Deoxyribonucleic acid
DPNH	Diphosphopyridine nucleotide, reduced
ESR	Electron spin resonance
PGA	2-phosphoglyceric acid
RNA	Ribonucleic acid
TPNH	Triphosphopyridine nucleotide, reduced

* * *

TABLE OF CONTENTS

Title page i

Approval page ii

Acknowledgments iii

Abbreviations to be used in text iv

Table of Contents v

List of Tables and Illustrations vii

INTRODUCTION 1

Statement of the Problem 1

Causes of Cancer 1

Prominent Theories of Carcinogenesis . . . 4

Principles of Electron Spin Resonance Spectroscopy . 23

ESR Studies of Biological Materials . . . 26

MATERIALS AND METHODS 31

Chemicals 31

Biological Preparations 32

Inorganic Studies of Manganese 39

Electron Spin Resonance Spectroscopy . . . 41

RESULTS 43

Whole Tissue Studies 43

Subcellular Components of Normal Mouse Liver and Hepatoma 43

"Minimal Deviation" Hepatoma and Normal Rat Liver Microsomes 47

Microsomal Manganese Isolation 69

Inorganic Manganese Studies 70

TABLE OF CONTENTS, Continued.

DISCUSSION 81

SUMMARY 104

REFERENCES 106

* * *

LIST OF TABLES AND ILLUSTRATIONS

FIGURE 1. The general Jacob-Monod model for regulation of enzyme synthesis 18

TABLE 1. List of normal and neoplastic mouse whole tissues 34

FIGURE 2. Outline for purification of microsomal manganese fraction 38

FIGURE 3. ESR spectra of mouse tumors and normal tissues 49

FIGURE 4. ESR spectra of mouse tumors 50

FIGURE 5. ESR spectra of mouse tumors 51

FIGURE 6. ESR spectra of mouse tumors 52

FIGURE 7. ESR spectra of mouse tumors 53

FIGURE 8. ESR spectra of mouse liver and hepatoma mitochondria 54

FIGURE 9. Theoretical ESR spectrum of microsomal Fe_x . . 55

FIGURE 10. ESR spectra of mouse liver and hepatoma smooth-surfaced microsomal fractions 56

FIGURE 11. ESR spectra of mouse liver and hepatoma rough-surfaced microsomal fractions 57

TABLE 2. ESR signal intensities of mouse liver and mouse hepatoma microsomes, per mg. protein 58

TABLE 3. Chemical analyses of microsomal fractions of mouse liver and mouse hepatoma 59

FIGURE 12. Reductive titration experiments with mouse liver and hepatoma microsomes 60

FIGURE 13. ESR spectra of oxidized and reduced mouse liver microsomal fraction 61

FIGURE 14. Reduced-direct optical spectra of rabbit, mouse, beef and rat liver microsomes 62

FIGURE 15. Electron micrograph of normal mouse liver microsomal fraction 63

LIST OF TABLES AND ILLUSTRATIONS, Continued.

FIGURE 16. Electron micrograph of normal mouse liver microsomal fraction 64

FIGURE 17. Antimycin A inhibition studies with mouse liver microsomal fraction 65

FIGURE 18. ESR spectra of rat liver and hepatoma microsomes 66

TABLE 4. ESR signal intensities of rat liver and hepatoma microsomes, and acetanilide hydroxylase activity, per mg. protein 67

FIGURE 19. Reduced-direct optical spectra of rat liver and hepatoma microsomes 68

FIGURE 20. ESR spectra of beef microsomal fraction and microsomal manganese aqueous fraction . . . 73

FIGURE 21. Low-temperature and room-temperature ESR spectra of manganous compounds and complexes . . 74

FIGURE 22. ESR spectra of samples of increasing anion/Mn^{++} ratio 75

FIGURE 23. ESR spectra of samples of manganous chloride in N,N-dimethylformamide, before and after addition of water 76

FIGURE 24. ESR spectra of manganous chloride in presence of proteins of increasing molecular weight . . 77

FIGURE 25. ESR spectrum of manganese associated with protein, where surface areas are equal 78

FIGURE 26. Experimental phosphoric acid titration curve . 79

FIGURE 27. ESR spectra of microsamples taken along phosphoric acid titration curve in presence of manganese 80

FIGURE 28. Postulated relationship of divalent cation to microsomal protein 102

I.

INTRODUCTION

A. Statement of Problem

Ideally, the worker in the field of cancer research should be aware of the known causes of cancer. Similarly, he should understand the strong points and the valid criticisms of each theory of carcinogenesis. Thirdly, he should decide upon the type of cancer research he wishes to undertake. Some research contributes to the knowledge of what is the initial event in carcinogenesis; other research helps clinicians in the treatment of cancers.

The problem of the initial events leading to carcinogenesis is the underlying question in this thesis. A new technic, low-temperature electron spin resonance (ESR) spectroscopy, was used in looking at normal and neoplastic biological material.

B. Causes of Cancer

Ultraviolet and ionizing irradiation are accepted as factors which may cause cancer. The incidence of cancers and leukemias in Japanese who were exposed to the atomic bomb has been markedly in-

creased. Early radiologists were found to have a higher incidence of tumors. Cancer of the tongue developed in many radium-dial painters who licked their brushes. The clinician is aware of increased squamous cell carcinoma in the weather-beaten skin of sailors and farmers.

Chemicals have been known to cause cancer since Pott described cancer of the scrotum in chimney sweeps some 200 years ago. In the industry of certain chemical dyes, as high as 11% of the workers in some British factories developed bladder cancer. Excessive doses of arsenic, selenium, iron (120) and other metals are known to cause a higher incidence of cancer, so that a theory of carcinogenesis on the basis of metal chelation with cellular constituents has been proposed (47). The recent proof of a cause-and-effect relationship between heavy cigarette smoking and epithelial lung cancer has emphasized the importance of chemical carcinogens. The theory of chemical carcinogenesis will be discussed later.

Tumorigenesis and tumor growth influenced by hormones have been seen clinically as well as experimentally. Some tumors seem to originate because of sustained, excessive hormonal stimulation (e.g., high levels of estrogen causing adenomatous hyperplasia, uterine carcinoma or breast cancer), while individual endocrine tumors may regress, disappear, or be enhanced on administration of hormones. Adrenal corticosteroids may promote the growth of some cancers, while steroids sometimes cause remissions in acute leukemia.

Poor hygiene and chronic infection are superficially accepted as causes of cancer. Absence of cancer of the cervix in nuns, increased

incidence of bladder cancer in schistosomiasis, and cancer of the penis only in the uncircumcised are all well-documented observations. Physical factors such as trauma and mechanical irritation should also be considered; cancer of the lip in pipe smokers and cancer of the mouth in patients with ill-fitting dentures are two good examples.

Present knowledge of oncogenic viruses in animals suggests that human cancer may be initiated or promoted by viruses or viral-like particles. A strong correlation between an African mosquito-borne virus and human malignant lymphoma suggests that viruses may be important in the causation of cancer. The theory of viral carcinogenesis will be discussed later.

"Embryonic rests" is a descriptive classification linked with embryologic tumors such as hepatic or renal embryoma, neuroblastoma and Wilm's tumor. Malignancy arising in "aberrant embryologic tissue" is no doubt explainable at a more fundamental level.

Cancer incidence is certainly influenced by genetic factors; certain types of cancer are more predominant in specific families or in certain races. Epidemiologic studies demonstrate geographic and national tendencies which influence the incidence of cancer. In any population study, too, one finds the incidence of any type of cancer subject to statistical distribution. Thus, the cancer research worker is faced with the dilemma: "a plethora of causes and an unpredictability of responses. Where do we go from here?" (131)

Among many scientists there is increasing agreement that malignant tumors arise and progress in stepwise fashion. Pathologists long

ago described microscopic changes in tissue undergoing malignant induction as a "field defect," and descriptive terms connoting the degree of irreversibility were metaplasia, dysplasia, anaplasia and neoplasia. Cancer research workers now generally agree on the stages of cancer development as: (a) initiation, which activates a normal cell to a precancerous cell, (b) promotion, which advances a precancerous cell to a dependent cancer cell, and (c) progression, which causes the cancer cell to become autonomous by further action of "initiators" and "promoters" (15,45,48,113,122,131,141). This concept of co-carcinogenesis suggests a complex etiology; two or more causative agents may act synergistically to initiate and promote malignancy.

Co-carcinogenesis still leaves some important questions unanswered, however. In terms of molecular biology, what is the irreversible initial event in carcinogenesis, and what are the steps leading to this primary event? Once understood, can these steps leading to the irreversible event be prevented?

C. Prominent theories of carcinogenesis

The theories of cancer etiology all agree that an alteration in genetic information occurs during the cell's irreversible malignant transformation. Why does the cancer cell stop obeying one or more of the "rules" which the normal cell unerringly follows? The "control mechanisms" in the normal cell have somehow changed in the neoplastic

cell, as evidenced by uncontrolled growth. The many theories of carcinogenesis attempt to explain how normal cellular functions have been altered.

The school of viral carcinogenesis contends that latent viral nucleic acid in a mammalian cell may be the cause of later neoplastic changes--similar to the symbiotic relationship of lysogenic bacteriophage in bacteria (5,131). The large Herpes symplex virus is a clinical example of a latent virus which may be activated by a number of agents such as emotional stress, heat or ultraviolet irradiation to form vesicular eruptions. Disappearance of virus from neoplastic cells previously induced by virus, and without trace of infective nucleic acid, suggests some type of "masking" phenomenon (50,134,139). Another possibility is that the viral nucleic acid may be so well integrated with the cell's nucleic acid that from our present experimental methods of detection we can only conclude that the virus is "masked." Perhaps no further influence of the virus is required to maintain the cell in its neoplastic state, because the virus has truly induced a somatic mutation.

Recent electron microscopy of cells from the Shope fibroma in rabbits, induced by the oncogenic Boerlage virus strain, has shown earliest changes occurring in the endoplasmic reticulum (17). This virus is an intracytoplasmic DNA-containing pox-virus and causes self-limiting subcutaneous fibromata in the wild rabbit and squirrel, and a fatal "infectious myxomatosis" in the domestic rabbit. Here arises the question of defining our terms: in causing a self-limited benign

tumor which may be only a hyperplasia of fibroblasts rather than a true "cancer," can the virus be truly called oncogenic? Proliferation of cells may be defined as tumorigenesis, and viruses which enhance the rate of cellular growth should be called tumorigenic or oncogenic. "Cancer" should be defined as irreversible cellular proliferation, with the capacity for metastasis and seeding, where this property of invasiveness statistically shortens the host's life span. Thus, oncogenesis need not always coincide with carcinogenesis. At any rate, the initial change effected by the invading virus was intracytoplasmic and, more important in relation to this thesis, occurred in the endoplasmic reticulum.

Another closely related theory of carcinogenesis suggests an "infectious," or growth-promoting, humoral substance. Two antagonistic substances, a promoter designated "promine" and a growth-retarding hormone "retine," have been found in thymus, aorta, muscle and tendon (136). These humoral agents have been roughly separated, in spite of similar solubilities in the solvents used for their extraction. "Promine" does not seem to induce malignancy by itself, but does make cancer cells grow faster, while "retine" tends to stop cancer cells' growth, causing tumors to actually regress. The value of the ratio between these two substances in any given tissue is postulated to be significant (136). Other workers have transplanted tumors of male birds into female birds, using the sex chromosome as a marker to distinguish the cells of the transplant from those of the host (108). Although the transplanted tumors grew and spread, all the new cancer

cells belonged to the host and none were derived from the transplant. This cancer-producing stimulation was therefore interpreted as due to viruses from the implanted tissues, or at least a filterable agent spreading into healthy cells of the host (108).

The immunological theory of Green contends that the etiology of cancer is due to loss of tissue-specific antigens, which are probably lipo-proteins located in the endoplasmic reticulum (56). Through mutation of unspecified cause, a genetic loss is equated to an antigenic loss in the cancer cell. The presence of antigens in nearby normal cells becomes "information" which is now "recognized" as "foreign" by the neoplastic cell. The antigen-deficient cells thus respond by reacting in the way in which normal lymphoid tissue reacts when confronted by a foreign antigen--production of antibodies against the tissue-specific antigens of nearby normal cells. The resulting (a) toxic effect on normal tissues, and (b) excessive selective growth of one abnormal clone or cell type, constitutes the phenomenon described as cancer (56,116,131). Electron microscopy of rat liver undergoing malignant induction by a carcinogenic dye in the diet (43, 109) demonstrated that the chemicals were bound first by the endoplasmic reticulum and soluble cell fraction; Green felt this evidence supported his immunological theory (56). His attempts to unify viral and chemical etiologic theories have little experimental support, however. For example, if a virus propagates in its nucleic acid form, (lacking its antigenic coat), it would neither elicit nor be affected by antibody (131).

There has been an attempt to unify all current theories of neoplasia on the basis of loss of regulatory controls of cell division (98). In addition to secondary control factors such as hormonal, nutritional and physical agents in the cell's microenvironment, Osgood feels that normal cell growth is regulated by a pair of specific feedback inhibitors, which are elaborated by the cell destined to differentiate, and which act upon the cell capable of division. He has postulated two types of daughter cells: (a) "α-cells" which remain immature and hence retain the ability to divide again, and (b) "n-cells" which differentiate and die, and which produce inhibitors that regulate α-cell division rates. Therefore, any somatic change in the α-cell resulting in early death of the corresponding n-cell leads to loss of inhibitor, resulting in uncontrolled, logarithmic neoplastic growth of the α-cells. Osgood contends that regeneration following removal of part of an organ is explained by a temporary decrease in inhibitor production. Embryonic tissues perhaps become malignant because of lack of sufficient inhibitor. Chemicals and viruses presumably effect the necessary "somatic genetic change" (98) whereby n-cell death occurs early and α-cell proliferation results.

One objection to Osgood's theory was experimental data by Lather and others demonstrating that the generation time of the more immature leukemic cells is prolonged rather than shortened (99), as measured by an index of mitosis. However, this criticism was disputed by Osgood, and leukemic leukocytes of the more immature cell type have been shown by DNA-incorporated radioactive phosphorus studies to probably have a

shorter survival time and actually an increased mitotic rate (100). The occasional successful transplantation of a malignant tumor with a single cell is another experimental observation difficult to explain by Osgood's theory. In individuals with erythroid hyperplasia (e.g., a marked acceleration in red cell turnover such as long-standing hemolytic anemia or congenital spherocytosis), an erythroleukemia never develops--another well-known fact contradicting Osgood's unifying concept. The isolation of the "regulator" or "inhibitor" substance would prove this theory (98), but thus far no one has succeeded.

The Warburg hypothesis of respiratory impairment as the etiologic basis of cancer (142,143) has been controversial for years (58,70,111, 146,147,148); recently Warburg's postulate has been experimentally disproved (37,113). Warburg stated that the transformation from aerobic to anaerobic energy production in the cell is the cause of cancer. After an irreversible injury to the normal cell's respiratory mechanisms, the normal cell adopts an anaerobic metabolism in order to survive, and this change is the malignant transformation. Because of the strong stand taken by Warburg, many studies of cellular metabolism have elucidated many metabolic pathways of the normal and neoplastic cell. However, the hypothesis that anaerobic glycolysis is a defect observed in all cancers has been shown not to be the case in the Morris "minimal deviation" hepatoma (2,37,113). The "minimal deviation" hepatoma refers to a class of transplantable rat hepatomas produced with very weak carcinogens (84,112). Thus, the "minimal deviation" hepatomas represent standardized transplantable animal cancers

in early stages of tumor progression.

Warburg's ideas on the significance of anaerobic glycolysis in all cancers must therefore be modified (2,117). The earliest stages of carcinogenesis more likely do not involve conversions to anaerobic glycolysis, but rather by natural selection in the Darwinian sense under partially anaerobic conditions, these neoplastic cells emerge with the secondary change of increased anaerobic glycolysis (113). In this regard, the type of lactate dehydrogenase tetramer associated with anaerobic tissues has been reported to be quantitatively increased by immunoelectrophoresis in tumor whole-tissue homogenates (52). This observation also suggests an emerging secondary change in cancer, in which the neoplastic cell is outgrowing its blood supply; due to the decreased oxygen partial pressure of the tissue, the tumor cell adapts to its more anaerobic environment by natural selection in the Darwinian sense.

As early as univalent oxidation-reduction mechanisms in the cell were postulated (79), free radicals have been implicated in the etiology of cancer (16,25,69,101). Because x-irradiation and radioactive isotopes, which sometimes alleviate cancer, cause free radical formation, Park suggested (101) that these therapeutic agents act by pairing, and thus cancelling, the unpaired electrons of the tumor. With the advent of newer and milder alkylating agents and antimetabolites which repress some types of cancer, however, this hypothesis was shown to be wrong. Perirenal sarcomas in rats and mice caused by wrapping the kidneys with certain plastic films was concluded to be

most likely a free radical mechanism (44,94,95,96). "Active centers" capable of binding proteins or other tissue components might consequently impair the metabolism of adjacent cells, resulting in neoplastic transformation (96). Relatively "free" electrons in synthetic plastic or protein polymers and areas of "high electron density" in carcinogens might supply the activation energy essential for carcinogenesis (85), and this concept is an attractive hypothesis.

The theory of chemical carcinogenesis is in agreement with most of the other previously discussed hypotheses. It is axiomatic in considering the mechanism of action of chemical carcinogens that the carcinogen, or its metabolite, must somehow interact with cellular constituents.

The microsomal fraction is that form of the endoplasmic reticulum isolated by homogenization of cells followed by differential centrifugation (14,60). Proteins of the microsomes and supernatant fractions bind considerably more carcinogenic dye than the proteins of the nuclei and mitochondria (80); this has been confirmed by electron microscopic studies (43,109). In hepatomas induced by carcinogenic dyes, there is an apparent loss of the cytoplasmic "h" proteins, a group of relatively basic proteins which takes up most of the protein-bound dye; this observation has been interpreted as the deletion of specific proteins as a consequence of their interaction with the carcinogen (129,130). The nature of the protein-bound dyes has now been partially explained. Data from liver protein (81) and from mouse skin protein (10,11,30) have shown that the protein binds the dye at a region of "high electron

density" of the carcinogens. Thus, the free radical mechanism previously mentioned must be kept in mind.

In contrast to the abundant experimental observations indicating that various carcinogens bind to microsomal and cytoplasmic proteins, data on nucleic acid binding are incomplete. While some workers have reported evidence for the more attractive theory of nucleic acid-bound carcinogens (3,63), others have convincingly pointed out by isotope and electron microscopic studies that nucleic acid-bound dyes could not account for more than 5% of the total protein-bound moiety (43,109, 130). The initial event of carcinogenesis, however, may involve only a very few molecules of carcinogen and a crucial component of DNA, RNA or protein. In such a case, the single event could not be feasibly detected, and the large-scale conjugation of microsomal and cytoplasmic protein may or may not be an important observation.

Therefore, the seemingly irreversible malignant transformation of a cell could occur in two general ways: (a) entrance of genetic information into the cell (the basis of the viral theory of carcinogenesis), or (b) an inheritable change occurring as a result of an inherent instability within the cell. This latter mechanism could be termed a <u>somatic mutation</u>, and the means by which this change in the cell's control system takes place must be explained in any plausible theory of carcinogenesis. The recent advances made in biochemical genetics indicate that basic alterations in either or both DNA and RNA molecules occur in the process of carcinogenesis. Since alterations of microsomal and cytoplasmic proteins also seem to occur, such

"information" from protein molecules could be stored and then transmitted to the nucleoprotein level in what is termed "cytoplasmic inheritance" (68,70,77,123,124,125,128). This idea, that cytoplasmic protein is altered, seems the most comprehensive in describing the events leading to cancer. Infective viral nucleic acid, immunological changes, and somatic mutations are all theoretical mechanisms for carcinogenesis which may be explained by assuming "information" is received from the cell's environment by way of the cytoplasm.

Nonchromosomal determinants are presumably cytoplasmic genetic factors which cannot be located on a chromosome. Such inheritance, called nonmapability, has been characterized in about 100 reported instances (125). Examples include the killer trait kappa in Paramecium (128), the iojap gene affecting male-sterility in maize (77), and streptomycin resistance in Chlamydomonas (123,124). Whether these entities of genetic information are infectious particles, cytoplasmic chromosomes or specialized structural proteins, is presently not well understood. Recent strong evidence (124) supports the postulate that the nonchromosomal determinants in Chlamydomonas are carriers of primary genetic information. These experiments demonstrating stability and retention of identity of the nonchromosomal genes in the face of cell division have fairly well excluded the alternative hypothesis--that nonchromosomal heredity merely reflects the existence of various cytoplasmic states which alter the expression of chromosomal genes.

One of the early theories that cytoplasmic inheritance plays a large role in the etiology of cancer was proposed by Woods and duBuy,

who felt that mitochondria in mutant states could become the continuing cause of neoplasia characterized by distinctive changes in cellular enzymatic activities (33). The mitochondrial hereditary system, designated chondriogenes, was investigated chiefly in higher plants where mutant mitochondria differentiate into plastids with characteristic abnormalities. While the extranuclear hereditary nature of plastids has been accepted by many investigators (149), the possibility has been suggested (119) that cases of so-called plastid mutation may actually be related to a permanently altered cytoplasmic condition in which normal plastid growth is impossible. Woods and duBuy demonstrated that many distinct forms of mutant mitochondria can be recognized in the cells of higher plants and that some of these abnormal derivatives were causing marked derangements in cellular growth and function--constituting a form of distinct malignancy. By introducing abnormal mitochondria into a certain cell and removing the mutant mitochondria by allowing them to segregate out in clonal multiplication, the authors demonstrated the disease symptoms to be directly related to the presence of these abnormal chondriogenes in the cell. The presence of a homozygous recessive chromosomal gene was associated with a much higher expression of chondriogene mutation. The authors felt they had fulfilled Koch's postulates in showing that this form of plant neoplasm was caused by the aberrant mutation of cytoplasmic mitochondria and promoted by the chromosomal genetic constitution (149).

One can postulate several indirect methods by which altered proteins may lead to heritable changes in nucleic acids. A considerable

amount of cytoplasmic protein is involved in the spindle formation during cellular division. Abnormal mitoses, a common phenomenon in neoplastic cells (62), could be due to faulty cytoplasmic protein structure or function. Altered protein may store and transmit distorted "information" to which the genetic center of the cell may respond by deletion of cellular molecules, or by abnormal growth. Nucleic acid, normally protectively encased by protein, may be attacked and altered or destroyed if the protective protein coat has been changed in some way. Immunological differences between tumor cells and their normal counterparts could also be produced by alterations in proteins (31,56). The initial event leading to malignancy may of course be a somatic mutation, but it might also be produced by "the transient action of an agent capable of complexing or inactivating temporarily a genetic locus, or a repressor, involved in the control of multiplication. It is clear that a wide variety of agents, from viruses to carcinogenes, might be responsible for such an initial event" (83).

The close relationship of cytoplasmic protein and its effects on regulation of gene function has brought about a flourish of activity among workers in biochemical genetics. During recent years the "one gene-one enzyme" hypothesis has become more precise. It is well known that a deoxynucleotide sequence which constitutes a gene can participate in two distinct chemical processes: (a) homocatalysis, or replication, where the DNA molecule forms a sequence identical to the original, and (b) heterocatalysis, or transcription, where the gene is

able to specify a certain polypeptide chain via the unstable intermediate messenger-RNA and the protein-synthesizing ribosomes associated with the endoplasmic reticulum. "Information" via the cytoplasm may affect the cell's genetic controls by any one of three well-known processes which appear to be widely different physiologically. Careful analysis of immunity, induction and repression, however, points to a common basic mechanism operating in all three systems.

When a bacterium is infected with a virus, usually viral nucleic acid and proteins are formed by the cell, and the cell is destroyed with release of new infective virus. However, if the viral nucleic acid is carried in the prophage state (lysogeny), the viral genes of the prophage replicate at the pace of the bacterial chromosomes, and viral proteins are not formed. If such a lysogenic bacterium is infected with bacteriophage of the same strain as that of the prophage, the viral genetic material enters the cell, but no viral nucleic acid or proteins are formed; this phenomenon, in which the "information" entering the bacterium does not appear to be "recognized" by the cell, is called immunity (66). As a result of ultraviolet, x-irradiation or certain chemical mutagens, however, the bacterium will respond to the viral nucleic acid "information" by producing infective viral particles; most chemical carcinogens apparently do not possess the activation energy necessary for re-expression of bacterial viruses. The mechanism by which a cell is temporarily immune to certain "information" is not understood. Possible explanations for immunity would be: (a) a genetic locus has been chemically altered, or (b) protein is

covering up a specific gene on the DNA helix. Perhaps the activation energy of irradiation and of mutagens changes the genetic locus, or uncovers the protein encasement, again allowing genic expression.

When bacteria are grown in the absence of a galactoside, only traces of β-galactosidase are found in the cells. If a galactoside is added to the medium, the bacterial synthesis of this enzyme increases by about 10,000-fold. This mechanism has been called induction, or derepression. The phenomenon is specific in that only enzymes concerned with the utilization of that specific substrate added to the environment are induced to high levels of activity (67).

The other form of bacterial adaptation is known as repression. A tryptophan-requiring bacterium, for example, synthesizes tryptophan when this essential amino acid is not present in the medium. If tryptophan is added to the environment, however, this "information" is somehow registered at the genetic level and tryptophan-synthesizing enzymes are promptly turned off--until such time as the external supply becomes exhausted. This extremely specific mechanism involves only the enzymes involved in the utilization of that substrate added to the environment; in the case of tryptophan-synthesizing enzymes, only tryptophan or its analogs can exert this effect of repression (68).

The similarity of these regulation systems in bacteria to the fundamental aspects of carcinogenesis lies in the fact that "information" via the cytoplasm can determine the rate of transcription of specific structural genes and hence can determine the destiny of that

FIGURE 1. The general Jacob-Monod model for the regulation of enzyme synthesis (68). A regulator gene produces a cytoplasmic repressor molecule, which associates reversibly with a specific operator gene, which in turn coordinates a unit of primary transcription--the operon. Presence of the effector (such as galactoside) inactivates the repressor, allowing transcription of polypeptides (formation of β-galactosidase) to take place. In repressible systems, only the modified repressor is active, and transcription of the operon is therefore prevented.

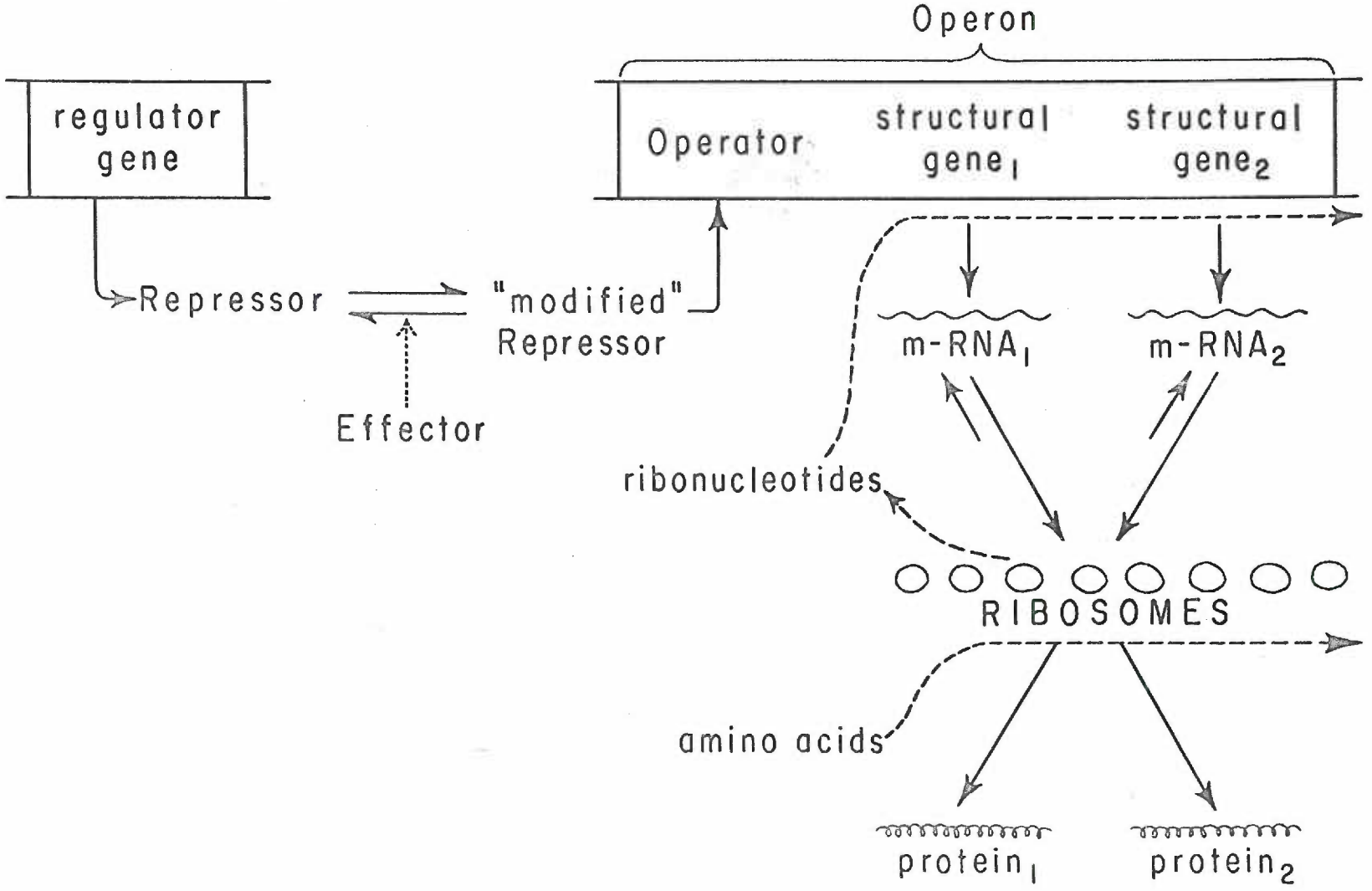
Operon
regulator gene
Operator
structural gene1
structural gene2
Repressor
"modified" Repressor
Effector
m-RNA1
m-RNA2
ribonucleotides
RIBOSOMES
amino acids
protein1
protein2

cell. The mechanism, as illustrated in Figure 1, which explains regulation of gene activity, involves a system of transmitters (regulator genes) and receivers (operator genes) of specific cytoplasmic signals in the form of repressor molecules (68). These cytoplasmic repressors must be capable of recognizing a particular metabolite and a particular operator gene. Through a mechanism still unknown, the metabolite may either (a) activate the repressor, which in turn would combine reversibly and specifically with that operator in order to inhibit transcription, or (b) inactivate the repressor, allowing the transcription of the operon and therefore the production of that specific group of proteins. The proteins then synthesized would be those enzymes specifically capable of utilizing the cytoplasmic metabolite which initially "informed" the cell of its presence in the cytoplasm.

This theoretical mechanism (68) would become more relevant to the field of carcinogenesis if these bacterial phenomena were also found in mammalian cells. A process analogous to, if not identical with, enzyme adaptation in microorganisms has been reported with the enzyme tryptophan pyrrolase in rat liver (71). Tryptophan or cortisone injected intraperitoneally in rats produces a two- to ten-fold increase in tryptophan pyrrolase activity in four hours' time (42,113). Recent data suggest that the energy-dependent activation of tryptophan pyrrolase reflects an enzymatic release of enzyme-protein from the microsomal particulate to a soluble form (41,104). In the presence of hematin, a divalent cation, ATP, phosphoenol pyruvate and PGA, the cell-soluble fraction designated the "peeling enzyme" solubilizes the

microsomal apo-enzyme, forming "active" tryptophan pyrrolase; this holo-enzyme, which includes the heme and usually manganous ion, forms kynurenine from tryptophan. Magnesium ion is slightly less effective than manganese, and other divalent cations are very inefficient (104).

Thus, in this mammalian system where tryptophan is the "effector," the tryptophan pyrrolase "operon" becomes active in order to take advantage of the excess substrate in the environment, and the destiny of the cell has been determined by cytoplasmic "information." According to the simplest form of the Deletion Hypothesis (63,80,110,113), repression of catabolic enzymes and derepression of anabolic enzymes could feasibly present the picture of malignancy--a condition of growth promotion, or uncontrolled growth.

Hormonal and drug induction of enzymes have different mechanisms which are not well understood. Cortisone appears to increase the number of template sites of the messenger-RNA (57). Stimulation of microsomal enzyme activity by administration of phenobarbital and other drugs has been reported (27), but this mechanism of enzyme derepression involves stimulation of the TPNH-oxidase system so that there is increased active oxygen available for drug and steroid hydroxylation (28,51) and probably differs from simple enzyme induction.

Differences between normal liver, precancerous liver and hepatomas have been summarized and thoroughly reviewed with few positive correlations (118). Numerous biochemical studies on all of the "minimal deviation" hepatomas have revealed that no two are exactly alike with respect to enzyme patterns and enzyme induction (2,12,13,21,

26,34,37,38,40,84,89,92,93,103,104,105,106,107,110,112,113,114,115, 121,133,140,145). Adamson and Fouts showed that the Morris 5123 was unable to metabolize codeine, p-nitrobenzoic acid, hexobarbital and aminopyrine (1). Because of the absence of drug-metabolizing enzymes from a wide variety of hepatomas (28,46), it was speculated that a deletion of these TPNH-dependent microsomal enzymes may have importance in hepatoma formation (1). Again, the more likely explanation is that deletion of microsomal enzymes in hepatomas is probably a secondary change in neoplasia in the Darwinian sense of natural selection, after the tumor has undergone the primary irreversible event of carcinogenesis and has gained autonomy.

It was felt (21,34,104,105) that it might be important to determine whether or not hepatoma tissue derived from normal liver still possesses the ability to respond to intraperitoneal administration of tryptophan. In the case of the Morris "minimal deviation" hepatoma 5123, there was no response after injections of tryptophan or cortisone, while a two- to ten-fold increase in tryptophan pyrrolase activity did occur in the livers of normal control rats and of rats hosting the hepatomas (104,105). The possibility that the lack of enzymatic induction was due to a failure of intraperitoneally injected material to reach the tumor was ruled out in subsequent experiments (13,21,34). Hepatoma 5123 has been found to respond to intraperitoneal methylcholanthrene administration by marked increases in demethylase activity, however; demethylase induction occurs in normal liver and has not been reported in the other "minimal deviation" hepatomas

to date (26,28,114).

Therefore, with respect to enzyme adaptation, the Morris hepatoma 5123 has been regarded as the least deviated of primary transplantable animal cancers, until very recently. Dyer's group has now shown (34) that "minimal deviation" hepatomas 7793, 7794-B and 7795 respond to substrate induction with elevated activity similar in behavior to the tryptophan pyrrolase activity of normal liver. The Reuber hepatoma H-35 and the Morris hepatoma 7793 were studied with respect to tryptophan and cortisone injections in adrenalectomized hosts, as well as in intact host rats; a significant substrate induction resulted in the intact but not in tumors of the adrenalectomized host (21). Differences in the tryptophan pyrrolase kinetics and electrophoretic mobilities between normal liver and hepatoma 7793 were not found, and tryptophan pyrrolase in the hepatomas was shown to have a dual (substrate and hormonal) control as in normal liver. The authors thus suggested that hepatomas may have lost the capacity to maintain a stable RNA template for tryptophan pyrrolase synthesis, so that the substrate induction in the hepatomas no longer occurs unless the RNA template is continuously renewed by corticosteroid stimulation (21).

"Minimal deviation" hepatomas progressively similar to normal rat liver will inevitably be characterized. The importance of cytoplasmic "information" and enzyme adaptation in "minimal deviation" hepatomas with respect to the fundamental aspects of cancer can only be speculative. The primary irreversible event in carcinogenesis therefore has probably not yet been uncovered, or perhaps the importance of a recent-

ly discovered difference between normal and neoplastic cells has not been fully appreciated. Again, perhaps no specific metabolic difference is an absolute requirement for neoplasia.

The problem of the initial events of carcinogenesis in this thesis first involved discovery of relative differences between the normal and neoplastic cell; these differences were then specifically traced to certain molecules associated with the endoplasmic reticulum. Those differences in one type of cancer which could also be demonstrated in a Morris "minimal deviation" hepatoma became far more significant. Most of the biochemical studies of normal and neoplastic biological material in this thesis centered around differences which were first discovered by low-temperature ESR spectroscopy, a new technic available to our laboratory.

D. Principles of Electron Spin Resonance Spectroscopy

ESR spectroscopy is the technic of observing unpaired electrons: free radicals such as possible enzymatic metabolic intermediates, and transition metal ions of the proper valence state (65). Paramagnetic behavior is shown when the magnetic effects of the individual electrons are not mutually neutralized, and paramagnetism is associated with the presence of either unpaired electrons or an incompleted electronic level. The permanent moments characterizing paramagnetic

materials are of sufficient magnitude as to make their diamagnetic properties appear relatively unimportant. Unlike diamagnetism, paramagnetism is dependent upon temperature, since it is associated with orientation of dipoles in a magnetic field. Although the presence of an odd number of electrons is commonly characteristic of paramagnetic substances, lack of electron pairing may occur when an even number of electrons is present if the principle of maximum multiplicity, or single occupancy of available orbitals, is obeyed.

The sample to be examined by ESR spectroscopy is placed in a static magnetic field which can be varied continuously, while at right angles to this field electromagnetic radiation of a fixed radio-frequency is applied. Absorption of energy from the radio-frequency oscillation by the sample is measured while the magnetic field strength is varied. The unpaired electron with its miniature magnetic moment may be compared to a spinning top. The rotating electron acts as a magnetic dipole, and the effect of the static magnetic field causes precession of this "gyroscope." The radio-frequency oscillation may be considered equivalent to a rotating magnetic field, and the rate of precession varies with the strength of the applied static magnetic field. Therefore, when the frequency of rotation coincides with the frequency of precession, the motion of the unpaired electron is affected and energy is absorbed.

Conditions for this "resonance absorption" in terms of quantum mechanics follow the fundamentals of the splitting of energy levels. If radiation of frequency ν is fed to the sample, some of the elec-

trons in the lower, or parallel, state will absorb energy and jump to the higher energy state while those electrons in the upper, or anti-parallel, state will be stimulated to emit radiation of frequency ν and fall to the lower energy state in the process, provided that

$$h\nu = g\beta H \qquad (i)$$

where h is Planck's constant, ν the radio-frequency of the microwave radiation, β the Bohr magneton constant, and H the strength of the static magnetic field in gauss. The term g is a dimensionless quantity designated the "spectroscopic splitting factor." The g-value determines the degree of splitting of the energy levels and is fundamentally the measure of contribution of the spin and orbital motion of the unpaired electron species being measured to its total angular momentum. Empirically, g was found to be 2.0023 for the completely "free" electron (65). Each free radical species or paramagnetic transition metal ion exhibits a characteristic and reproducible g-value, just as any compound displays a constant molecular weight, boiling point or magnetic susceptibility measure.

Absorption measurements of the sample when Equation (i) is satisfied are recorded as the first derivative of microwave energy absorption with respect to field strength, in order to increase the signal-to-noise ratio. The ESR signals are therefore presented as microwave energy absorption as a function of magnetic field strength. Unpaired electrons in biological samples can thus be measured for (a) absolute

concentration and (b) frequency of species occurrence, by respectively recording the intensity of the ESR signal (i.e., deviation of the pen from the baseline), and scanning the magnetic field.

E. ESR Studies of Biological Materials

The early ESR studies of biological tissues were based on frozen-dried samples (23). Presence of water in the ESR spectrometer cavity then available caused an appreciable loss in ESR detection sensitivity, as water in the cavity is an effective absorber of microwave energy. Recent development of more sensitive ESR devices has now permitted direct investigations of living animal tissues in the presence of liquid in the cavity (7,25).

Pioneering work in the application of the technic of ESR spectroscopy to living normal and neoplastic whole tissue was reported by Commoner and Ternberg (25), who found that "in contrast with normal liver, free radicals are undetectable in rat and mouse hepatoma," and that all of the ESR studies of neoplastic tissues up to this time indicate that they are distinguished by "relatively low, or wholly undetectable, free radical contents." Their samples included normal and neoplastic rat and mouse liver, rat livers at intervals from birth, normal human liver and human liver from several clinical cases of obstructive jaundice; all tissue samples were suspended in a 5% glucose solution in the ESR cavity. The wholly empirical observations of

decisive differences in free radical concentrations related to certain pathological changes in animal and human tissues suggested to the authors certain useful lines of investigation such as differential diagnosis, insight into metabolic differences among tumors, and metabolic studies of the response of tumors to anticancer agents. They postulated that the remarkable absence of detectable ESR signals in tumor tissue reflected the relatively small concentration of mitochondria, since the free radicals most likely were originating in the mitochondrial redox enzymes (25).

More recently, Russian workers detected free radicals in carcinogenic preparations with ESR spectroscopy and felt this pointed to the possible role of free radicals in the etiology of malignant tumors (69). They studied the semiquinone free radical in varying conditions of oxygen partial pressure, alkalinity and tissue protein concentration. It was concluded that semiquinone free radicals, formed by alkalinizing the medium, adsorbed to protein polymers, and this free radical mechanism was offered as the initial event in carcinogenesis.

These ESR studies were all made at room temperature, however, a technic having the advantage of direct observation of living cells but having the disadvantage of relatively low sensitivity compared with spectroscopy at lower temperatures (65). Increased sensitivity in ESR analysis can be shown to occur at lower temperatures by the Maxwell-Boltzmann expression in which the ratio of the number of electrons in the higher energy state, n_1, to the number of electrons in the lower energy state, n_2, is given by

$$\frac{n_1}{n_2} = e^{-\frac{\Delta E}{kT}} \qquad \text{(ii)}$$

where ΔE is the separation between the two levels of electrons, k the Boltzmann constant, and T the absolute temperature. At low temperatures where T is reduced, therefore, the difference between the n_1 and n_2 levels is increased, so that a larger net absorption and greater sensitivity occurs (65).

Many biological materials have been studied with ESR spectroscopy in the last few years. For purposes of interpretation of results and later discussion, the ESR characteristics of important biological substances are summarized here.

Melanins have a narrow absorption around g=2.00 (24,76), characteristic of free radical signals. Mitochondria and submitochondrial particles from beef heart and other tissues absorb at g=1.94 and 2.00, probably due to non-heme iron associated with flavin or flavin semiquinone (6,7). Mitochondria also have absorption at g=4.3, probably due to ferric iron in the high-spin state (126), and absorption at g=2.03 and 2.17, presumably due to cupric copper in cytochrome oxidase (8). Smooth- and rough-surfaced microsomes (ribosome-free and ribosome-containing, respectively) have absorptions at g-values of 1.91, 2.25 and 2.41, owing to the presence of an otherwise unidentified heme protein, designated microsomal Fe_x by this laboratory; microsomes also absorb at g=2.00, probably due to either a flavin or another

semiquinone free radical (61,88,150). Hematin compounds have complex absorptions dependent upon their high- or low-spin states and may give signals in the regions of g=6, 4 or 2 (35). A complex six-line absorption centered about g=2.00, found in a number of biological materials, is attributed to the manganous ion associated with its structural environment in a special way (4,74,86,138).

While melanin, free radicals and inorganic systems of paramagnetic transition metal ions can be observed at room temperature, all the other resonances mentioned above were seen only with low-temperature ESR spectroscopy for several reasons. As previously mentioned, increased sensitivity of the spectrometer can be shown mathematically as well as experimentally to occur at low temperatures, so that this technic was advantageous in detecting small concentrations of biological paramagnetic substances. Because liquids absorb microwave energy, sample size is very limited at room temperature, while in the frozen state a considerably larger sample may be studied. In addition, the handling of samples and the operation of the instrument are simpler and more reproducible at low temperatures. Also, a reaction may be stopped at a desired state by quick-freezing and then studied at leisure (9,65).

There are distinct disadvantages to low-temperature ESR analysis, however. The mechanics of the liquid nitrogen flow system for cooling the ESR cavity can be a problem. The state observed in the frozen sample at -170° C. cannot be assumed to be necessarily the state which prevailed at room temperature. Equilibrium shifts, complex formations

and pH shifts may occur. Kinetic studies at liquid nitrogen temperatures are generally cumbersome (9).

The interaction of nuclear magnetic moments of a molecule with an unpaired electron may lead to fine detail in the ESR spectrum, designated hyperfine structure. This splitting can be of great value in interpreting the species of free radical or the environmental structure of bound paramagnetic transition metal ions in a biological sample. An unpaired electron may interact with the nuclear magnetic moment of the same molecule or of neighboring molecules. In the liquid state, molecular tumbling (Brownian motion) cancels the influence of the nuclei of neighboring molecules, so that only the hyperfine structure stemming from the nuclear magnetic moment of the parent molecule is detected and recorded with room-temperature ESR technic. However, in the rigid environment with low temperatures, powder or viscous solvents, this anisotropic interaction is continuous, leading to hyperfine splitting from neighboring molecules as well as the parent molecule. The multiplicity of energy levels results in a general broadening of the ESR signal with no resolved hyperfine structure, and this can be a distinct limitation to ESR spectroscopy at liquid nitrogen temperatures (9,65).

For a paramagnetic species in a rigid environment, more than one g-value can occur, causing asymmetric ESR spectra. This phenomenon depends upon the orientation of the symmetry axes of the crystal field with respect to the magnetic field H. Values for both parallel and perpendicular orientation are then observed (9,65).

II.

MATERIALS AND METHODS

A. Chemicals

In experiments where extraneous paramagnetic impurities would be undesirable, all water was doubly distilled and then passed through a Barnstead standard mixed-bed ion-exchange column. The conductivity of the column was $\angle 1.0$ μmho; the meter remained below 0.1 p.p.m. sodium chloride. All articles of glassware used in such experiments were thoroughly rinsed in water which had been doubly distilled and deionized.

Buffers were prepared according to directions given in Methods of Enzymology (53,55). The pH of each buffered solution was checked against Coleman pH standards. The sodium and potassium phosphates, alcohols, acids and bases used in all experiments were American Chemical Society reagent grade chemicals.

Sodium dithionite, manganous sulfate and sodium chloride were obtained from Mallinckrodt Chemical Works. Sucrose and manganous chloride were supplied as a reagent grade from Baker and Adamson. Tetrasodium-EDTA, lithium chloride and acetanilide were purchased from Matheson, Coleman and Bell Co. The reagent grade ammonium sulfate was recrystallized before use. Succinic acid, tryptophan, protamine sul-

fate and sodium choleate were obtained from Nutritional Biochemicals Corp. DPNH and TPNH were obtained from C. F. Boehringer & Soehne Co. Bovine albumin, antimycin A and ovalbumin were purchased from Mann Research Laboratories, Inc. Phosphatidyl-serine and cytochrome c were supplied by Sigma Chemical Co. The reagent grade p-phenylenediamine from Eastman Organic Chemicals Co. was sublimed before use, the fraction between 90° and 92° C. being collected. N,N-dimethylformamide and β-glycerophosphate were also obtained from Eastman. Phenol was purchased from Hartman-Leddon Co. Pyridine was supplied by Merck & Co., Inc. Trypsin was obtained from Calbiochem Corp. for Biochemical Research, and β-lactoglobulin was obtained from the Bureau of Agricultural and Industrial Chemistry, Philadelphia.

Emasol 1130, a nonionic synthetic detergent (polyoxyethylene-sorbitan-monooleate), was obtained from the Kao Soap Co., Tokyo. Emasol 1130 and 4130 are probably identical to Tween 80, except for minor differences in the lengths of the polyoxyethylene side chains--indicated by slight differences in the index of hydrophilic/lipophilic balance (151).

B. Biological Preparations

Twenty-nine mouse tumors were purchased from the Roscoe B. Jackson Laboratories, Bar Harbor, Maine. Each type of cancer was freshly inoculated subcutaneously into three mice at Bar Harbor and shipped by

air on a schedule convenient to this laboratory. The tumors were allowed to mature, and when the mass was clearly visible the animal was sacrificed by cervical dislocation; the tumor was dissected free and kept on ice. As much blood as possible was removed, and the firmest, most viable regions were dropped directly into liquid nitrogen. After being frozen the samples were rapidly weighed and then placed in a cold quartz ESR sample tube, which was kept immersed in liquid nitrogen to avoid any thawing of the sample. The procedure from cervical dislocation of the mouse to immersion of the sample in liquid nitrogen averaged three to five minutes. The average weight was 170 mg. This provided a very rough, qualitative comparison of the frozen whole tissue samples. Quantitative technics employed for subcellular fractions are described below. The list of tumors and normal tissues which were studied appears in Table 1.

Hepatoma BW 7756 in the C57/LJ mouse was used for the preparation of cell particulates; liver from the same mouse strain was used for normal subcellular counterparts. Cell organelles were prepared from the pooled tissues of six to ten animals. Mitochondria were prepared by a modification of the method of Schneider (127) and examined in 0.25 M sucrose after repeated centrifugal washings. Rough- and smooth-surfaced microsomes were prepared by a modification of the method of Fouts (46), which was shown to produce essentially homogeneous fractions by electron microscopy (61). All ESR and biochemical analyses were standardized to microsomal protein concentrations, as determined by the biuret method (54). Spectrophotometric readings at 540 mu were

TABLE 1. List of normal and neoplastic mouse whole tissues which were studied by low-temperature ESR spectroscopy. Twenty-nine Bar Harbor mouse tumors and two normal tissues were included in the survey.

TUMORS

Name	Bar Harbor Classification	Mouse Strain
Mammary Adenocarcinoma	H 2712	C3H/HeJ
	d br B	DBA/1J
	BW 11301	A/J
	BW 10232	C57 BL/6J
	Ca D 1	DBA/1J
	Ca D 2	DBA/2J
	C 3 HBA	C3H/HeJ
Melanoma	S 91	DBA/1J
	H-P	BALB/cJ
	B/16	C57BL/6J
Myeloid Leukemia	(DBA/2 in ♂) MY-1	DBA/2
	(DBA/2 in ♀) MY-1	DBA/2
	C 1498	C57BL/6J
Spindle Cell Sarcoma	S 37	DBA/1J
	S 180	BALB/cJ
	SI	A/J
Lymphatic Leukemia	P 1534	DBA/2J
Rhabdomyosarcoma	BW 10139	CE/J
Osteogenic Sarcoma	T 283	AKR/J
Induced Lymphosarcoma	6C 3 HED	C3H/HeJ
Anaplastic Carcinoma	15091 A	A/J
Ovarian Granulosa-Cell Tumor	E 11731	A/HeJ
Ovarian Granulosa-Cell Tumor (Hormonal)	H 4929	DBA/1J
Preputial Gland Tumor	ESR 586	C57 BL/6J
Round Cell Tumor	C 1300	A/J
Hemangioendothelioma	BW 6473	129/J
Testicular Interstitial-Cell Tumor (Hormonal)	H 10119	BALB/cJ
Adrenal Cortical Tumor	E 12529	C57BL/10J
Hepatoma	BW 7756	C57/L J

NORMAL TISSUES

Cardiac Muscle	A/J, BALB/cJ, and C57/L J
Liver Tissue	A/J, C57 BL/10J, 129/J, and C57/L J

carried out 24 to 48 hours after addition of the biuret reagent; this allowed time for the formation of a visible phospholipid net, which was filtered off by glass wool before the spectrophotometric reading. Chemical analyses of the mouse liver and mouse hepatoma microsomes included total iron content (52), pyridine hemochromogen (102) and cytochrome b_5 (49).

Electron microscopy of mouse microsomal preparations was done by Dr. Kakefuda at City of Hope Research Center, Duarte, California. The frozen microsomal samples were shipped by air; at City of Hope Research Center the specimens were immediately fixed with osmium tetroxide, dehydrated, and embedded in Epoxy-resin. Thin sections were later cut and stained with uranylacetate and lead for electron microscopic sections.

Oxidation-reduction experiments utilizing low-temperature ESR spectroscopy (61) were conducted on normal mouse liver and hepatoma microsomes. The possibility of a new microsomal a-type cytochrome was studied by spectrophotometry at liquid nitrogen temperatures (39). Cytochrome oxidase activity was determined by Warburg manometry (64) and by enzyme kinetics with the recording spectrophotometer (82). Antimycin A inhibition studies were also carried out (132).

Seven female Buffalo strain rats inoculated subcutaneously and intramuscularly with Morris hepatoma 5123-B, Generation 39, and thirteen female Buffalo strain rats of the same age for controls were obtained through the generosity of Dr. H. P. Morris of the National Can-

cer Institute, Bethesda, Maryland. Eight weeks after inoculation the animals were sacrificed by cervical dislocation, and the tumors and livers were excised and immediately frozen in liquid nitrogen. Three groups of tissues were defined: (a) livers from normal healthy rats, (b) livers from animals hosting the tumors, and (c) Morris "minimal deviation" hepatoma 5123-B tissue. These tissues were then separately homogenized in 0.88 M sucrose, and the combined smooth- and rough-surfaced microsomal fractions of the three respective groups were compared by low-temperature ESR spectroscopy (88,89), studied by spectrophotometry at liquid nitrogen temperatures (39), and assayed for acetanilide hydroxylase activity (72,89). The results were quantitatively compared on the basis of microsomal protein concentration, also determined by the previously mentioned modification of the biuret method (54).

A substrate induction experiment (21) was carried out with fifteen other Buffalo strain rats. Five animals received injections of 4.0 ml. 0.25 M suspension of L-tryptophan in 0.9% sodium chloride, five animals received 10 mg. cortisone acetate, and five "control" rats received injections of 4.0 ml. 0.9% sodium chloride. The injections were administered intraperitoneally at time zero and at three hours, and all rats were sacrificed by cervical dislocation six hours after the first injection. All livers were excised and immediately frozen in liquid nitrogen. Later, the three respective liver microsomal fractions were isolated and examined by low-temperature ESR technic (88,89).

The paramagnetic manganous ion appeared to be very intimately associated with every microsomal preparation. Therefore, numerous attempts at purifying manganese in its natural association with the microsomal membrane were carried out. Fresh, frozen beef liver was purchased from Swift & Co., and microsomal preparations, starting with 400 g. whole liver at a time, were done. Separation of a manganese fraction by ammonium sulfate fractional precipitations, precipitations by pH, column chromatography and continuous-flow electrophoresis proved unsuccessful. The ESR signal height per mg. microsomal protein was the only available means by which microsomal manganese could be accurately measured; thus, the microsomal manganese fraction could not be successfully followed in the above-mentioned technics, due to either (a) too much dilution, or (b) contamination with paramagnetic impurities, commonly cupric ion.

Solubilization of the microsomal manganese component after trypsin digestion was unsuccessful in acid or base solutions, or in ethyl alcohol, methyl alcohol or ether. Emasol solubilization after trypsin digestion produced the most satisfactory purification, resulting in an aqueous phase of quite concentrated manganese per mg. protein. The procedure used in solubilizing a microsomal manganese moiety is outlined in Figure 2.

FIGURE 2. Procedure used in solubilizing and purifying a microsomal manganese fraction. This outline to date is the most satisfactory method. The two-fold and six-fold purifications refer to ESR signal height of manganese, per mg. microsomal protein.

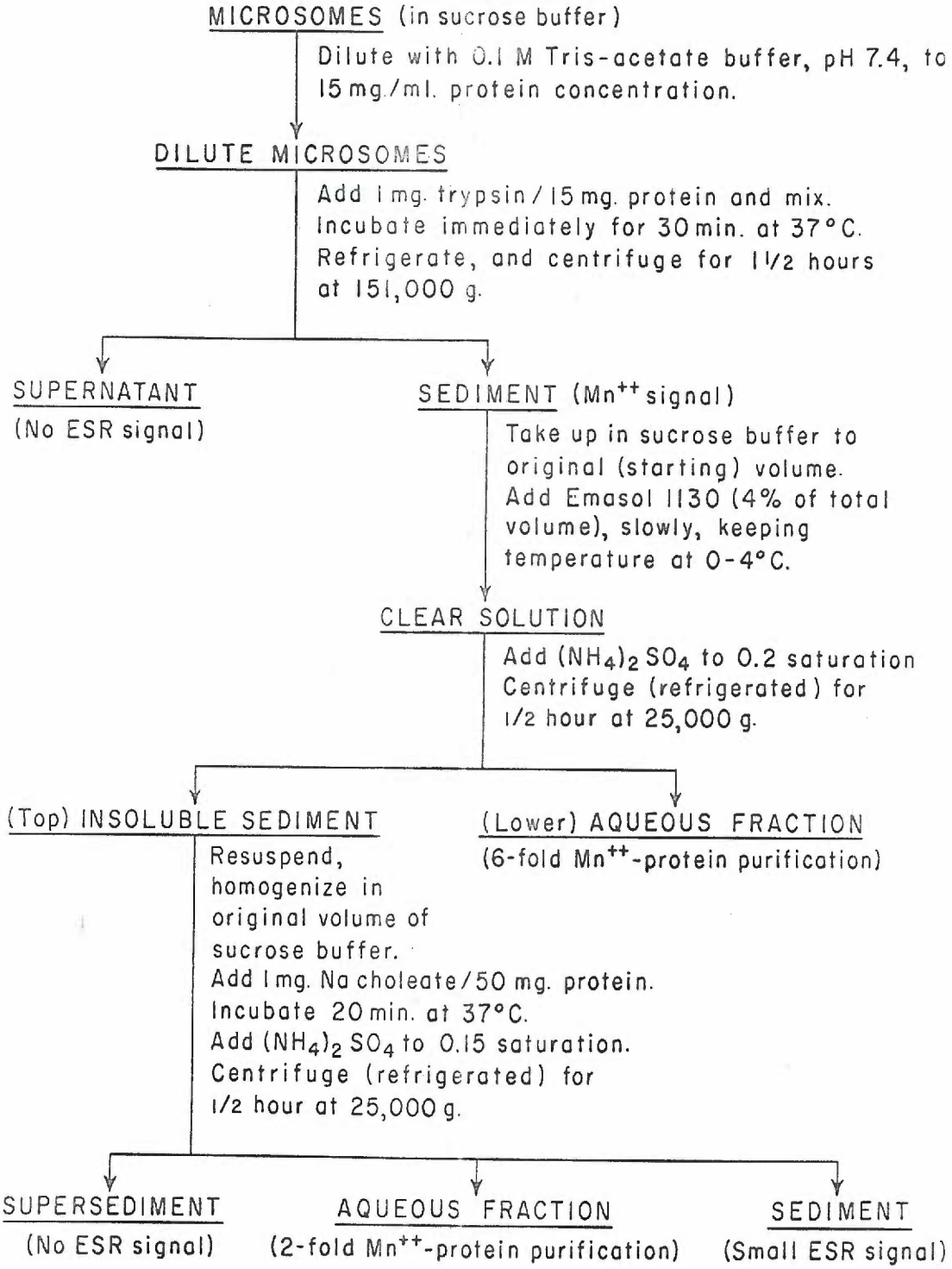
MICROSOMES (in sucrose buffer)
Dilute with 0.1 M Tris-acetate buffer, pH 7.4, to 15 mg./ml. protein concentration.
DILUTE MICROSOMES
Add 1 mg. trypsin / 15 mg. protein and mix. Incubate immediately for 30 min. at 37°C. Refrigerate, and centrifuge for 1 1/2 hours at 151,000 g.
SUPERNATANT
(No ESR signal)
SEDIMENT (Mn^{++} signal)
Take up in sucrose buffer to original (starting) volume. Add Emasol 1130 (4% of total volume), slowly, keeping temperature at 0-4°C.
CLEAR SOLUTION
Add $(NH_4)_2 SO_4$ to 0.2 saturation Centrifuge (refrigerated) for 1/2 hour at 25,000 g.
(Top) INSOLUBLE SEDIMENT
(Lower) AQUEOUS FRACTION
(6-fold Mn^{++}-protein purification)
Resuspend, homogenize in original volume of sucrose buffer. Add 1 mg. Na choleate / 50 mg. protein. Incubate 20 min. at 37°C. Add $(NH_4)_2 SO_4$ to 0.15 saturation. Centrifuge (refrigerated) for 1/2 hour at 25,000 g.
SUPERSEDIMENT
(No ESR signal)
AQUEOUS FRACTION
(2-fold Mn^{++}-protein purification)
SEDIMENT
(Small ESR signal)

Oxidative phosphorylation appears to require manganous ions; in studies of mitochondrial respiration (19,20), low concentrations of manganous ion stimulated the respiratory rate, suggesting the possible presence of a redox pump located in the mitochondrial membrane. The possibility of redox function of manganese in the microsomal membrane was therefore entertained. The experimental procedure of Strittmatter (132) measures microsomal respiration, by following the reduction of exogenous cytochrome c at 550 mu. This experimental system was prepared, and both smooth- and rough-surfaced mouse liver microsomes were examined. The effect on microsomal respiration was studied--with and without the presence of 1 mM manganous chloride in the system.

C. Inorganic Studies of Manganese

The problem of explaining the observed low-temperature ESR spectrum of microsomal manganese, compared to the simple six-line absorption seen at room temperature, led to basic study with numerous inorganic experimental systems. Manganous chloride, manganous sulfate, and manganous phosphate (prepared from dilute manganous chloride and concentrated phosphoric acid (59)), were studied by ESR in acid solutions of varying anion/Mn^{++} ratios of chloride, sulfate and phosphate, respectively.

The additional influence of fluoride, cyanide, lithium chloride, sodium chloride, bovine albumin, ovalbumin, β-lactoglobulin, cyto-

chrome c, protamine sulfate, numerous amino acids, β-glycerophosphate and phosphatidyl-serine on manganous chloride was examined by ESR at room temperature as well as low temperatures. Water, methanol, ethanol, acetone and N,N-dimethylformamide were used as solvents for manganous chloride in experiments studying the effects of solvent on the manganous ion.

The titration curve of phosphoric acid was established by measuring the pH of 900 umoles of phosphoric acid before and during the stepwise addition of 2700 umoles of sodium hydroxide. A volume of 1.0 ml. base was added to a starting volume of 10.0 ml. phosphoric acid. In further experiments, 10, 20 and 100 umoles of manganous phosphate was added to 890, 880 and 800 umoles of starting phosphoric acid, respectively. Stepwise addition of sodium hydroxide was again carried out in each of these experiments, and microsamples of each solution were taken at various points along the titrations for low-temperature ESR analysis. By this method, the concentrations of each phosphate species were known at any given point along the titration curve, and the effect of each anion species upon the manganous cation could therefore be accurately determined by low-temperature ESR technic.

D. Electron Spin Resonance Spectroscopy

A Varian V-4500 ESR spectrometer with 100-kc. field modulation was used, with modulation amplitudes between 8 and 16 gauss. Klystron frequencies were determined with a Hewlett-Packard K532B frequency meter, and field strengths were monitored with a Hewlett-Packard 5240 electron frequency counter coupled to a proton resonance meter. The spectra shown in the figures are derivative curves of the actual energy absorption, with magnetic field H always increasing from left to right. The maximum and minimum slope positions of some of the spectra may be reversed in phase, but this is unimportant.

Instrumental response times were set at 0.3 or 1.0 second for ESR analysis of the biological materials, and at 0.01 second for the more sensitive inorganic systems of manganese. The gain was as low as 20 for the inorganic experiments where manganous ion concentration was usually 10^{-3} M, and as high as 1000 for the less concentrated biological materials. The magnetic field was scanned from 1000 to 4000 gauss, which covers the g-value regions of 6, 4 and 2. Purified nitrogen passed through a heat-exchanger in liquid nitrogen kept the cavity temperature at about -160° C., although the temperature could be regulated between -190° and -50° C. by adjusting the rate of nitrogen gas flow through the heat-exchanger.

Sample size in the ESR cavity was normally 0.20 ml., with the exception of room temperature experiments and the titration study with manganese, when sealed capillary tubes (with the solution to be

examined) were placed in the bottom of ESR quartz tubes normally used for low-temperature work. The ESR quartz sample tubes were of approximately 3 mm. bore. The prepared samples were always stored in liquid nitrogen prior to placement in the ESR cavity. The quartz tubes were tested prior to use, to eliminate those giving spurious ESR signals in the absence of experimental material.

III.

RESULTS

A. Whole Tissue Studies

The ESR spectra of typical whole tumor and whole normal tissues of the mouse are depicted in Figures 3 through 7. The comparison signals from normal liver and cardiac muscle are shown in Figure 3.

B. Subcellular Components of Normal Mouse Liver and Hepatoma

The mouse hepatoma BW 7756 was compared to presumably related normal mouse liver. The ESR spectra of mitochondria obtained from normal and neoplastic liver are shown in Figure 8. Curves A and B represent the spectra of normal and cancerous mitochondria, respectively, washed and centrifuged twice; curves C and D depict the corresponding samples washed and centrifuged six times.

The theoretical ESR derivative spectrum of microsomal Fe_x is pictured in Figure 9, with absorptions at g_m=2.25 and s_m=2.41 and 1.91.*

* "g_m" is the position, in terms of g-value, of maximal absorption, while "s_m" is the position of maximum or minimum slope in the spectrum plotted as a derivative curve (61).

This heme protein has not been purified, so that actual ESR spectra of microsomal preparations always show this absorption superimposed on signals of other paramagnetic substances. Again looking at Figure 8, we can see that microsomal Fe_x decreases in proportion to the number of times the mouse liver mitochondria are washed. No significant paramagnetic differences exist between the mouse liver and hepatoma mitochondria, once the microsomal contamination has been washed out.

Typical ESR spectra of normal and neoplastic smooth-surfaced and normal and neoplastic rough-surfaced microsomes are shown in Figures 10 and 11, respectively; the protein concentrations of both comparisons are approximately equal. The mouse hepatoma microsomal spectra contain roughly the same ESR signals but at lower magnitude, while a definitely greater intensity in the absorption at g_m=2.00 is seen in the mouse hepatoma rough microsomes.

The changes in signal height per mg. microsomal protein at the various g-values are given in Table 2. One "unit" of signal height was arbitrarily chosen as 1 cm. of recorder-pen deviation at 1000 gain. Protein concentration of the samples ranged between 35 and 70 mg./ml. The hepatoma microsomal Fe_x as measured by the g_m=2.25 signal is 4½ times decreased in the smooth microsomes, and 3½ times decreased in the rough fraction, compared with the corresponding values for normal liver microsomes. In the neoplastic rough microsomes, the microsomal g_m=4.3 signal is 1½ times greater, while the free radical signal at g_m=2.00 is twice as large. The g_m=1.91 signal of smooth hepatoma microsomes is one-third that of the corresponding signal from smooth

microsomes of normal mouse liver. Other differences are not significant at the p = .01 level of confidence (87,88).

The concentrations of several microsomal components determined by chemical analysis are listed in Table 3. Of interest is the relatively large amounts of heme iron other than that accounted for by microsomal cytochrome b_5 in both the normal and cancerous mouse liver microsomal fractions.

Reductive titrations of microsomal Fe_x in normal mouse liver and mouse hepatoma microsomes were studied by ESR in an attempt to elicit any difference in the binding or redox state between normal and neoplastic microsomal Fe_x. As seen in Figure 12, the mouse hepatoma microsomes paralleled the normal liver microsomes in every phase of the experiment; only a large concentration difference was observed. As had been previously observed (61), TPNH was preferred to DPNH in enzymatically reducing microsomal Fe_x.

In Figure 13 the ESR spectrum of oxidized normal mouse liver microsomes is compared to that of enzymatically TPNH-reduced microsomes. In the TPNH-reduced ESR spectrum, the absorptions responsible for microsomal Fe_x are clearly diminished with respect to s_m=2.41 and g_m=2.25, but a discrepancy was repeatedly observed in the s_m=1.91 region. An increase in signal height in this region upon reduction with phosphopyridine nucleotides suggested mitochondrial contamination of the normal mouse liver microsomal fraction (6,7), and numerous experiments were performed to rule this possibility in or out.

Reduced-direct spectrophotometry at liquid nitrogen temperatures

(39) was done on microsomal fractions of rabbit, mouse, beef and rat liver. Figure 14 demonstrates the optical spectra characteristic for microsomes--a predominance of cytochrome $\underline{b_5}$ with twin α-bands at 552 and 558 mu, a β-band at 525 mu and the Soret band at 420 mu. In all microsomal fractions, but especially those of the mouse, a persistent optical peak at 599 mu was observed. To distinguish whether this absorption was due to an $\underline{a}$- or $\underline{a_5}$-type cytochrome, carbon monoxide bubbling and saturation of reduced mouse liver microsomes in the absence of light was carried out. A band at 450 mu was repeatedly produced (91), but the 599-mu peak was not decreased in size.

Normal mouse liver microsomes were carefully examined by electron microscopy for mitochondrial contamination. Figures 15 and 16 are electron micrographs at high magnification which showed no intact mitochondria, or traces of mitochondrial fragments.

Cytochrome oxidase activity, a specific determination for the presence of the mitochondrial electron transport chain, was carried out by Warburg manometry (64). While normal mitochondrial preparations gave values between 50 and 200 ul oxygen consumed/mg. protein/hr., a value of $\underline{7.3}$ ul oxygen/mg. protein/hr. for the normal mouse liver microsomal fraction was obtained. This suggested mitochondrial contamination of 3 to 14%. Cytochrome oxidase kinetics (82) were studied by recording spectrophotometry; a value of $\underline{7.23}$ ul. oxygen consumed/mg. protein/hr. confirmed the data obtained by Warburg manometry. Further calculations showed that the mitochondrial electron transport chain present in the supposedly "pure" mouse liver microsomal fraction

was able to reduce 5.4 mumoles of oxygen/mg. protein/min.

Antimycin A inhibition studies were carried out on the recording spectrophotometer. This technic is a very sensitive test, because antimycin A specifically and completely inhibits the mitochondrial electron transport chain (152). The results of several experiments are summarized in Figure 17, where reduction of exogenous cytochrome c was followed at 550 mu during six minutes' reaction time. Addition of antimycin A to the system partially inhibited the supposedly "pure" mouse liver microsomal fraction, lending strong support to the supposition that mitochondrial electron transport chain contamination is probably present.

C. "Minimal Deviation" Hepatoma and Normal Rat Liver Microsomes

Typical ESR microsomal spectra of normal rat liver, host rat liver and "minimal deviation" hepatoma 5123-B are depicted in Figure 18. As can be seen by the g_m=2.25 signal height, the three- to four-fold concentration decrease in microsomal Fe_x is again apparent in the "minimal deviation" hepatoma. The free radical signal at g_m=2.00, previously twice as large in the more anaplastic mouse hepatoma rough microsomal fraction, is now not statistically different among these three microsomal groups. The hepatoma microsomal manganese (detectable by measuring the ESR signal height at g_m=2.18, the lowest magnetic field strength splitting of the six absorption lines of manganese) is

two-fifths that of normal rat liver microsomes (89).

The significant ESR signal heights per mg. protein are listed in Table 4, where one "unit" was arbitrarily chosen as 1 cm. of recorder-pen deviation at 400 gain. Protein concentrations of the microsomal samples ranged from 38 to 60 mg./ml. In addition to the ESR differences just mentioned, the microsomal acetanilide hydroxylase activity of these three fractions was assayed and found not to differ statistically. When the reduced-direct optical spectra of these three groups were studied at liquid nitrogen temperatures, no significant differences were apparent; the optical spectra are compared in Figure 19.

The three respective rat liver microsomal fractions which were isolated following tryptophan pyrrolase induction were examined by low-temperature ESR technic. The signal heights of microsomal Fe_x, manganese and free radicals were compared in the same method (88,89) of standardizing ESR signal height per mg. microsomal protein. No statistically significant difference was found among the three goups of rat liver microsomes: tryptophan-injected, cortisone-injected and the physiological saline-injected (control) animals.

FIGURE 3. ESR derivative spectra of the various mouse tumors and normal liver and cardiac tissue, all whole-tissue samples. Magnetic field strength in gauss increases from left to right, and the arrows indicate the g-value of the free electron, 2.0023.

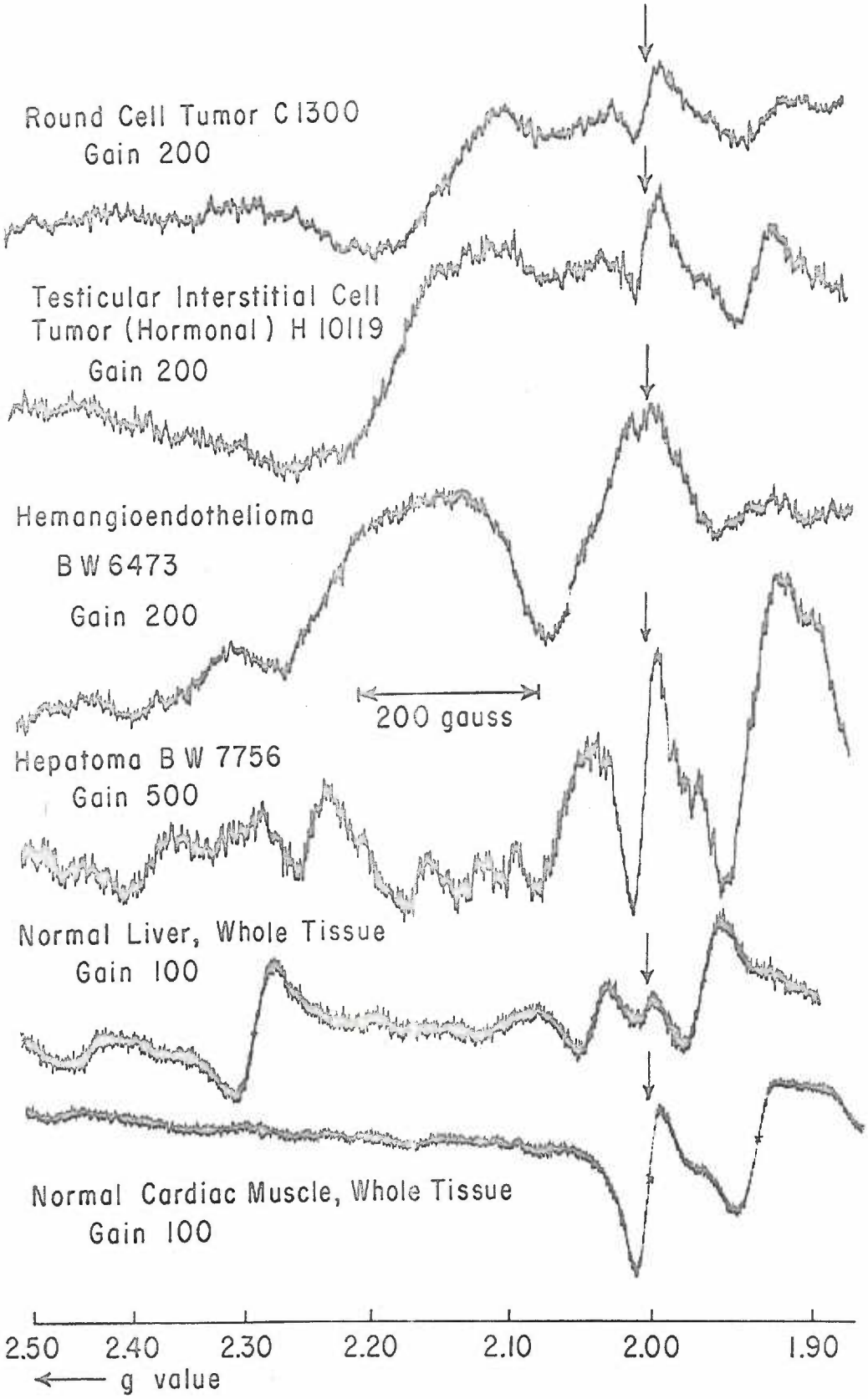
Round Cell Tumor C1300
Gain 200
Testicular Interstitial Cell
Tumor (Hormonal) H 10119
Gain 200
Hemangioendothelioma
B W 6473
Gain 200
200 gauss
Hepatoma B W 7756
Gain 500
Normal Liver, Whole Tissue
Gain 100
Normal Cardiac Muscle, Whole Tissue
Gain 100
2.50
2.40
2.30
2.20
2.10
2.00
1.90
g value

FIGURE 4. ESR derivative spectra of the various mouse tumors, whole-tissue samples. Magnetic field strength in gauss increases from left to right, and the arrows indicate the g-value of the free electron, 2.0023.

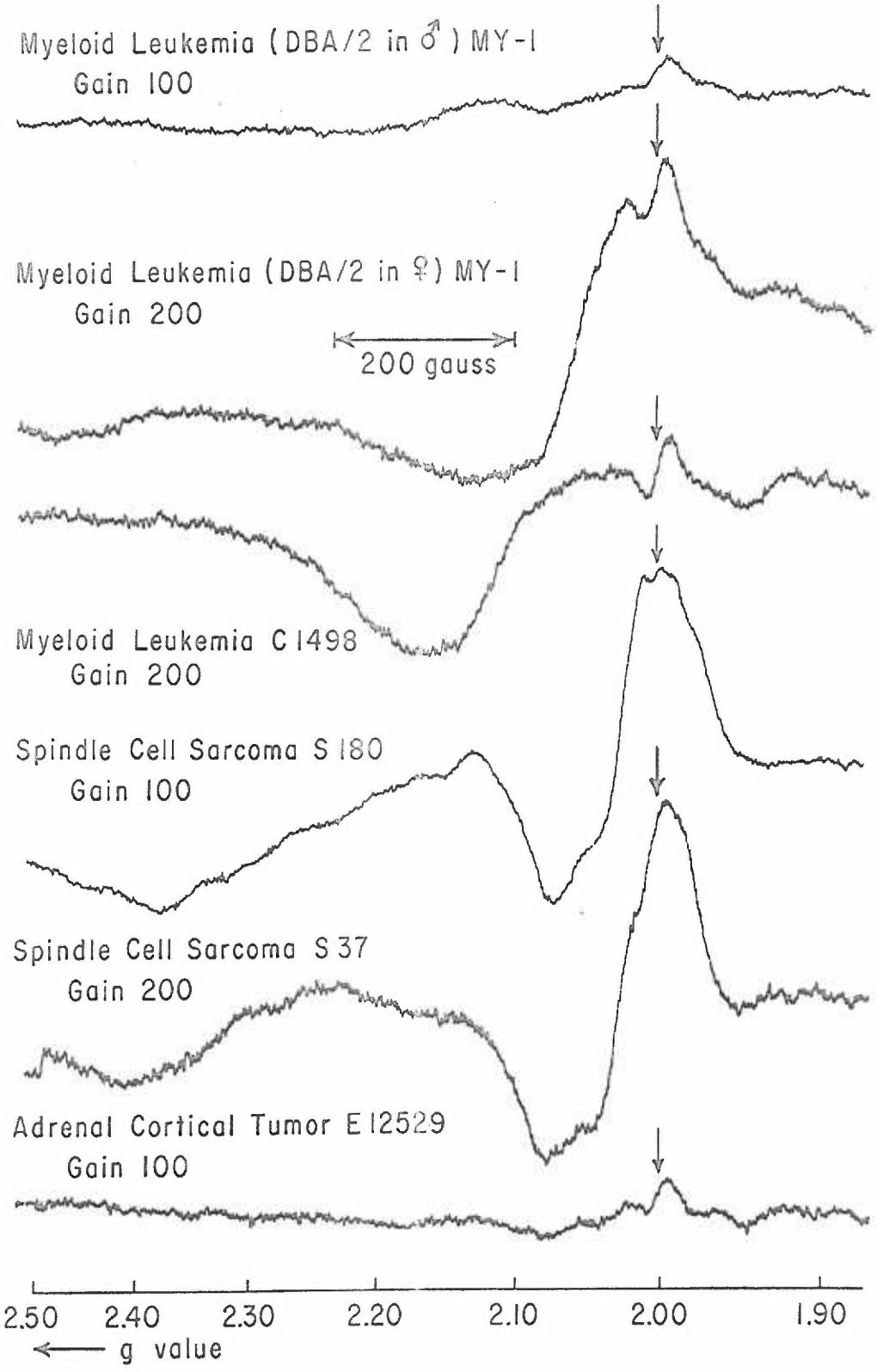
Myeloid Leukemia (DBA/2 in ♂) MY-1
Gain 100
Myeloid Leukemia (DBA/2 in ♀) MY-1
Gain 200
200 gauss
Myeloid Leukemia C1498
Gain 200
Spindle Cell Sarcoma S180
Gain 100
Spindle Cell Sarcoma S37
Gain 200
Adrenal Cortical Tumor E12529
Gain 100
2.50
2.40
2.30
2.20
2.10
2.00
1.90
g value

FIGURE 5. ESR derivative spectra of the various mouse tumors, whole-tissue samples. Magnetic field strength in gauss increases from left to right, and the arrows indicate the g-value of the free electron, 2.0023.

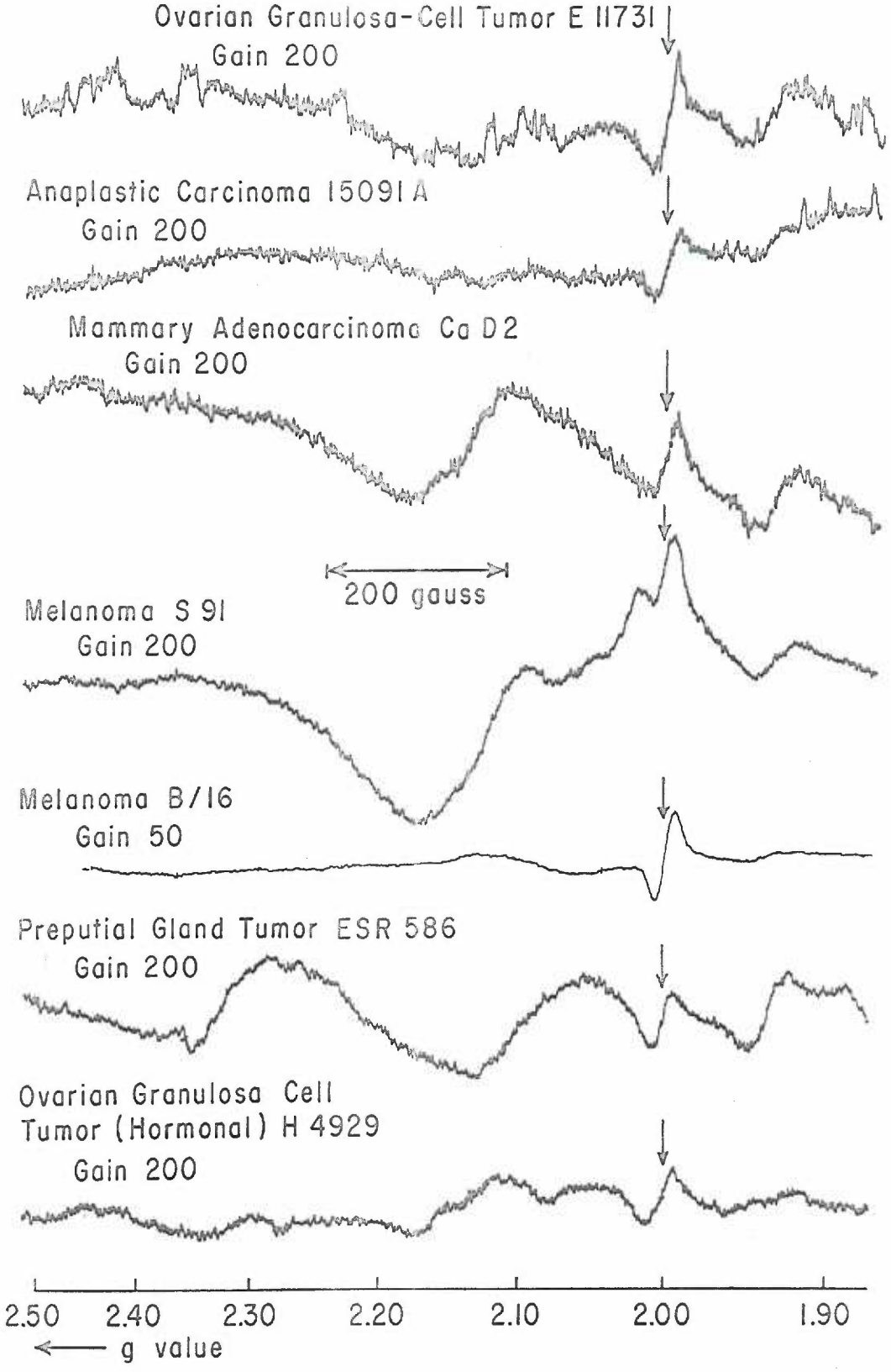
Ovarian Granulosa-Cell Tumor E 11731
Gain 200
Anaplastic Carcinoma 15091 A
Gain 200
Mammary Adenocarcinoma Ca D2
Gain 200
200 gauss
Melanoma S 91
Gain 200
Melanoma B/16
Gain 50
Preputial Gland Tumor ESR 586
Gain 200
Ovarian Granulosa Cell
Tumor (Hormonal) H 4929
Gain 200
2.50
2.40
2.30
2.20
2.10
2.00
1.90
g value

FIGURE 6. ESR derivative spectra of the various mouse tumors, whole-tissue samples. Magnetic field strength in gauss increases from left to right, and the arrows indicate the g-value of the free electron, 2.0023.

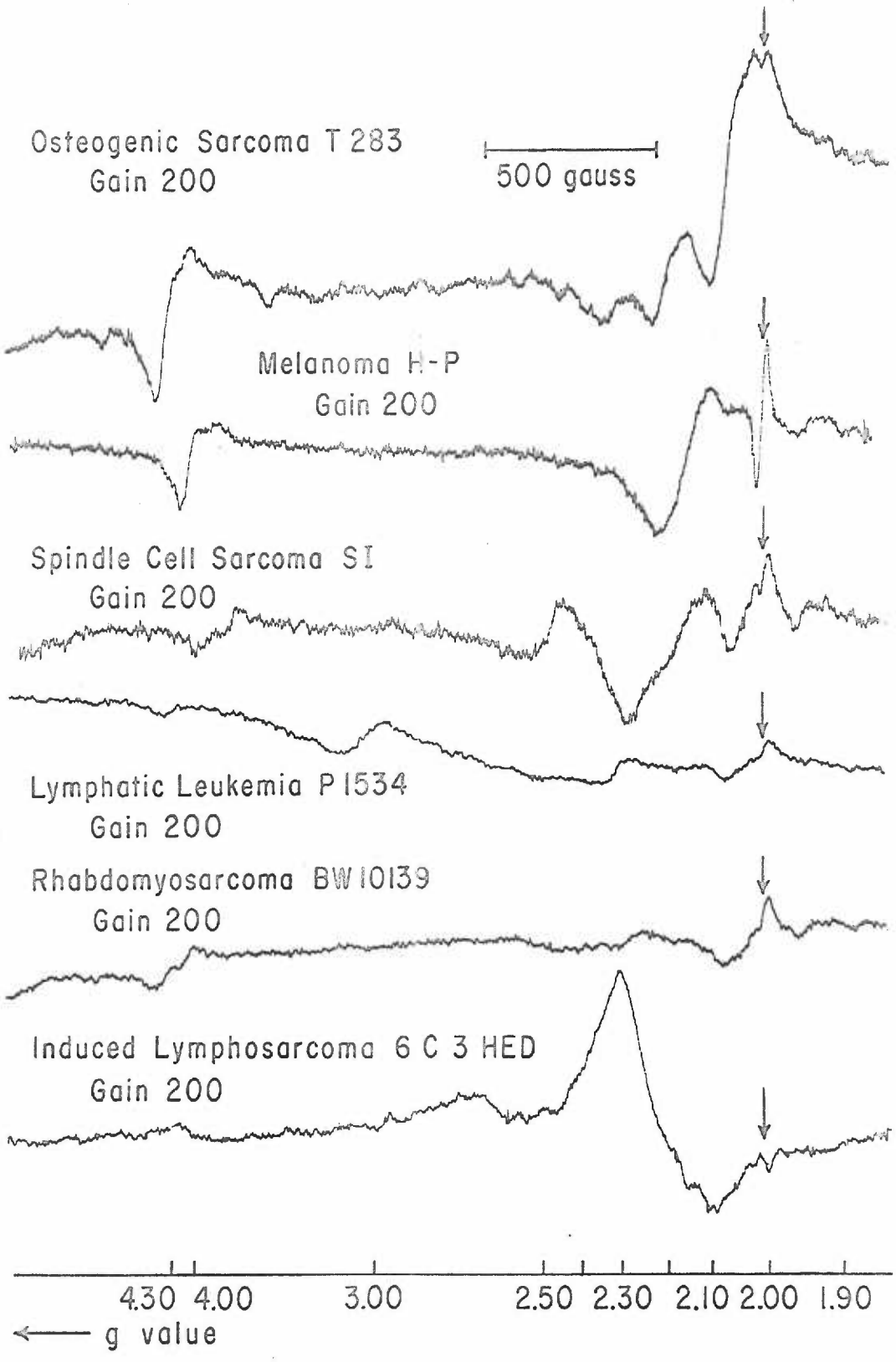
Osteogenic Sarcoma T 283
Gain 200
500 gauss
Melanoma H-P
Gain 200
Spindle Cell Sarcoma SI
Gain 200
Lymphatic Leukemia P 1534
Gain 200
Rhabdomyosarcoma BW 10139
Gain 200
Induced Lymphosarcoma 6 C 3 HED
Gain 200
4.30 4.00 3.00 2.50 2.30 2.10 2.00 1.90
g value

FIGURE 7. ESR derivative spectra of the various mouse tumors, whole-tissue samples. Magnetic field strength in gauss increases from left to right, and the arrows indicate the g-value of the free electron 2.0023.

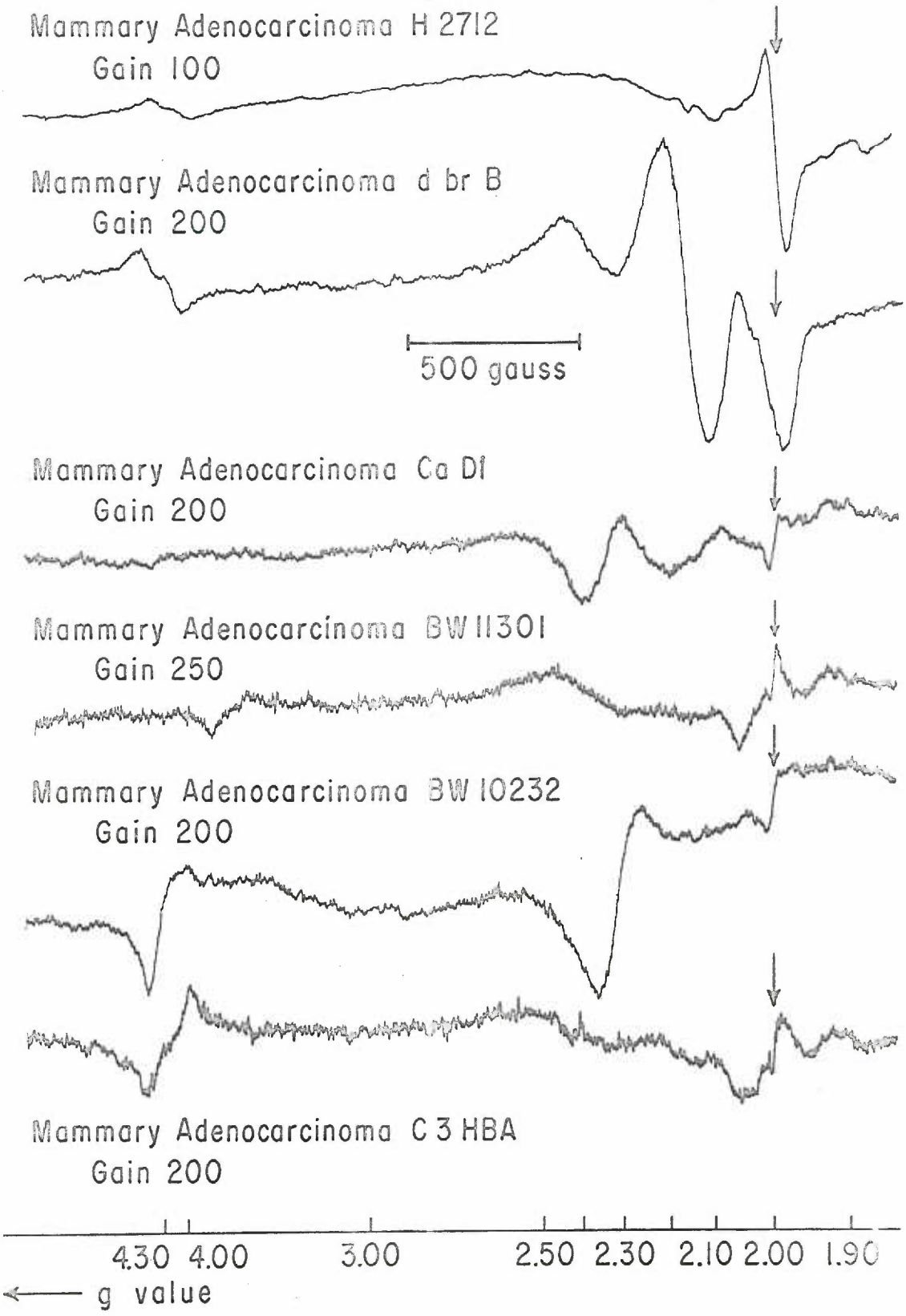
Mammary Adenocarcinoma H 2712
Gain 100
Mammary Adenocarcinoma d br B
Gain 200
500 gauss
Mammary Adenocarcinoma Ca DI
Gain 200
Mammary Adenocarcinoma BW 11301
Gain 250
Mammary Adenocarcinoma BW 10232
Gain 200
Mammary Adenocarcinoma C 3 HBA
Gain 200
4.30 4.00 3.00 2.50 2.30 2.10 2.00 1.90
g value

FIGURE 8. ESR derivative spectra of mitochondrial fractions, of normal mouse liver (A) and of hepatoma (B) washed twice with isotonic sucrose; ESR derivative spectra of the same normal liver mitochondria (C) and hepatoma mitochondria (D) after six such washings. Magnetic field strength increases from left to right, and the g-values of importance are designated by arrows.

Protein concentrations of the four samples are all about 50 mg./ml., as determined by the biuret method.

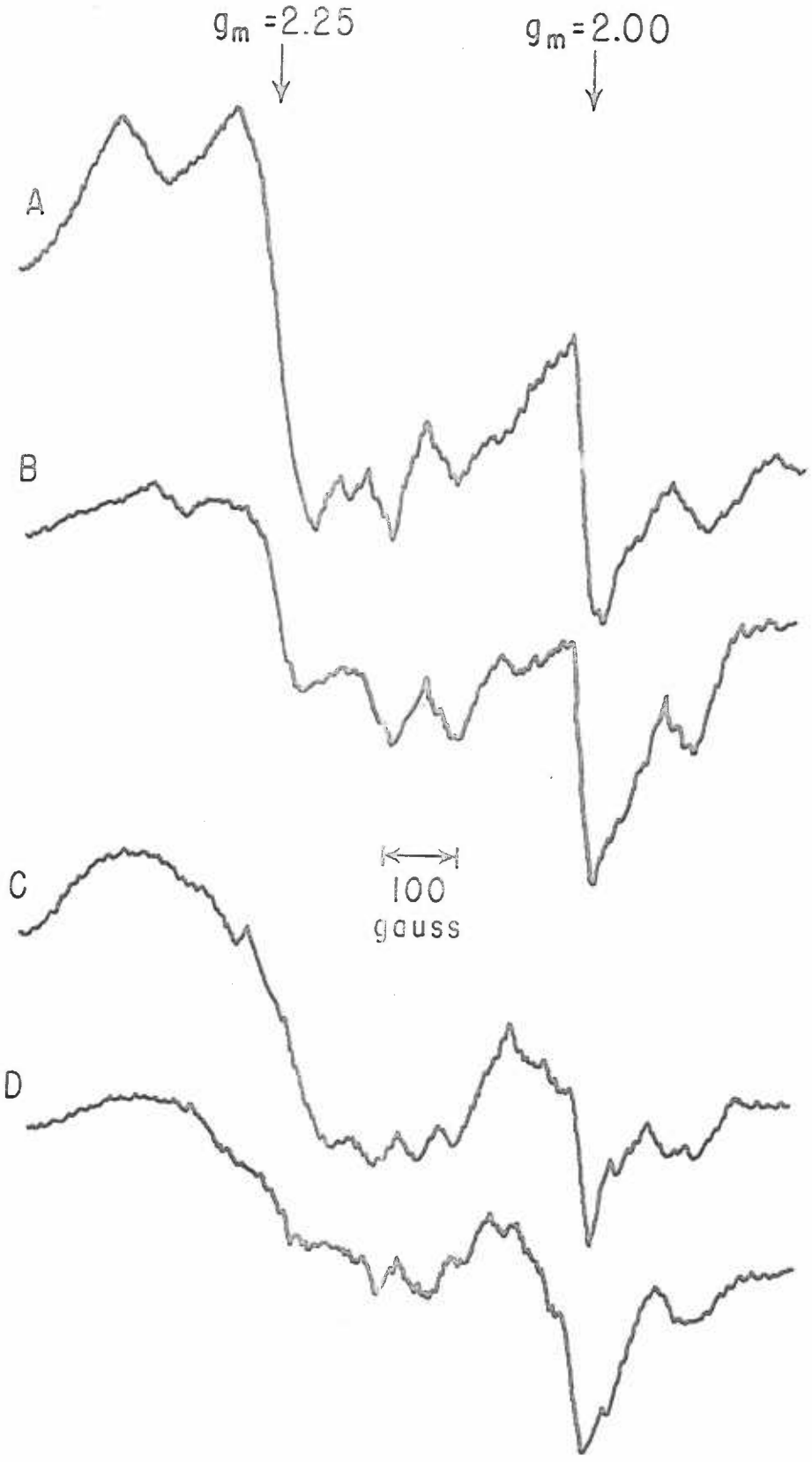
g_m = 2.25
g_m = 2.00
A
B
C
D
100
gauss

FIGURE 9. The theoretical ESR derivative spectrum of microsomal Fe_x with the characteristic absorptions at $g_{\perp}$=2.25, and s_m=2.41 and 1.91. The octahedral configuration of this heme protein results in this asymmetric ESR spectrum of microsomal Fe_x in the frozen state, and g-values for both parallel and perpendicular orientation are illustrated. Magnetic field strength increases from left to right.

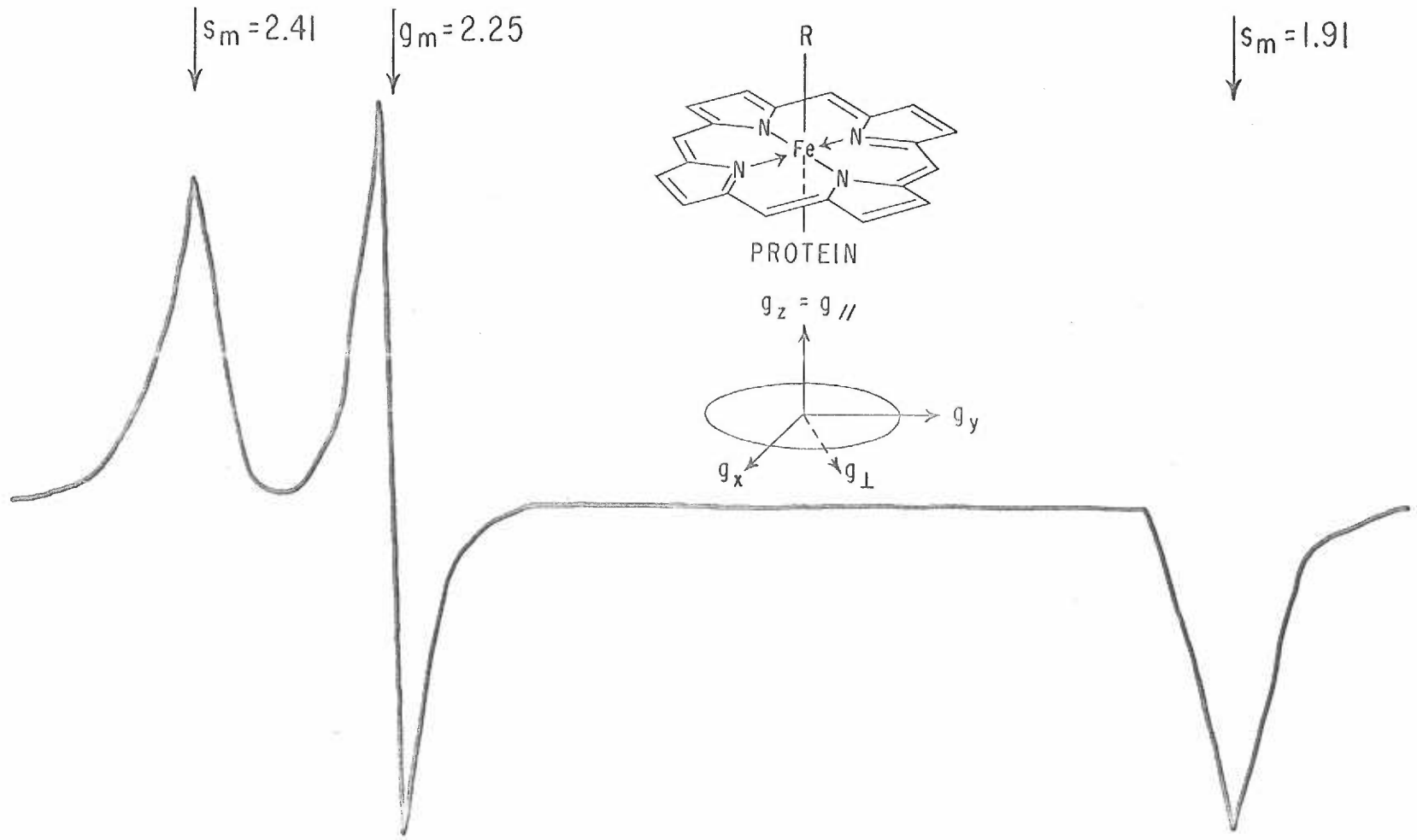
$s_m = 2.41$
$g_m = 2.25$
$s_m = 1.91$
R
N
Fe
N
N
N
PROTEIN
$g_z = g_{//}$
g_y
g_x
$g_\perp$

FIGURE 10. ESR derivative spectra of normal (A) and neoplastic (B) mouse liver smooth-surfaced microsomes. Protein concentration in these two samples is approximately equal, around 50 mg./ml. Magnetic field strength increases from left to right, and g-values of importance are designated by arrows.

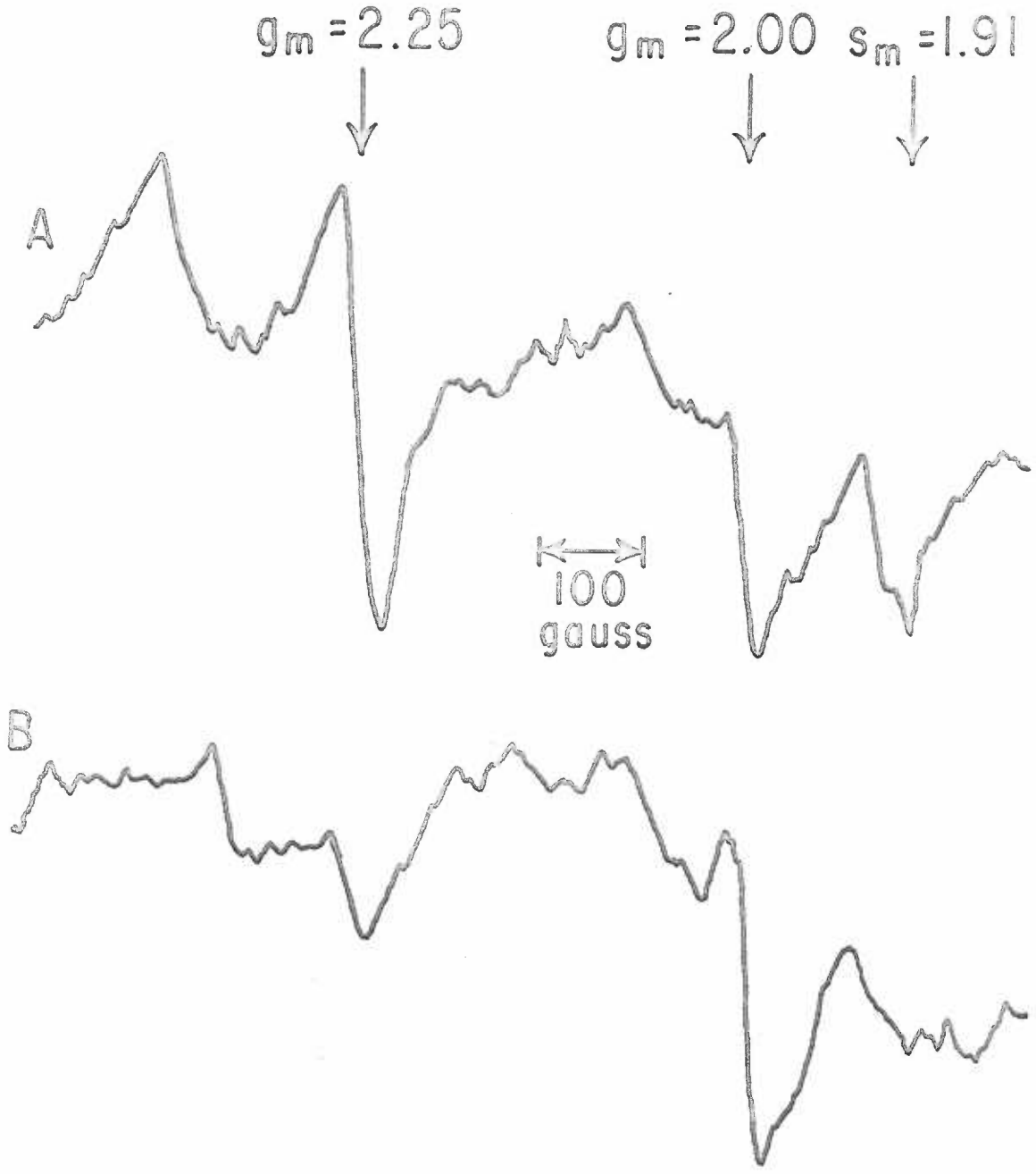
$g_m = 2.25$
$g_m = 2.00$
$s_m = 1.91$
A
100
gauss
B

FIGURE 11. ESR derivative spectra of normal (A) and neoplastic (B) mouse liver rough-surfaced microsomes. Protein concentration in these two samples is approximately equal, around 55 mg./ml. Magnetic field strength increases from left to right, and g-values of importance are designated by arrows.

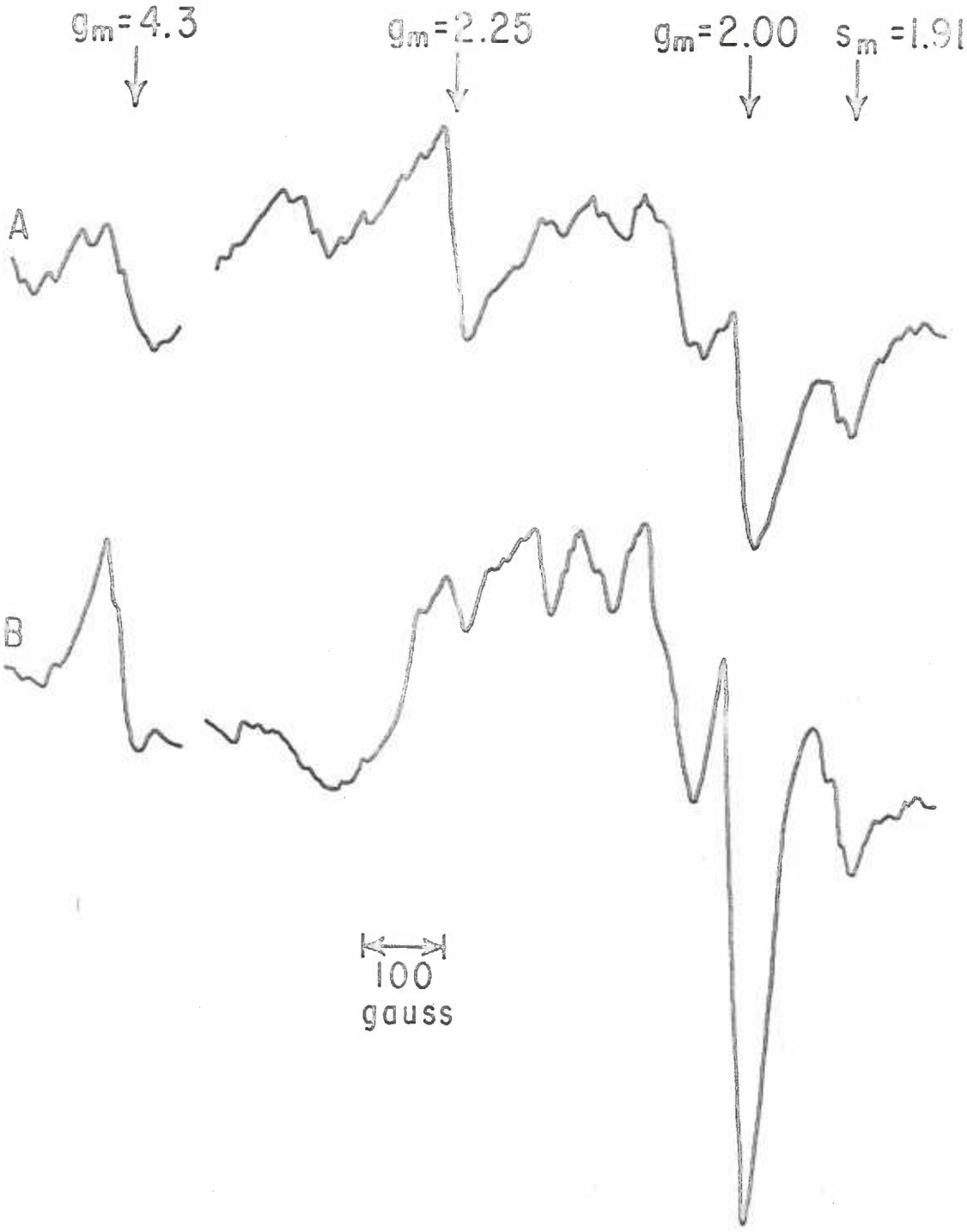
$g_m = 4.3$
$g_m = 2.25$
$g_m = 2.00$
$s_m = 1.91$
A
B
100
gauss

TABLE 2. The ESR signal intensities of mouse liver and mouse hepatoma microsomes, per mg. microsomal protein. The g_m=4.3 signal is concerned with ferric (high-spin) iron in the microsomes, the g_m=2.00 signal measures the free radical content, and the g_m=2.25 and s_m=1.91 signals are measurements of microsomal Fe_x absorption.

Tissue	Signal	Signal Height Centimeters at Gain 1000 Per Milligram Protein Smooth Fraction N samples*	Mean	S.D.	Rough Fraction N samples*	Mean	S.D.
Liver	$g_m = 4.3$	—	—	—	22	0.33	0.12
Hepatoma		—	—	—	16	0.52	0.16
Liver	$g_m = 2.25$	15	0.98	0.53	22	0.64	0.28
Hepatoma		14	0.23	0.16	15	0.18	0.26
Liver	$g_m = 2.00$	15	0.51	0.27	22	0.51	0.30
Hepatoma		14	0.48	0.21	16	1.01	0.21
Liver	$s_m = 1.91$	15	0.31	0.13	22	0.20	0.12
Hepatoma		13	0.10	0.03	16	0.18	0.07

*Samples of 0.20 ml. were taken from two or three separate preparations of mouse liver or hepatoma microsomes, where each preparation was made up of pooled tissues of six to ten mice. Thus, each mean value represents normal or neoplastic microsomes of twelve to thirty mice.

TABLE 3. Chemical analyses of the smooth- and rough-surfaced microsomal fractions of normal mouse liver and mouse hepatoma.

Microsomal Fraction	Total Fe[a]	Heme Fe[b]	Total Fe / Heme Fe ratio	Non-Heme Fe	Cyto-chrome b_5	Heme Fe other than Cyt. b_5
SMOOTH						
Normal liver	6.1	0.67	9.1	5.5	0.25	0.42
Hepatoma	6.3	0.77	8.2	5.5	0.16	0.61
ROUGH						
Normal liver	10.5	1.00	10.2	9.4	0.17	0.83
Hepatoma	7.3	0.69	10.6	6.6	0.12	0.57

[a] Total iron and non-heme iron values are in terms of mμatoms/mg. protein.

[b] Heme iron and cytochrome b_5 values are in terms of mμmoles/mg. protein.

FIGURE 12. The reductive titration experiments with normal mouse liver and hepatoma microsomes. Addition of DPNH or TPNH to the smooth-surfaced microsomal fractions resulted in the enzymatic reduction of microsomal Fe_x, measured by the g_m=2.25 signal height. When the anaerobic system was then exposed to air, reoxygenation would occur, with oxidation of microsomal Fe_x back to the paramagnetic ferric form.

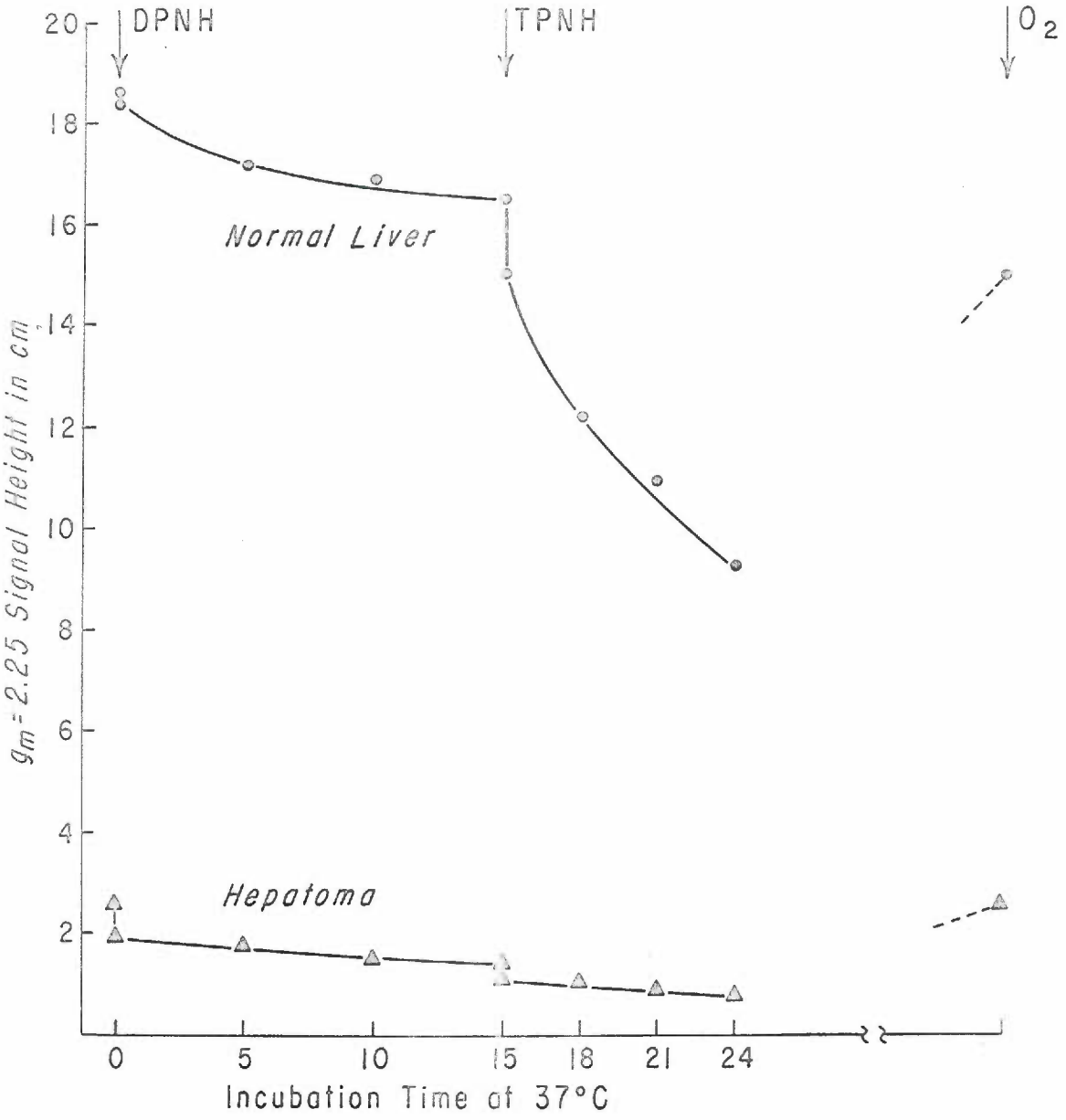
DPNH
TPNH
O_2
Normal Liver
Hepatoma
g_m=2.25 Signal Height in cm
20
18
16
14
12
10
8
6
4
2
0
5
10
15
18
21
24
Incubation Time at 37°C

FIGURE 13. ESR derivative spectra of the same sample of mouse liver rough-surfaced microsomes--oxidized and enzymatically reduced by TPNH addition and incubation. Magnetic field strength increases from left to right, and g-values of importance are designated.

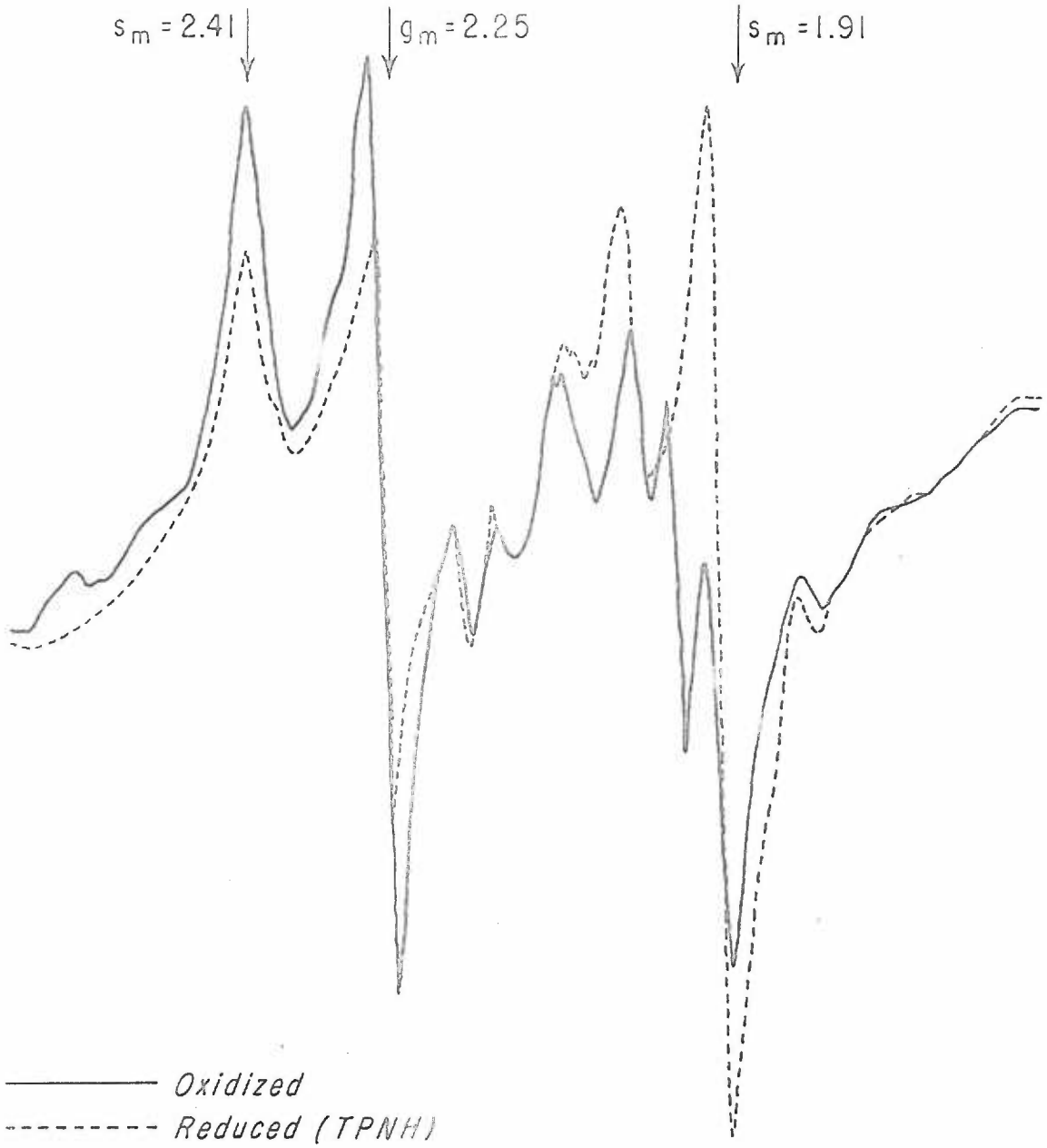
$s_m = 2.41$
$g_m = 2.25$
$s_m = 1.91$
Oxidized
Reduced (TPNH)

FIGURE 14. Reduced-direct optical spectra of liver microsomes of rabbit, mouse, beef and rat at liquid nitrogen temperatures. The smooth-surfaced microsomal fractions were used in the case of rabbit and mouse liver spectra, while the combined smooth- and rough-surfaced fraction was used in the case of beef and rat liver preparations.

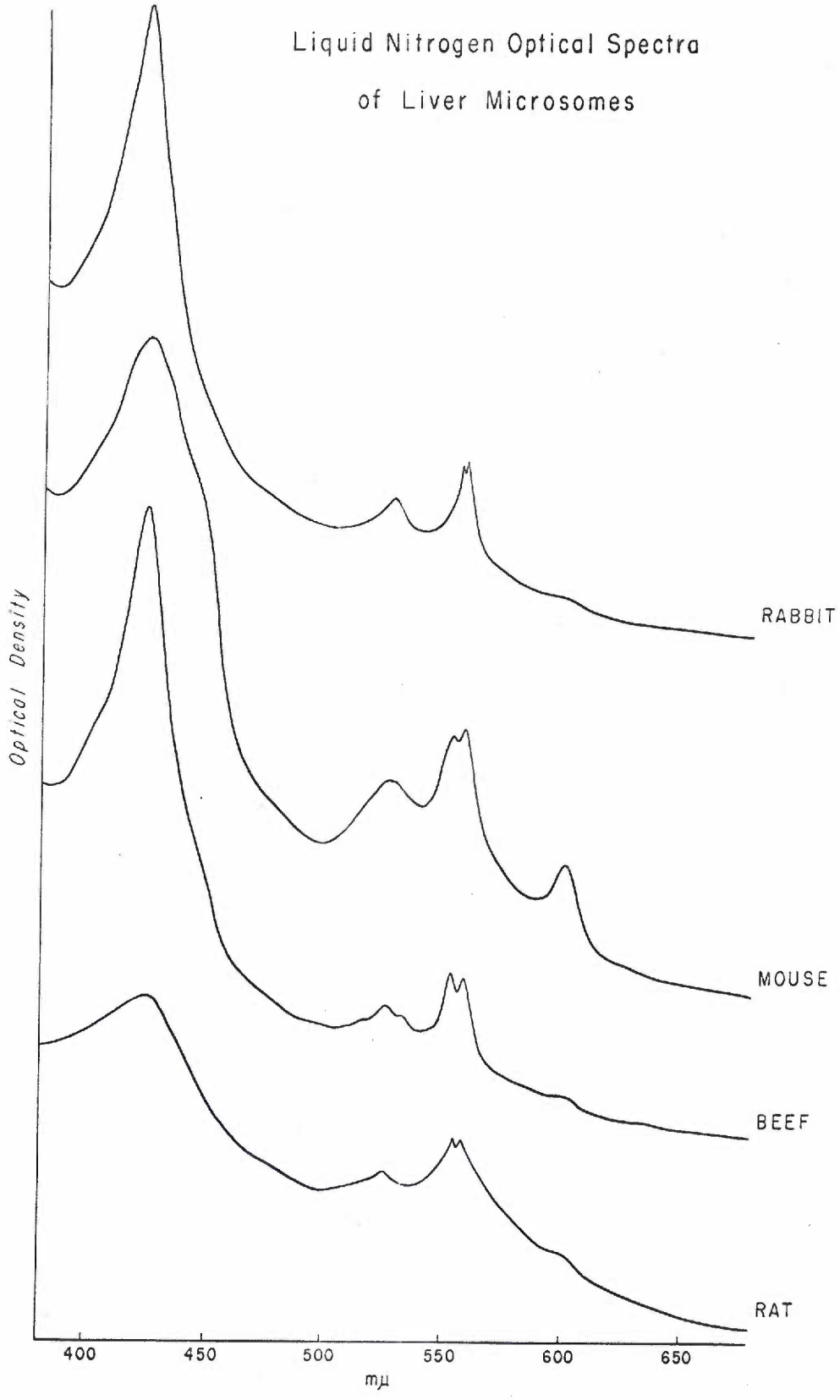
Liquid Nitrogen Optical Spectra
of Liver Microsomes
Optical Density
RABBIT
MOUSE
BEEF
RAT
400
450
500
550
600
650
mμ

FIGURE 15. Electron micrograph of normal mouse liver rough-surfaced microsomal fraction, fixed with 1% osmium tetroxide and stained with uranylacetate and lead. Magnification 45,000X. This micrograph was taken through the generosity of Dr. Kakefuda, City of Hope Research Center, Duarte, California.

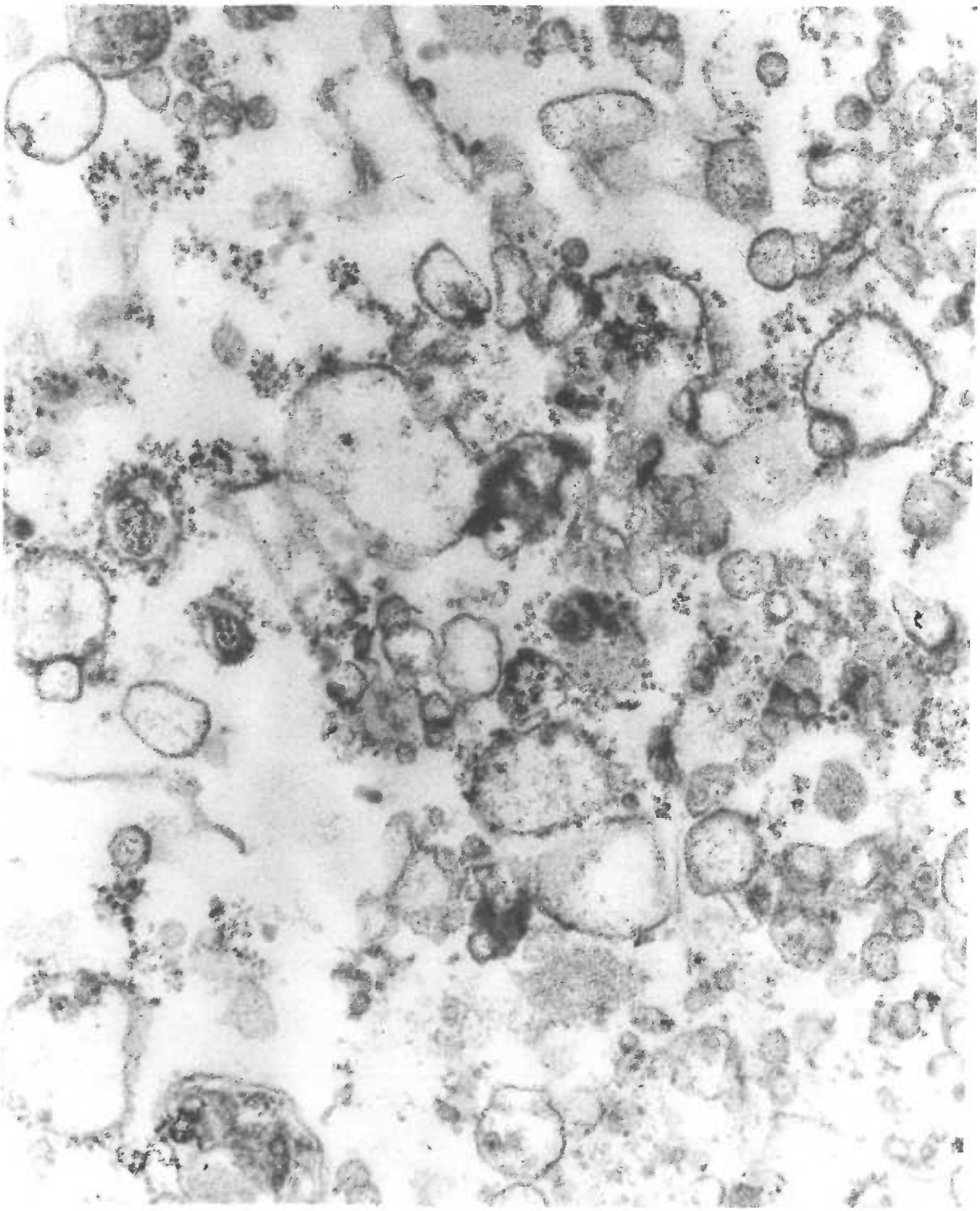

FIGURE 16. A second electron micrograph of normal mouse liver rough-surfaced microsomal fraction, fixed with 1% osmium tetroxide and stained with uranylacetate and lead. Magnification 45,000X. This micrograph was taken through the generosity of Dr. Kakefuda, City of Hope Research Center, Duarte, California.

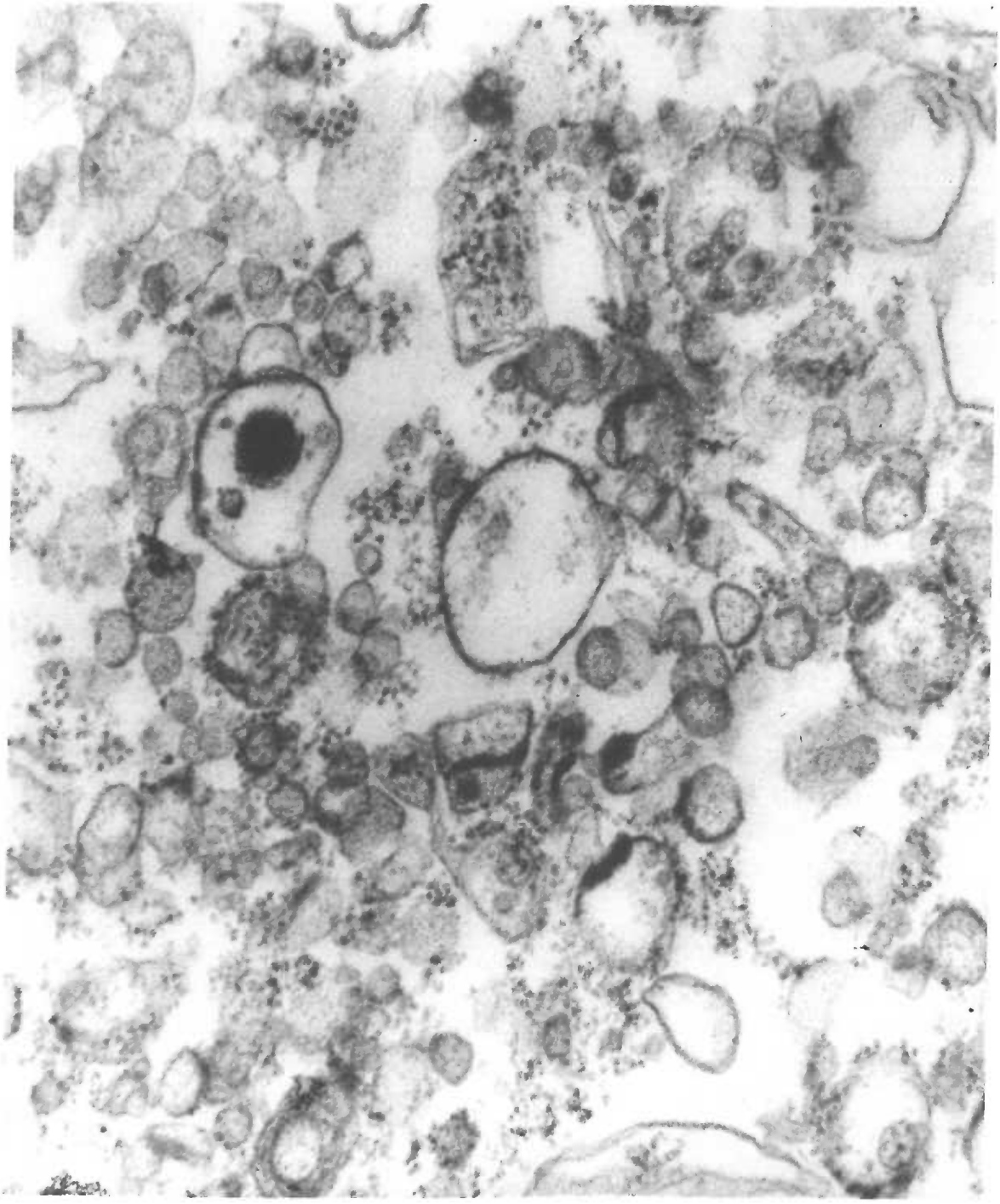

FIGURE 17. Antimycin A inhibition studies of supposedly "pure" mouse liver rough-surfaced microsomal fraction. Microsomal respiration is followed spectrophotometrically by observing the rate of reduction of exogenous cytochrome c at 550 mu.

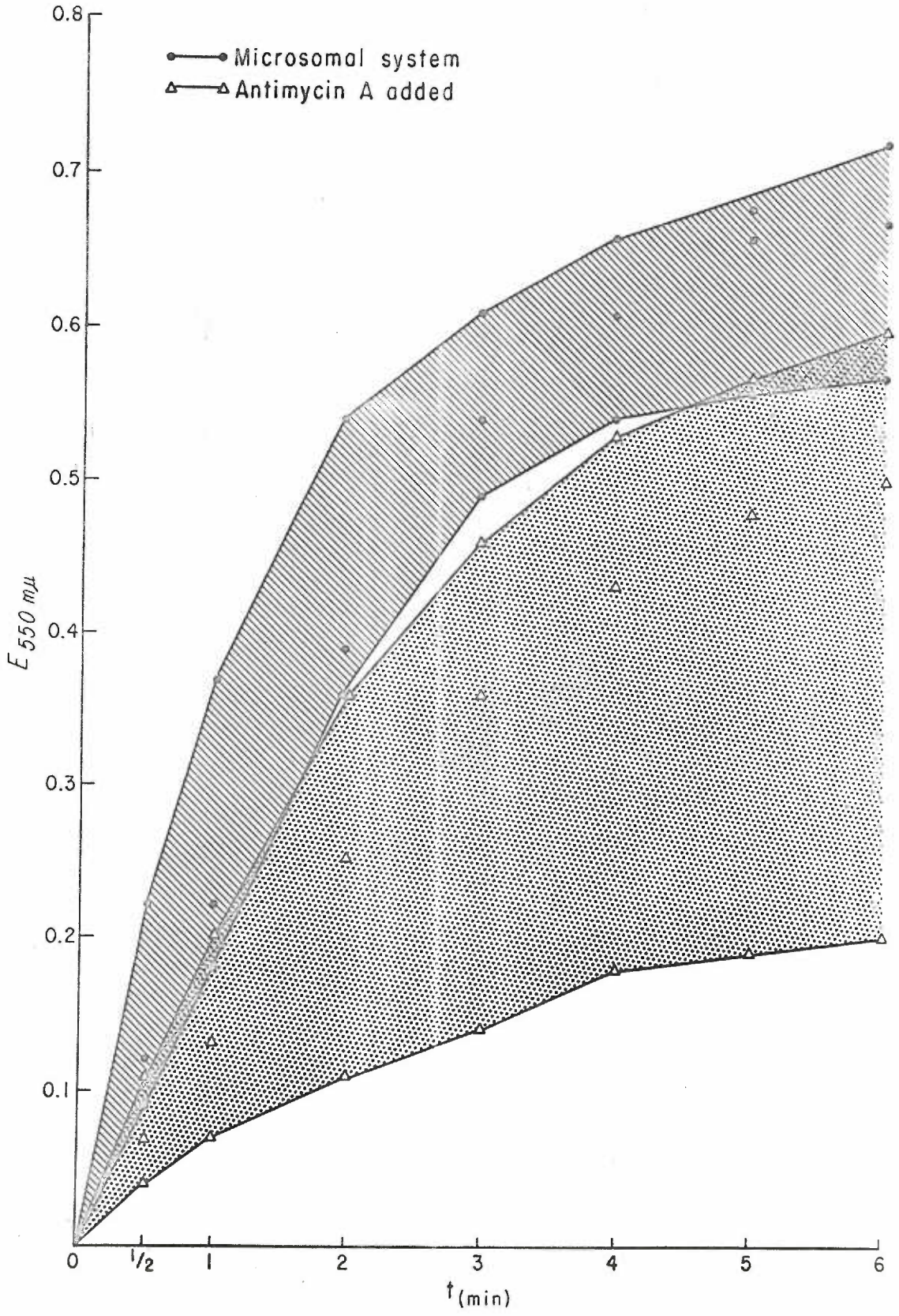
Microsomal system
Antimycin A added
0.8
0.7
0.6
0.5
0.4
0.3
0.2
0.1
$E_{550\,m\mu}$
0
1/2
1
2
3
4
5
6
t (min)

FIGURE 18. ESR derivative spectra of normal rat liver, host rat liver, and "minimal deviation" hepatoma 5123-B, microsomal fractions. Protein concentrations were 51, 41 and 57 mg./ml., respectively. Magnetic field strength increases from left to right, and g-values of importance are designated.

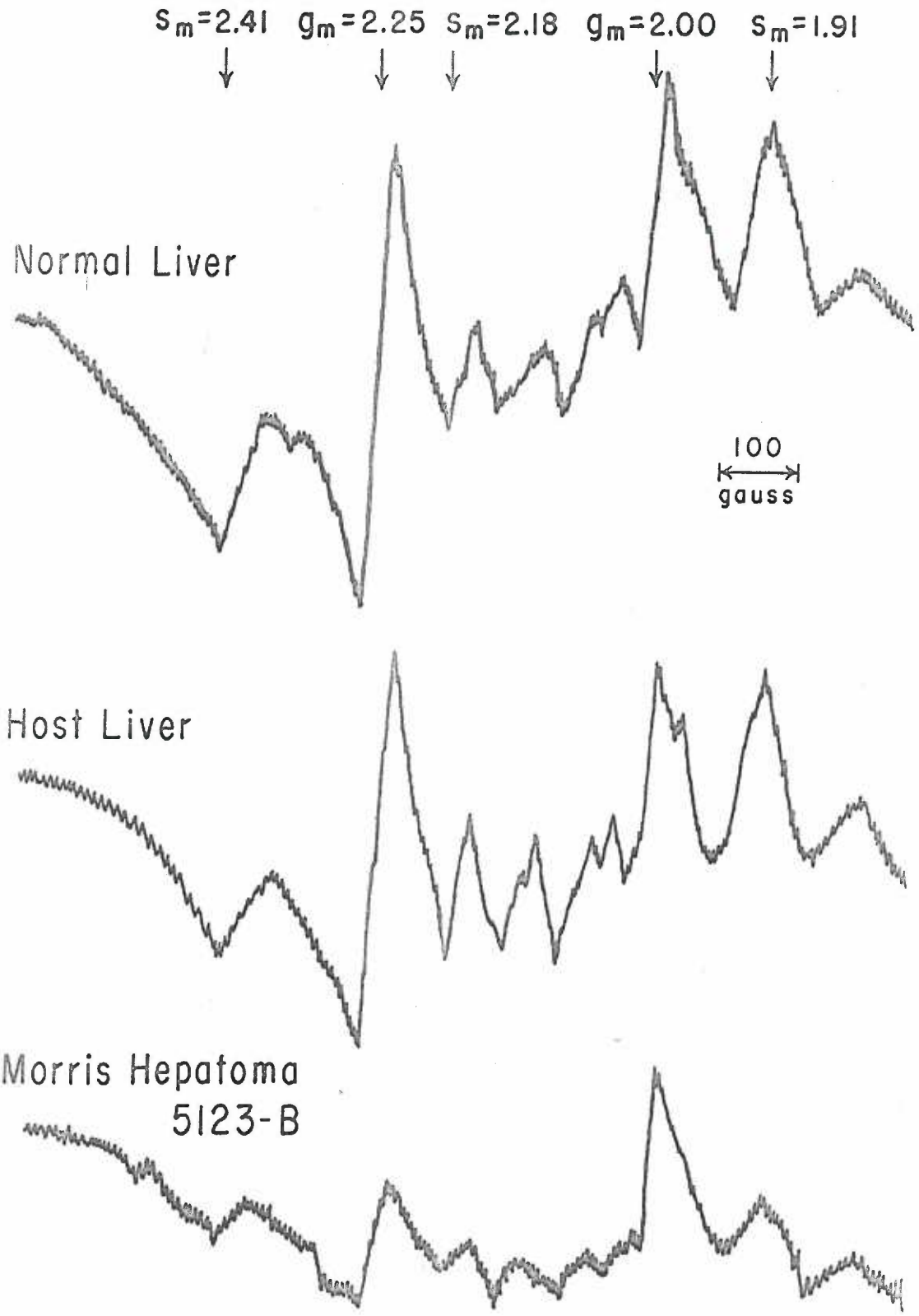
s_m=2.41
g_m=2.25
s_m=2.18
g_m=2.00
s_m=1.91
Normal Liver
100
gauss
Host Liver
Morris Hepatoma
5123-B

TABLE 4. The ESR signal intensities and acetanilide hydroxylase activity of normal rat liver, host rat liver, and "minimal deviation" hepatoma 5123-B, microsomal fractions, per mg. protein. The mean value represents the average of twenty microsomal samples.

MICROSOMAL PREPARATIONS

		Normal Rat Liver	Host Rat Liver	Morris Hepatoma 5123-B
Microsomal Fe_x ($g_m = 2.25$)	Mean	.452*	.396	.144
	S.E.	.013	.016	.008
Microsomal Mn^{++} ($s_m = 2.18$)	Mean	.112	.114	.045
	S.E.	.012	.003	.004
Free Radical Content ($g_m = 2.00$)	Mean	.178	.181	.165
	S.E.	.011	.029	.011
Acetanilide Hydroxylase Activity	Mean	20.3**	17.1	20.7
	S.E.	2.1	1.0	3.2

* ESR signal height in mm pen deviation / mg protein

** Enzyme activity in mμmoles acetanilide hydroxylated / mg nitrogen / minute

FIGURE 19. Reduced-direct optical spectra of microsomal fractions of normal rat liver, host rat liver and hepatoma 5123-B. Protein concentration was 15 mg./ml. in all three cases.

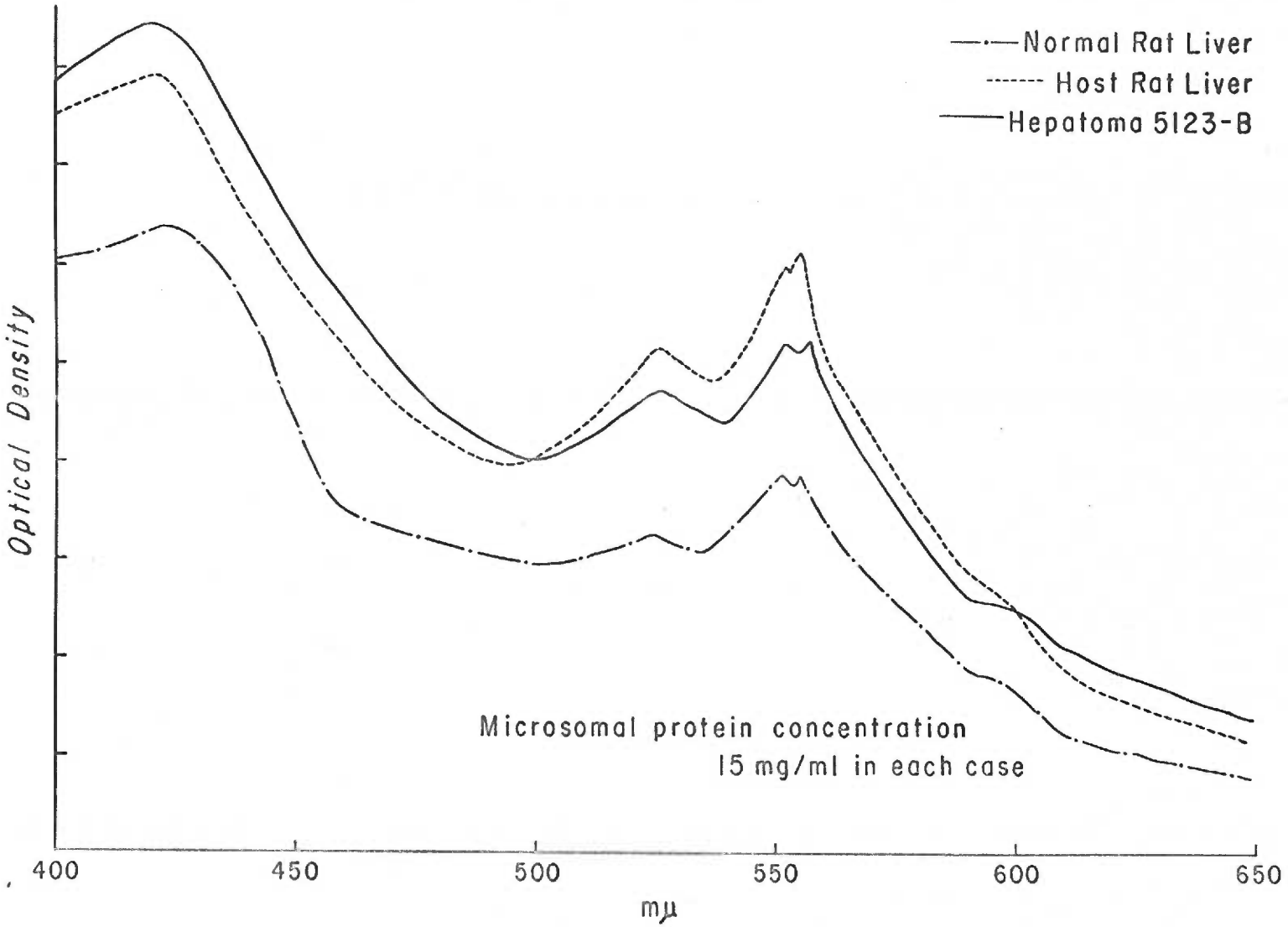
Normal Rat Liver
Host Rat Liver
Hepatoma 5123-B
Optical Density
Microsomal protein concentration
15 mg/ml in each case
400
450
500
550
600
650
mμ

D. Microsomal Manganese Isolation

After trypsin digestion and Emasol treatment as outlined in Figure 2, the pale yellow aqueous phase was found to have a six-fold increase in microsomal manganese; this was determined by the s_m=2.18 ESR signal height/mg. protein. Further treatment with sodium choleate extracted more microsomal manganese from the sediment, so that the second aqueous fraction had a two-fold increase in microsomal manganese, when compared to the starting material.

A typical low-temperature ESR derivative spectrum of beef liver microsomes with a concentration of 53.5 mg. protein/ml. is depicted in Figure 20 A. The ESR spectrum of the aqueous phase of microsomal manganese after trypsin digestion and Emasol treatment is shown in Figure 20 B; the protein concentration is 5 mg./ml.

Further characterization of this aqueous microsomal manganese fraction has not been carried out. Reduced-direct spectrophotometry at liquid nitrogen temperatures (39) gave no interesting information. The manganous ion could be separated from its protein moiety by passing the microsomal manganese fraction through Chelex or Sephadex G-25 chromatography columns; ESR analysis of the concentrated protein after passage through these columns showed loss of the characteristic low-temperature manganous ion signal.

Microsomal respiration was found not to require manganous ions. The presence of 1 mM manganous chloride added to Strittmatter's

system (132), as measured by reduction of exogenous cytochrome c, repeatedly inhibited rather than enhanced the oxidation-reduction activity of the microsomal electron transport system.

E. Inorganic Manganese Studies

Typical low-temperature and room-temperature ESR spectra of various manganous compounds and complexes are summarized in Figure 21. In each case, the manganous ion concentration is 10^{-3} M. When compared to the characteristic manganous six-line absorption at room temperature, the differences in the low-temperature curves are obvious. The manganous cyanide complex is an exception, where no signal is seen at either -180° C. or room temperature.

Hydrochloric acid was added to a constant concentration of 10^{-3} M manganous chloride; the resulting ESR low-temperature spectra are depicted in Figure 22. As the Cl^{-}/Mn^{++} ratio increases and the pH drops, the manganese spectra demonstrate not only the characteristic broad signal superimposed on an increasing six-line spectrum, but resolution of hyperfine structure among the six lines becomes apparent. This same phenomenon is seen when lithium chloride or sodium chloride is added to manganous chloride, sulfuric acid or excess sulfate ion is added to manganous sulfate, or phosphoric acid or excess phosphate ion is added to manganous phosphate (4).

Addition of water to a relatively "water-free" alcohol solution

tends to also increase the hyperfine resolution of the low-temperature six-line manganese signal. The effect of adding water to a relatively "water-free" solution of manganous chloride dissolved in N,N-dimethylformamide is seen in Figure 23. There is an apparent increased resolution and overall signal height, when water is added.

The effect of proteins of varying molecular weight on the manganous low-temperature ESR signal is seen in Figure 24. Proteins of 10^{-3} M concentration were each dissolved in aqueous solutions of 10^{-3} M manganous chloride. Molecular weight varied from 5,600 for protamine sulfate (salmine) to 67,000 for bovine albumin; the other proteins used were cytochrome c, β-lactoglobulin and ovalbumin. Increased hyperfine splitting is apparent as the manganous ion is associated with protein molecules of increasing size. This hyperfine resolution of the ESR signal seems to be associated with the surface area of the protein molecule, as illustrated in Figure 25, where the same surface area of three different proteins was exposed to the same concentration of manganous ion.

The experimental phosphoric acid titration curve, in the absence and presence of 50 umoles of manganous ion, is depicted in Figure 26. The effect of manganese was much less marked when only 10 or 20 umoles of manganous ion was present in the titration mixture. Arrows designate the points along the titration curve at which microsamples of solution were taken for low-temperature ESR analysis.

The ESR spectra of these microsamples are shown in Figure 27. The phosphate anion species which, in association with the manganous

ion, is responsible for the low-temperature six-line spectrum is decreased in sample D and disappears altogether in sample E. The superimposed broad signal, which has a peak-to-peak line width of almost 600 gauss in samples A, B and C, concomitantly disappears with the six-line component in spectra D and E. The broad signal arising in samples F and G has a peak-to-peak line width of about 300 gauss and a different shape, and this signal must represent a different manganous ion-phosphate anion species.

FIGURE 20. Typical low-temperature ESR derivative spectra of beef liver microsomes (A) and the microsomal manganese aqueous fraction (B) after trypsin digestion and Emasol solubilization. Protein concentrations are 53.5 and 5 mg./ml., respectively. Magnetic field strength increases from left to right, and the important g-values are designated.

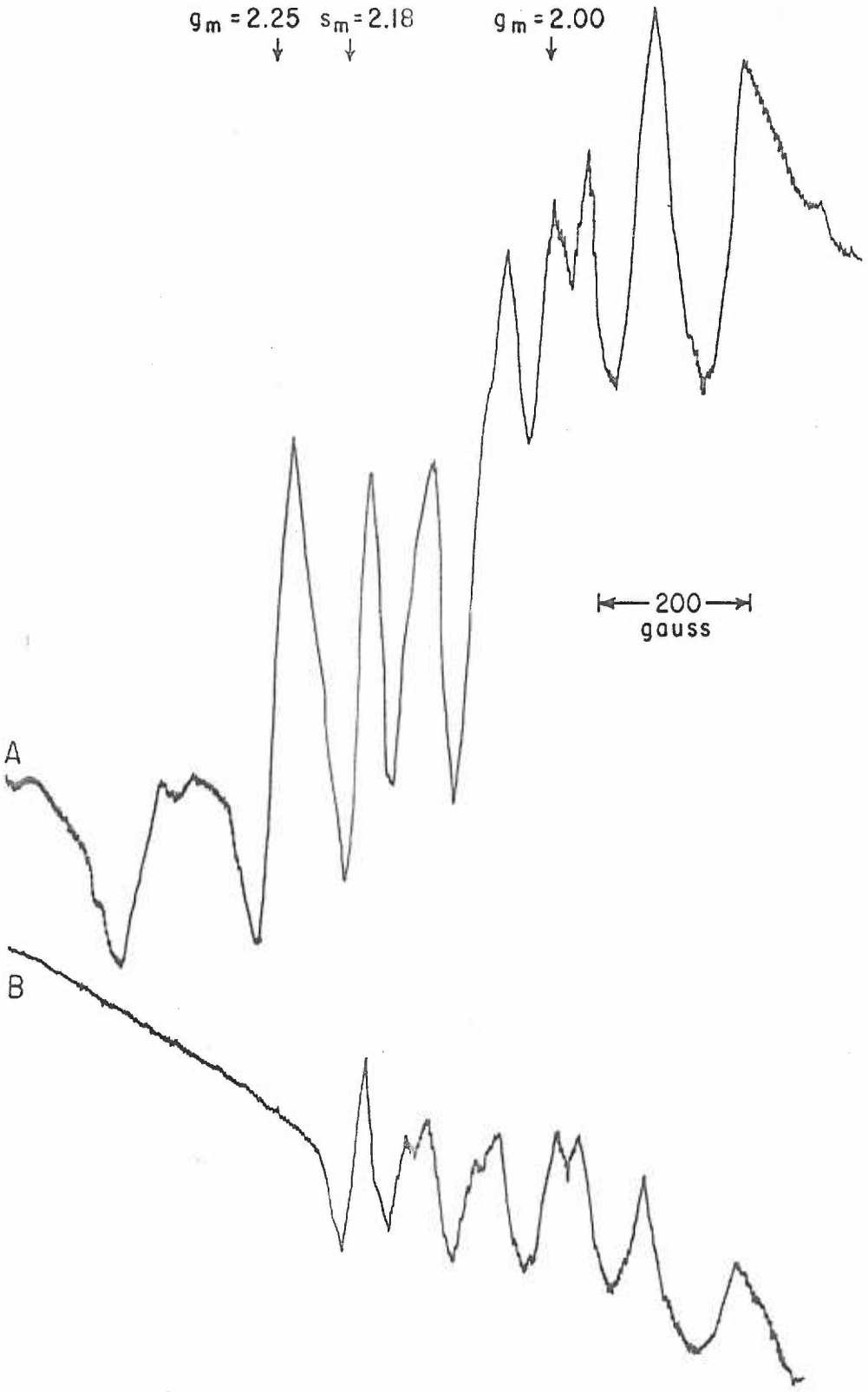
$g_m = 2.25$
$s_m = 2.18$
$g_m = 2.00$
200
gauss
A
B

FIGURE 21. Typical low-temperature and room-temperature ESR derivative spectra of various manganous compounds and complexes, where the manganous ion concentration was always 10^{-3} M. The gains vary from one sample to the next.

Magnetic field strength increases from left to right in all of the spectra, and the 600-gauss signal is always centered at g=2.00.

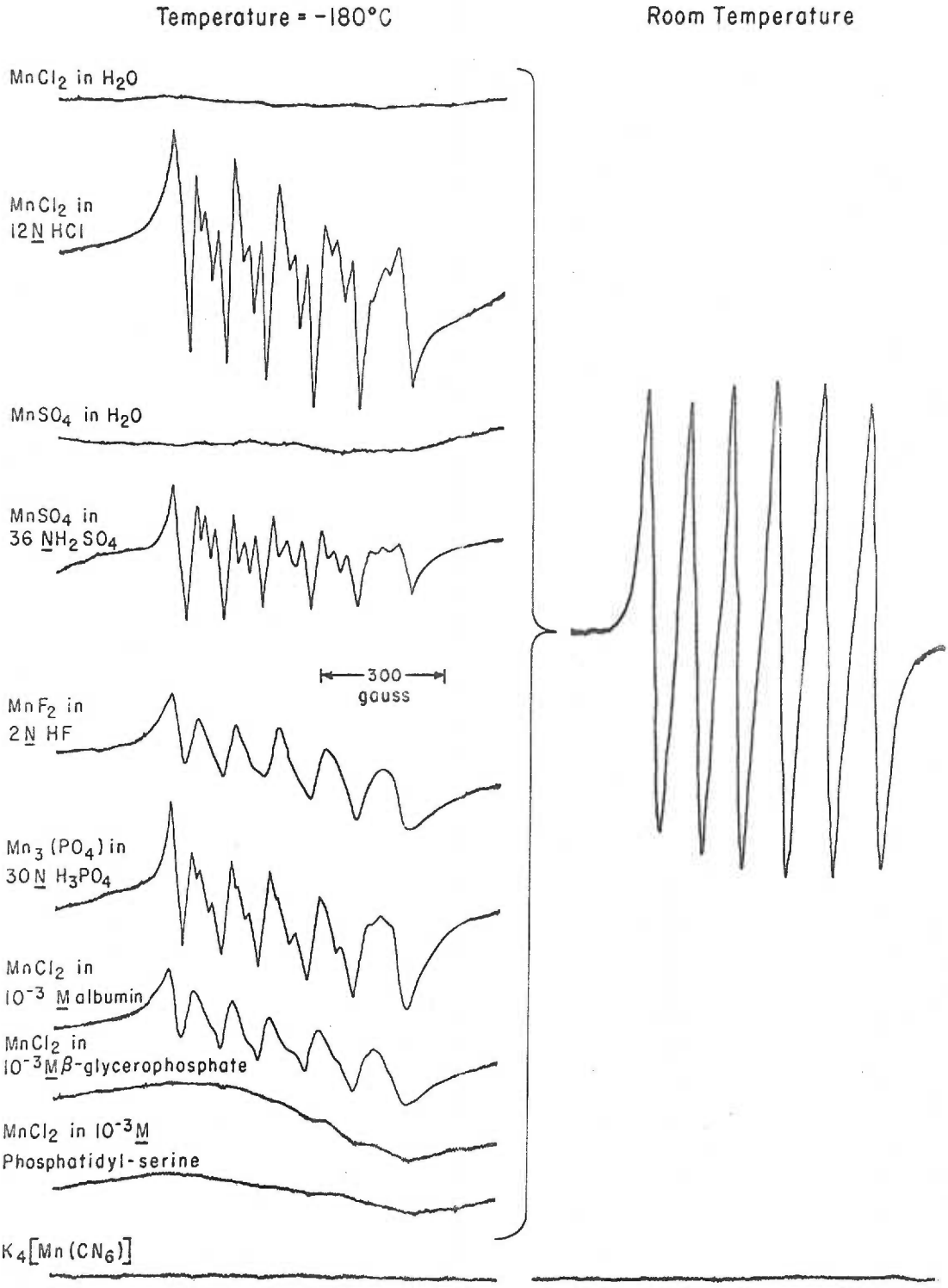
Temperature = −180°C
Room Temperature
$MnCl_2$ in H_2O
$MnCl_2$ in 12 N HCl
$MnSO_4$ in H_2O
$MnSO_4$ in 36 N H_2SO_4
300 gauss
MnF_2 in 2 N HF
$Mn_3(PO_4)$ in 30 N H_3PO_4
$MnCl_2$ in 10^{-3} M albumin
$MnCl_2$ in 10^{-3} M β-glycerophosphate
$MnCl_2$ in 10^{-3} M Phosphatidyl-serine
$K_4[Mn(CN_6)]$

FIGURE 22. The ESR low-temperature spectra of samples of increasing chloride ion/manganous ion ratio. Manganous ion concentration was 10^{-3} M throughout.

Magnetic field strength increases from left to right.

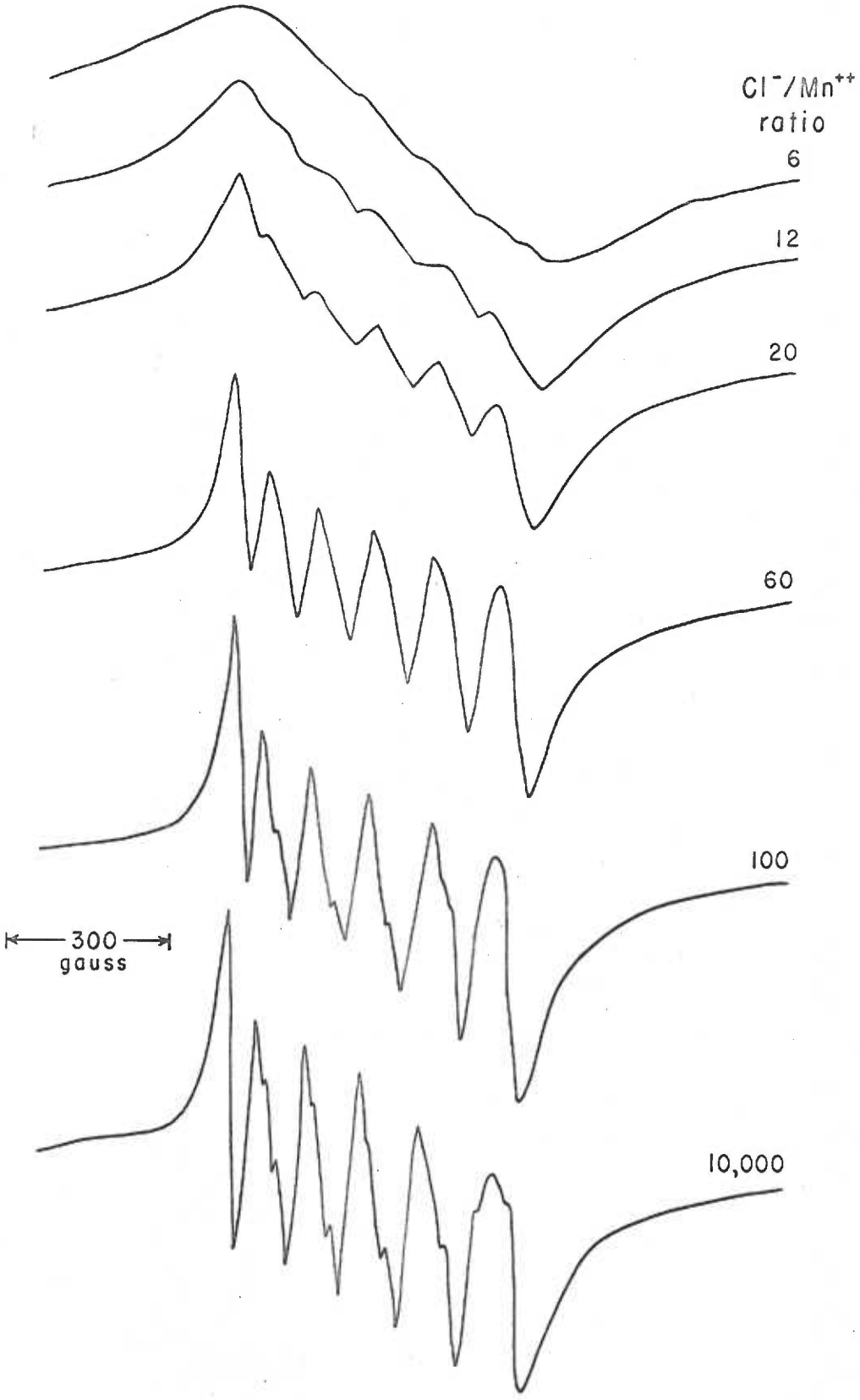
Cl⁻/Mn⁺⁺
ratio
6
12
20
60
100
10,000
300
gauss

FIGURE 23. The ESR low-temperature spectra of samples of "water-free" manganous chloride in N,N-dimethylformamide, before and after addition of water.

Magnetic field strength increases from left to right.

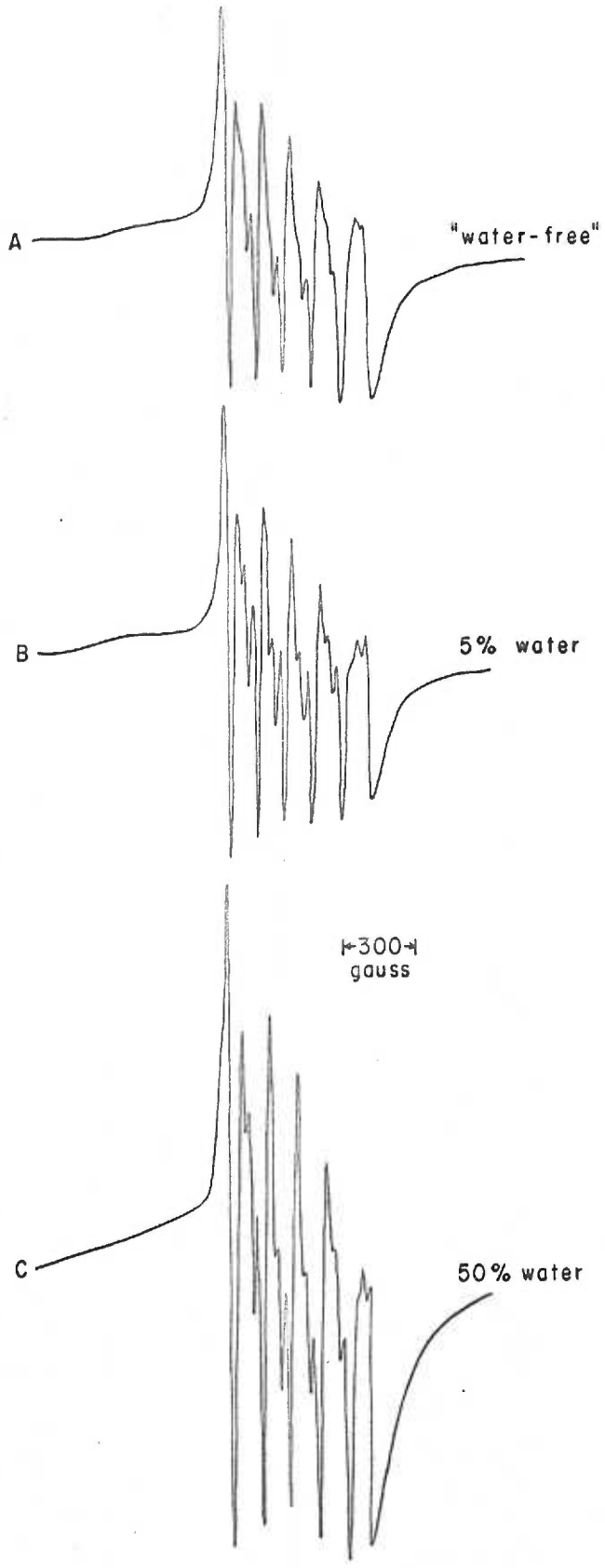
A
"water-free"
B
5% water
⊢300⊣
gauss
C
50% water

FIGURE 24. The ESR low-temperature spectra of samples of 10^{-3} M protein in the presence of 10^{-3} M manganous chloride. The molecular weights of protamine sulfate, cytochrome c, β-lactoglobulin, ovalbumin and bovine albumin, respectively, are listed in order of increasing molecular weight.

Magnetic field strength increases from left to right.

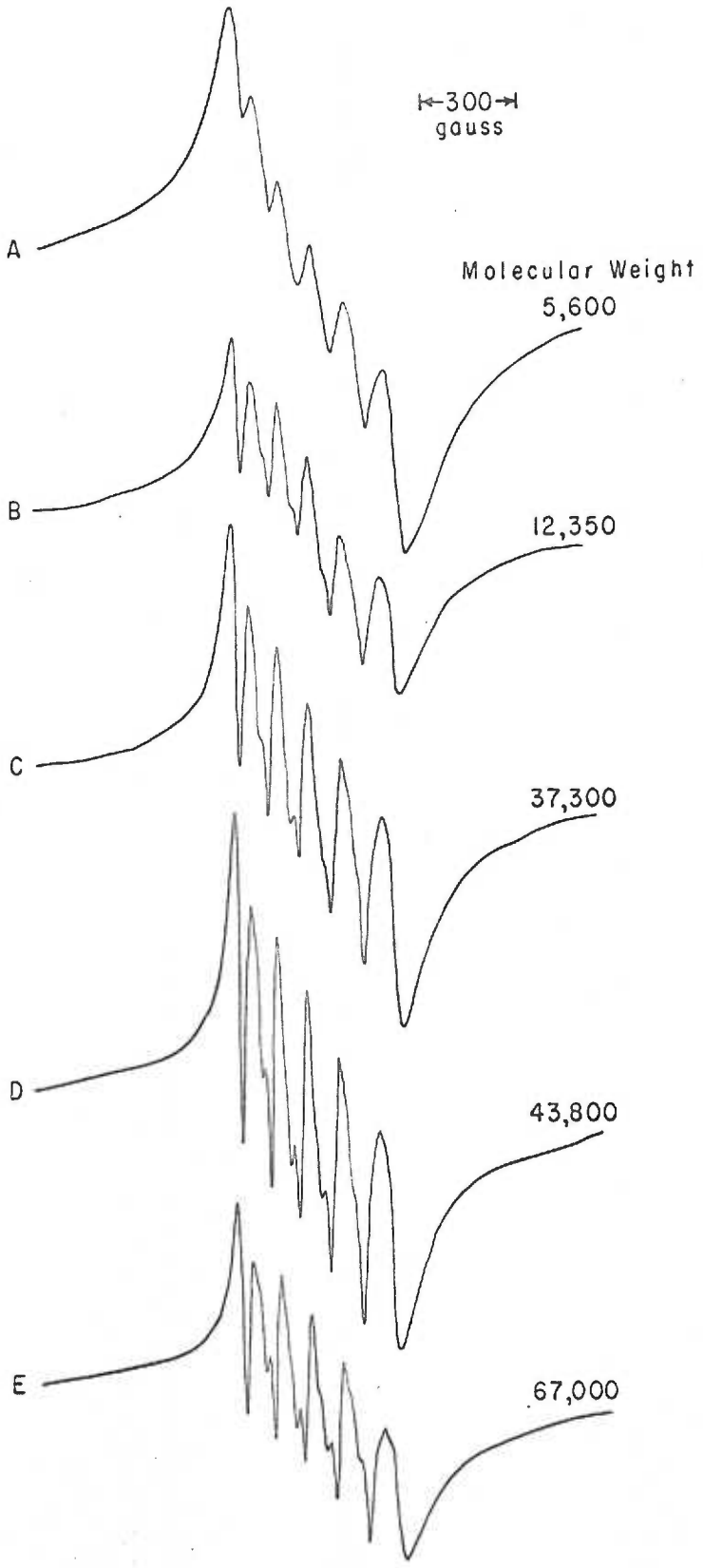
300
gauss
A
Molecular Weight
5,600
B
12,350
C
37,300
D
43,800
E
67,000

FIGURE 25. An ESR low-temperature spectrum of manganous ion in association with protein. The molarity required for an equal surface area was calculated in the case of protamine sulfate, cytochrome c and bovine albumin. Resolved hyperfine structure, measured by the AB/CD ratio, compares the interaction of the manganous ion with the same surface area from three different protein molecules.

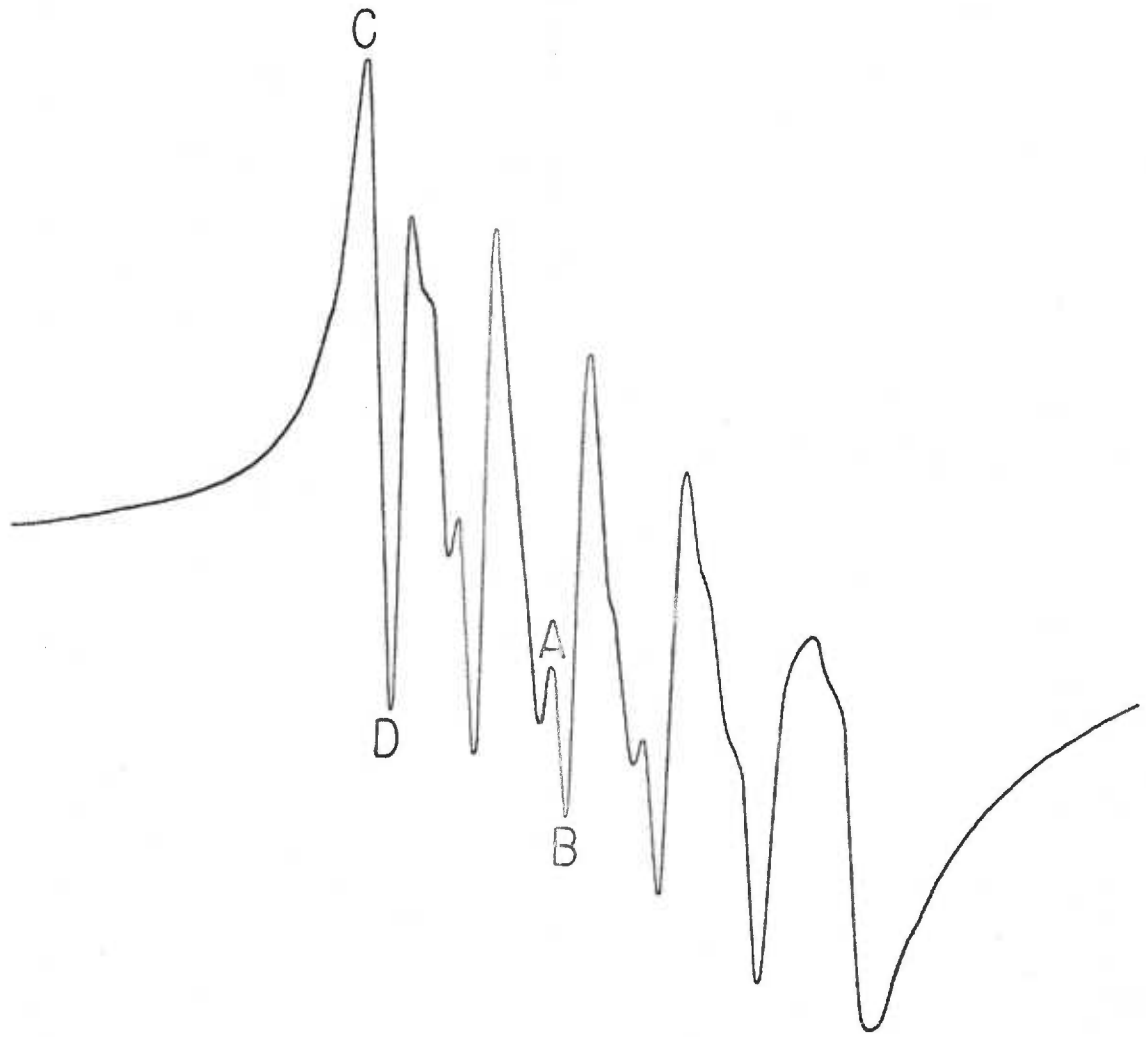

Resolution (AB/CD ratio)	M.W	M required for equal S.A.
86.5/32 = 2.7	5,600	5.3×10^{-3} M
43.5/16 = 2.7	12,350	3.1×10^{-3} M
79.5/21 = 3.8	67,000	1.0×10^{-3} M

1×10^{-3} M $MnCl_2$ used throughout

FIGURE 26. The experimental phosphoric acid titration curve. 2700 µmoles of base was added gradually to 900 umoles of phosphoric acid. In the presence of 50 umoles of manganous ion added in the form of manganous phosphate, less phosphoric acid was required to maintain a constant concentration of 900 umoles in the titration mixture.

Arrows designate the points along the titration curve at which microsamples of solution were taken for low-temperature ESR analysis.

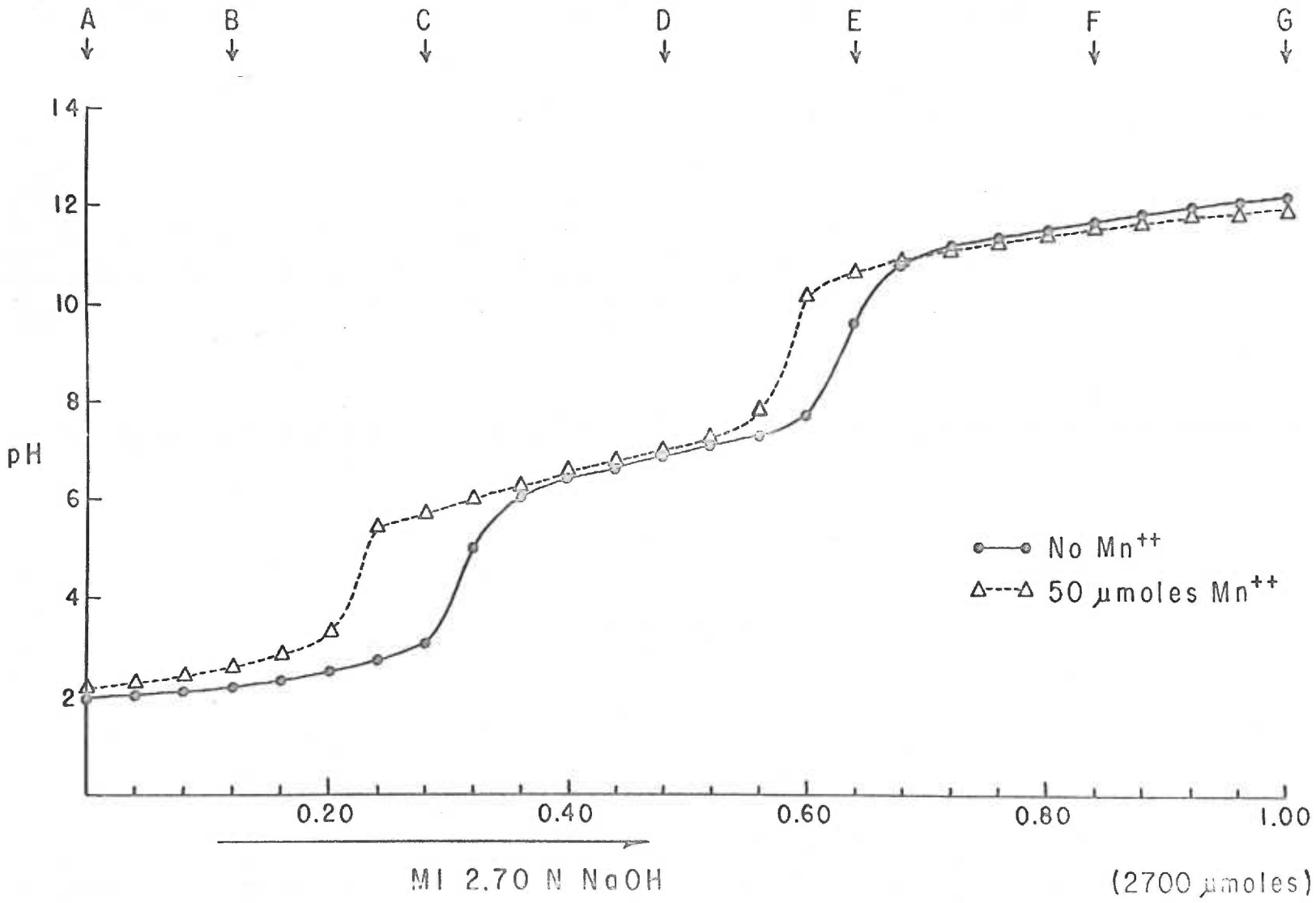
A
B
C
D
E
F
G
14
12
10
8
6
4
2
pH
0.20
0.40
0.60
0.80
1.00
No Mn++
50 µmoles Mn++
Ml 2.70 N NaOH
(2700 µmoles)

FIGURE 27. Low-temperature ESR spectra of microsamples taken at the seven points along the phosphoric acid titration curve. Because of a large increase in signal intensity, the last two samples were examined at lower gain. Manganous ion concentration remains constant, while the phosphate anion species is changing throughout the titration.

Magnetic field strength increases from left to right.

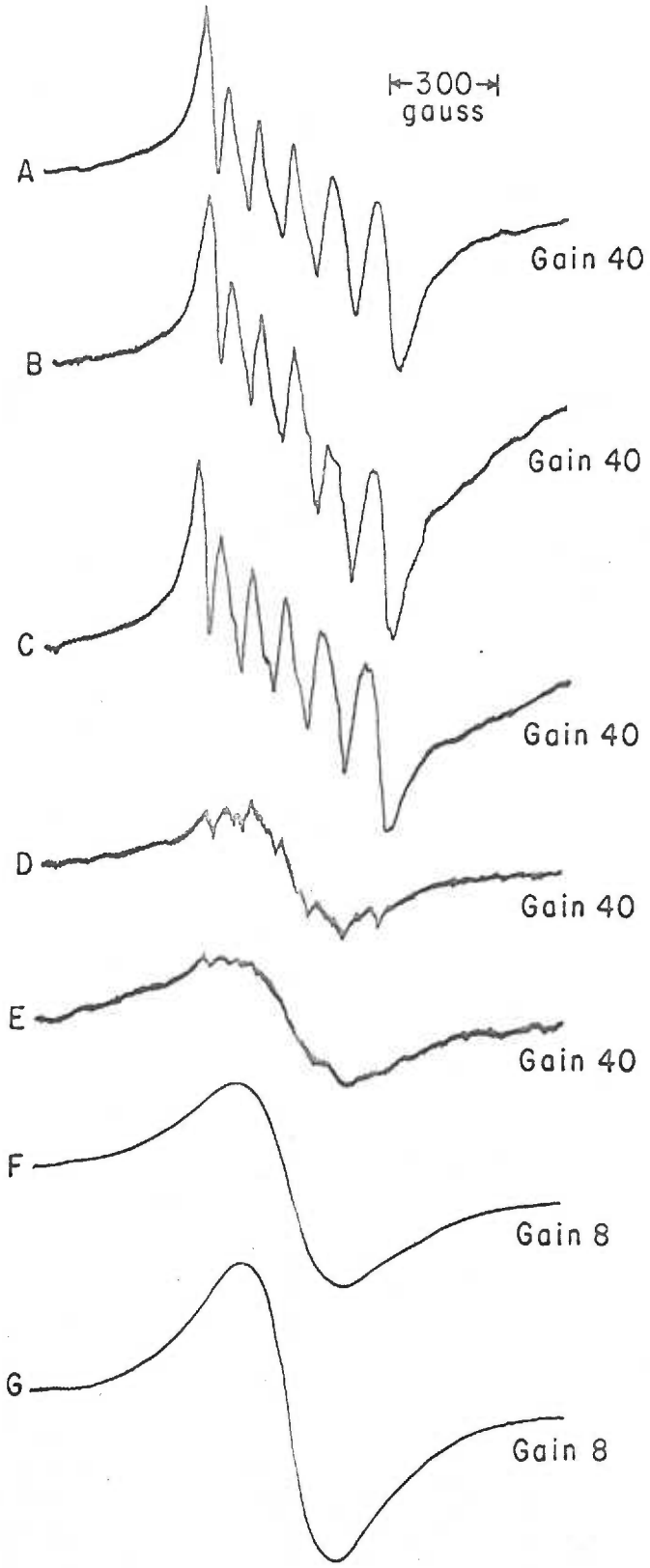
300
gauss
A
B
Gain 40
C
Gain 40
Gain 40
D
Gain 40
E
Gain 40
F
Gain 8
G
Gain 8

IV.

DISCUSSION

The mouse cardiac muscle whole tissue in Figure 3 has an ESR signal typical of heart tissue from other species and is primarily made up of absorptions from the components of mitochondria (7). Normal mouse liver gives a signal which is a summation of absorptions from mitochondria and microsomes, but in the hepatoma BW 7756 a weak mitochondrial absorption predominates, indicating a loss of paramagnetic substances relatively greater for microsomes than for mitochondria. This observation has been confirmed by whole tissue electron microscopy of this mouse hepatoma, when compared to normal mouse liver from the same mouse strain.*

Without normal tissue with which to compare the other tumors, it is difficult to generalize about characteristic differences between the ESR spectra of normal and neoplastic whole tissue. However, certain observations can be made. All tissues, normal and neoplastic, have absorptions in the region of g=2 at -165° C., in contrast to their properties at room temperature (25). The hemangioendothelioma in Figure 3, the spindle-cell sarcomas in Figures 4 and 6, and the

* Unpublished data of work done in collaboration with Dr. T. Kakefuda, City of Hope Research Center, Duarte, California.

osteogenic sarcoma in Figure 6 are all characterized by a fairly narrow, intense absorption in the region of g=2.03, possibly due to cupric copper (8). In Figures 5 and 6 the melanomas show strong, narrow absorptions at g=2.00, almost certainly due to the presence of melanin (76). The mammary adenocarcinomas in Figures 5 and 7 show markedly different spectra. Mammary adenocarcinoma H 2712 has a remarkably strong signal probably of the free radical type at g=2.00, d br B has a highly differentiated spectrum of a hitherto unobserved type, and Ca D1 and BW 10232 appear to have related spectra, although only the latter has absorption in the g=4.3 region. It is obvious that each of the ESR spectra of these whole tumors could require substantially more investigation (88).

This mouse tumor whole tissue survey utilizing ESR spectroscopy at low temperatures directly contradicted the room-temperature work of Commoner and Ternberg (25); there is little basis for their conclusions and speculations. Our qualitative study thus pointed out the usefulness of low-temperature ESR analysis as a promising new tool for observing comparative differences between normal and neoplastic biological material.

It is probable that the modified Schneider preparation of mitochondria (127) from normal mouse liver and mouse hepatoma BW 7756 gives a fraction grossly contaminated with microsomes, because the ESR absorption at g_m=2.25 due to microsomal Fe_x can be slowly washed out of the mitochondrial fraction, as seen in Figure 8. This difficulty

to separate subcellular organelles in the mouse liver will be referred to again later in this discussion. It is evident that there are no significant paramagnetic differences between normal mouse liver and mouse hepatoma mitochondria, once the microsomal contamination has been substantially removed.

The characteristic microsomal ESR spectra seen in normal mouse liver in Figures 10 and 11 are similar to those observed with purified rabbit liver microsomes (61), as well as microsomal fractions from beef, rat and dog.* Generally, the free radical absorption at g_m=2.00 is of somewhat greater intensity in the mouse than in rabbit liver (61,88) or rat liver (89). The absorption at g_m=4.3, seen in the rough microsomes in Figure 11, is known to be associated with high-spin (ionic) iron (126).

The differences between the ESR signals of normal mouse liver and mouse hepatoma microsomes in Table 2 could not be correlated with analytical differences for total iron, non-heme iron, pyridine hemochromogen or cytochrome $\underline{b}_5$, as listed in Table 3. Cytochrome $\underline{b}_5$ concentration was found to be decreased in mouse hepatoma microsomes, but cytochrome $\underline{b}_5$ does not give an ESR signal under the conditions of these experiments. The fact that there are always appreciable amounts of heme iron other than that accounted for by cytochrome $\underline{b}_5$ strongly suggests the presence of one or more other microsomal cytochromes, and this hypothesis is being investigated in our laboratory. Heme iron other than that accounted for by cytochrome $\underline{b}_5$ has a variable concen-

* Work from this laboratory to be published.

tration in normal and neoplastic smooth microsomes and normal and neoplastic rough microsomes; therefore, there seems to be no correlation between this unaccounted-for heme iron and the large concentration decrease seen at g_m=2.25 in the mouse hepatoma microsomes.

There is a discrepancy in the proportional change of signal height at g_m=2.25 and s_m=1.91; in normal mouse liver and hepatoma microsomes the g_m=2.25/s_m=1.91 signal height ratio is .98/.23 = 4.25 and .31/.10 = 3.10, respectively. Since in other work with smooth-surfaced microsomes from normal rabbit liver (150) the temperature dependency and relative heights during reductive titration were shown to be identical for the three peaks ascribed to microsomal Fe_x, the differences in relative heights now observed may be important. They could be due to a change in the nature of the heme binding, or to a contribution by some other absorption in the s_m=1.91 region to the hepatoma microsomal Fe_x absorption.

The apparent increase in free radical concentration in hepatoma rough-surfaced microsomes, judged by signal height at g_m=2.00 per mg. protein, has an unknown significance.

The large diminution in the g_m=2.25 ESR signal in mouse hepatoma microsomes could be due to (a) change in chemical binding, (b) change in the oxidation-reduction state, or (c) concentration decrease, of microsomal Fe_x. Denaturation by heat or acid irreversibly destroys microsomal Fe_x, as detected by ESR; the g_m=2.25 signal disappears with the appearance of a large g_m=4.3 signal. This may mean that paramag-

netic iron, in its special structure of particulate microsomal Fe_x (as diagrammed in Figure 9), has been released by denaturation to the soluble, high-spin (ionic) ferric form. A proportionally smaller g_m=4.3 signal in the mouse hepatoma after similar denaturation strongly suggests a neoplastic decrease in the amount of microsomal Fe_x rather than a mere change in chemical binding. In the enzymatic reductive titrations shown in Figure 12, any change in the redox potential between normal mouse liver and hepatoma microsomal Fe_x can be ruled out. The rate of reduction, rate of reoxygenation, and the substrate preference appears identical when measured by the ESR g_m=2.25 signal height; only a large concentration decrease in the hepatoma is apparent. The conclusion of these studies, then, is that mouse hepatoma microsomal Fe_x is markedly decreased in concentration, when compared to normal mouse liver microsomal Fe_x.

In Figure 13, with enzymatic reduction of the normal mouse liver microsomes by TPNH, there is a discrepancy in the s_m=1.91 region of the ESR spectrum. With respect to the signal heights at s_m=2.41 and g_m=2.25, microsomal Fe_x is reduced by TPNH (from the paramagnetic ferric to the diamagnetic ferrous form); the absorption decrease of microsomal Fe_x at s_m=1.91, however, is cancelled out by the presence of another compound which develops an ESR signal on TPNH reduction. A biological material with these properties has been reported (6,7,9), and this mitochondrial non-heme iron component characteristically appears at g=1.94 on DPNH reduction. Mitochondrial contamination of

the mouse liver microsomal fraction must therefore be considered.

This discrepancy in the s_m=1.91 region of the ESR spectrum could also account for the difference in the previously mentioned g_m=2.25/s_m=1.91 signal height ratio between normal liver and mouse hepatoma microsomes. This observation could be explained by an increased amount of hepatoma mitochondrial contamination, some of which is reduced, thus giving a large ESR absorption in the s_m=1.91 region; the resulting g_m=2.25/s_m=1.91 ratio would thus be lowered in the hepatoma.

The reduced-direct optical curves of rabbit, mouse, beef and rat liver microsomes at liquid nitrogen temperatures are shown in Figure 14. In each type of animal liver a shoulder in the 600 mu region can be seen, while a large peak at 599 mu is persistent in normal mouse liver microsomes. This region is suggestive of an a-type cytochrome, while there is no evidence for the presence of mitochondrial cytochromes b or c. The hepatoma microsomal fraction gives an identical optical spectrum, except for an overall diminution in concentration. Carbon monoxide saturation of the reduced mouse liver microsomes in the absence of light produces the characteristic band at 450 mu, called P-450 and postulated to represent a new microsomal cytochrome (91). The absorption peak at 599 mu does not change in size with carbon monoxide saturation of the reduced microsomes, however. This evidence strongly suggests that we are dealing with an a-type cytochrome, rather than cytochrome a_3 (the latter reversibly binds with carbon monoxide in the absence of light (151), causing a decrease in the 600 mu region).

The question then arises as to whether we are observing mitochondrial cytochrome a contamination of the mouse liver microsomal fraction

or the presence of a new a-type microsomal cytochrome. The fact that no mitochondrial fragments were observed by electron microscopy cannot by itself rule out mitochondrial contamination. Figures 15 and 16 are only two examples of many electron micrographs in which mitochondrial contamination was never observed.

Cytochrome oxidase activity, determined by Warburg manometry (64) and confirmed by enzyme kinetics spectrophotometrically (82), is claimed to be the best method for determining the presence of the mitochondrial electron transport chain in any biological preparation. By these technics, then, it is concluded that the mouse liver microsomal fraction was contaminated with 3 to 14% mitochondria, relative to protein concentration. Further confirmation of this contamination came with the antimycin A studies; antimycin A is a known inhibitor of the mitochondrial oxidation-reduction system (132). If no mitochondrial electron chain contamination were present, addition of antimycin A would have no inhibitory effect on a microsomal preparation. The partial inhibition, as seen in Figure 17, supports the idea of mitochondrial contamination of the mouse liver microsomal fraction.

In Figure 14 it is possible that the mouse microsomal cytochrome b_5 is obscuring the presence of mitochondrial cytochrome b contamination. A few shoulders in the optical spectra of the mouse and beef liver microsomes do suggest that some substance other than pure cytochrome b_5 must be present. Mitochondrial cytochrome c is the most freely diffusible, most soluble and easiest to extract of all the mitochondrial cytochromes, so that loss of this cytochrome into the soluble

phase would be quite likely during the microsomal preparatory procedure. Cytochrome $\underline{a}_3$ (cytochrome oxidase) has been shown to be present in this mouse liver microsomal fraction by Warburg manometry and enzyme kinetics, although it could not be demonstrated by carbon monoxide binding. Thus, it can be rationalized that we are seeing mouse liver mitochondrial contamination in the form of cytochrome $\underline{a}$ at 599 mu in the reduced-direct optical spectrum, while the other mitochondrial cytochromes are either obscured by the large absorption peaks of microsomal cytochrome $\underline{b}_5$, or the other mitochondrial cytochromes have been washed out of the microsomal fraction during the differential centrifugation procedure.

In Figure 14, there is very little spectrophotometric absorption in the 600 mu region of the rabbit, beef or rat liver microsomal fractions, prepared by the same method as the mouse liver microsomes. Microsomal contamination of the mouse liver mitochondrial fraction was discussed earlier, and the results of washing the mitochondria free of microsomes are seen in the ESR spectra of Figure 8. The mouse liver therefore seems to be a good example of a tissue whose subcellular components have a strong affinity for each other. Preparations of mitochondria (127) and microsomes (46) which may prove to be homogeneous in one tissue might not necessarily produce satisfactory separations of other tissues, or of the same tissue from other animal species. Mitochondria, microsomes and other subcellular components are not always separated like so many marbles of varying sizes within a cellular sack.

These studies with mouse liver suggest this difficulty of subcellular organelle preparations and further show that electron microscopy is unable to establish homogeneity at the molecular level. The assays of cytochrome oxidase activity (64,82) and antimycin A inhibition studies (132) are thus shown to be valuable in determining degree of mitochondrial contamination of a biological material, while low-temperature ESR spectroscopy (87,88,89) is shown to be a valuable technic in determining the degree of microsomal contamination of a biological material. In the liquid nitrogen optical spectra of liver microsomes in Figure 14, perhaps the absorption in the 600 mu region is a further index of the degree of mitochondrial contamination. The presence of an a-type microsomal cytochrome remains a possibility, but this is very unlikely in the presence of proven mitochondrial contamination.

The importance of studying differences between normal and neoplastic cells in "minimal deviation" tumors was previously emphasized, so that the three- to four-fold concentration decrease in microsomal Fe_x of the Morris "minimal deviation" hepatoma 5123-B now becomes highly significant. Since the free radical concentration is now not significantly different between the microsomes of normal rat liver and rat hepatoma 5123-B, we may conclude that the increased free radical content observed in the more anaplastic mouse hepatoma rough-surfaced microsomes is probably not important in the study of the initial events of carcinogenesis, but rather an unexplained, secondary change (113). The

importance of intracytoplasmic information (10,11,30,81,129,130) and early changes in the endoplasmic reticulum (17,43,56,80,109) during carcinogenesis was previously emphasized. Therefore, differences between microsomal fractions of normal rat liver and a "minimal deviation" hepatoma may be important in studying which mechanisms operate in giving a normal cell the "information" necessary to initiate malignant transformation.

In Table 4 acetanilide hydroxylase activities do not differ significantly between normal rat liver, host rat liver and the "minimal deviation" hepatoma. This important enzyme occurs in the microsomal oxidation-reduction chain as one of the liver's detoxifying mechanisms to handle drugs given to the animal (72). Animals with hepatomas have been reported (1) to be more easily affected by certain drugs, presumably because of the neoplastic deletion of the necessary detoxifying enzymes. The fact that many drug metabolizing enzymes are deleted from hepatomas (28,46), while acetanilide hydroxylase activity is not diminished in hepatoma 5123-B, further points out the similarity of this "minimal deviation" tumor to normal rat liver. Microsomal Fe_x has also been postulated to be important in the microsomal electron transport chain (61,150). When the "minimal deviation" Morris hepatoma 5123-B is compared to normal rat liver, however, no significant difference in acetanilide hydroxylase activity is seen. This observation, plus the fact that there is a large concentration decrease in hepatoma microsomal Fe_x, suggests that acetanilide hydroxylation is a microsomal function apparently independent of the microsomal Fe_x electron pathway.

As previously discussed, hepatoma 5123 was unable to respond to tryptophan pyrrolase induction (104,105). Breakdown of tryptophan to kynurenine in the mammalian system requires, among other things, manganous ion and hematin (41,104). Tryptophan pyrrolase is a heme-containing enzyme, so it is tempting to speculate that perhaps microsomal Fe_x is the particulate source for the hematin necessary in tryptophan pyrrolase induction. When tryptophan pyrrolase induction was attempted, using the same rat strain and same experimental procedure (21), however, no paramagnetic differences between the tryptophan-injected rats, the cortisone-injected animals and the control rats were found. It is therefore concluded that, although microsomal Fe_x concentration is very small in hepatoma 5123-B and tryptophan pyrrolase induction does not occur in hepatoma 5123, no correlation between these two observations could be found by low-temperature ESR technic.

Microsomal manganese, as measured by ESR signal height, is listed in Table 4; the "minimal deviation" hepatoma 5123-B has two-fifths the microsomal manganese of normal rat liver, when related to protein concentration (89). It is further tempting to speculate that tryptophan pyrrolase induction may be influenced by the concentration of microsomal manganese--which is a paramagnetic measurement of this cation associated with the endoplasmic reticulum membranes. However, tryptophan pyrrolase cannot be induced at all in hepatoma 5123 (104,105), while the presence of manganous ion can be seen in hepatoma 5123-B by ESR. Thus, any influence of the microsomal manganese concentration

on the fact that tryptophan pyrrolase induction does not occur in hepatoma 5123 could not be determined by low-temperature ESR experiments.

These studies with rat liver and "minimal deviation" hepatoma support the fact that there is a concentration decrease of microsomal Fe_x in hepatomas. Microsomal manganese in hepatoma 5123-B is two-fifths that of normal rat liver, while no difference in free radical content exists between normal and cancerous liver. The microsomal enzyme glucose-6-phosphatase in hepatoma 5123 is one-third to one-half that of normal rat liver (145). Certainly morphological changes occur early in the endoplasmic reticulum during the process of carcinogenesis (17,43,109), but it is difficult to evaluate and predict the significance of differences like these observed in the microsomal fraction of a "minimal deviation" tumor. The fact that cancer may be initiated by "multiple pathways" (12) is also a possibility one must keep in mind.

The relationship of the manganous ion to the microsomal membrane has been difficult to determine. By trypsin digestion and Emasol treatment, the resultant aqueous phase was purified six-fold, as determined by manganese ESR signal height per mg. protein; the low-temperature ESR spectra of microsomal manganese before and after this purification are shown in Figure 20. The ESR spectrum of superimposed microsomal Fe_x can be seen in the starting beef microsomes, while this particulate component is not present in the microsomal manganese aqueous fraction. The fact that the manganous ion can be separated

from its protein moiety when chromatographed on Chelex or Sephadex G-25 gel suggests a very weak type of bonding between the divalent cation and electronegative areas of the protein.

Trypsin digestion, lubrol solubilization, sonication and the Mickel shaker are all methods which can be used in breaking down the microsomal membranes and isolating a manganese fraction. The same question of all these methods is raised, however--is the structural relationship of manganese to the microsomal membrane in vivo and in vitro the same as that in the isolated aqueous fraction? Further isolation and characterization of microsomal manganese remains to be done.

Addition of manganous ion to the mouse liver microsomal system did not enhance microsomal respiration. In the microsomal reductive titrations, too, the ESR manganous signal always remained stable. The redox potential of the stable d^5 manganous ion oxidized to the manganic form is +1.51 volts, far above most cellular reactions of -0.32 to +0.36 volts. Possible molecular relationships of cellular manganese have been studied and proposed (36,73), however, in which the redox potential of a manganese compound can be considerably changed by complexing the cation with some organic molecule or macromolecule. Most likely the manganous ion functions as other divalent cations probably do--stabilization of negative charges along cellular membranes. It has long been known, for example, that the structure of isolated mitochondria is preserved by adding manganese in trace amounts to prevent swelling (29).

Low-temperature ESR spectra of the manganous ion in various compounds and complexes are markedly different from the corresponding room-temperature solution spectra, as seen in Figure 21. The gain is variable, as is the anion/Mn^{++} ratio, so no conclusions can be drawn from this figure. These spectra were early data and led to further experiments in an attempt to determine the cause of these observations. Generally, six absorption lines over a range of 600 gauss are always seen, centered about g=2.00. In the low-temperature spectrum an underlying broad signal of a 600-gauss peak-to-peak line width is usually concomitant with the six-line signal. In the case of high anion concentrations or very low pH, a hyperfine structure develops, with a doublet between each of the six absorption lines. A very weak, broad signal occurs in the low-temperature ESR spectra of aqueous manganous chloride, aqueous manganous sulfate, and manganous chloride in association with β-glycerophosphate and phosphatidyl-serine. The manganous cyanide complex has no ESR signal at either room temperature or low temperatures, probably because the cyanide ion has sufficiently high ligand-field strength to forcibly alter the high-spin d^5 manganous ion to a low-spin manganous cyanide ($Mn(CN)_6^{-4}$) state (97), and an ESR signal is not observed under these conditions.

It can be seen from Figure 22 that as the pH is lowered or the anion concentration in solution is raised, the six observed lines of the manganous ESR low-temperature spectrum increase in intensity, and are further resolved until a 16-line spectrum develops (4). This has been shown with hydrochloric acid, lithium chloride or sodium chloride

as the chloride ion source added to manganous chloride. Sulfuric acid or excess sulfate ion added to manganous sulfate, and phosphoric acid or excess phosphate ion added to manganous phosphate, also can reproduce the same phenomena. It is difficult to fit the low-temperature spectra into any one energy scheme, since the six observed lines are not split evenly; the distance between each absorption varies from about 70 to 120 gauss apart, increasing from low to high magnetic field. However, the fully resolved spectra of the manganous ion in the frozen state, as in the case of a high anion/Mn^{++} ratio, can be explained in terms of a spin hamiltonian if we consider some of the hyperfine lines to be due to forbidden transitions (4).

The highly resolved, 16-line ESR spectrum, similar to that seen with high anion concentrations, can be seen in frozen solutions of manganous chloride in organic solvents such as ethanol, methanol or acetone (4). A manganous chloride powder was baked at 200° C. to a constant weight. When this theoretically anhydrous form was added to relatively "water-free" doubly-distilled methanol, the hyperfine resolution of the low-temperature ESR spectrum was less than that seen when water is abundant in the experimental system. The same phenomenon is observed in the ESR spectra of Figure 23, where "anhydrous" manganous chloride was dissolved in N,N-dimethylformamide and then water was added to the system; the same gain is used in all three spectra. Just the fact that the manganous chloride powder could be dissolved in the N,N-dimethylformamide solvent suggests that enough water molecules were present in the "water-free" system to hydrate the manganous and chlor-

ide ions among the organic solvent molecules. We have observed, therefore, that when precautions are taken to rid the system of water, the hyperfine resolution of the low-temperature ESR signal is decreased. Perhaps the water molecule is important in the species-complex which causes the characteristic manganese low-temperature six-line signal with its underlying broad signal component.

Proteins of increasing molecular weight exert an influence on the low-temperature ESR manganese spectrum similar to the effect of high anion concentrations or very low pH. Figure 24 shows greater resolution of the low-temperature ESR signal with increasing protein molecule size. The degree of resolution is best measured by a ratio of signal heights, for example, AB/CD, as illustrated in Figure 25. Thus, it was speculated that perhaps the hyperfine structure of the low-temperature manganese signal could be correlated with the surface area of the protein environment. Molecular weight was assumed to be proportional to volume, and a relative radius in arbitrary units was calculated for assumed spheroid molecules of protamine sulfate, cytochrome c and bovine albumin. From this, relative surface areas of each were estimated, and the concentration of each protein required for equal surface area is listed in Figure 25. The resolution of hyperfine structure was very similar in all three cases, being identical in the two lower molecular weight proteins, which were easier to dissolve in the aqueous manganous chloride solution. These results are certainly within experimental error of the system used. The association of the manganous ion with the surface area of protein molecules is therefore

probably similar to the association of the manganous ion with high anion concentration in causing the characteristic six-line low-temperature spectrum.

The phosphoric acid titration curve is seen in Figure 26. Each plateau of the curve represents an equilibrium between two phosphate species: at point B the $H_2PO_4^-$ concentration and the undissociated H_3PO_4 concentration are equal; at point D, the midpoint of the second dissociation, there is an equilibrium between the $HPO_4^=$ and the $H_2PO_4^-$ species; at point F the $PO_4^{\equiv}$ and the $HPO_4^=$ species are equal in concentration. At point G, the predominant phosphate species would be the $H_2PO_4^-$ ion, while the undissociated H_3PO_4 has disappeared for all practical purposes. Similarly, the $HPO_4^=$ ion would predominate at point E, while the $PO_4^{\equiv}$ species is in excess at point G. The presence of manganous phosphate appears to shorten the dissociation plateaus slightly and to make the slopes in between plateaus considerably steeper. This phenomenon indicates that fewer protons are available in the titration system. The reason is simple: in order to maintain a phosphate concentration of 900 umoles in the system, less phosphoric acid (and therefore fewer protons) was added in the presence of 50 umoles of manganous phosphate. This also explains why the pH is slightly higher in the case of manganous phosphate addition. Most important in Figure 26 is the fact that the predominant phosphate species at any point along the titration curve can be predicted.

The question of which phosphate species accounts for the six-line low-temperature ESR spectrum of the manganous ion is answered in

Figure 27. The signal remains prominent in samples from points A, B and C of the titration curve. The six-line signal is markedly reduced in the sample from point D, however, when the $H_2PO_4^-$ species is half gone, and total disappearance of the six-line signal in the sample from point E coincides with the total disappearance of the $H_2PO_4^-$ ion. The underlying broad signal, which seems to always occur with the six-line absorption, disappears with the six-line signal, and a broad signal with a 300-gauss peak-to-peak line width develops in intensity as the other signal disappears. This narrower broad signal has the same characteristic shape as the ESR spectrum of manganous phosphate ($Mn_3(PO_4)_2$) powder. As mentioned previously, the procedure for making manganous phosphate powder was combining dilute manganous chloride with concentrated phosphoric acid, with precipitation and washing at an alkaline pH (59); by this method complete purity is difficult to obtain because of slight contamination with hydroxyl and chloride ions in the flocculent manganous phosphate precipitate. In the experimental titration system, a similar white flocculent precipitate appears at about pH 9 and a different brown powder appears in very small amounts above pH 10. The white substance most likely represents a mixture of manganous phosphate with hydroxyl ion contamination, while the brown, metallic-appearing precipitate must represent diamagnetic manganese oxide (MnO_2).

The interpretation of these ESR results is therefore clear. The univalent anion is that phosphate species which, in association with the manganous ion, accounts for the commonly observed six-line ESR

spectrum. The underlying broad signal of 600 gauss peak-to-peak line width which is always associated closely with the six-line signal is not well understood. The broad signal of 300 gauss peak-to-peak line width is the $Mn_3(PO_4)_2$ species, which visibly precipitates in the system above pH 9. The number of univalent anions which associate with the manganous cation cannot be determined; the formula $Mn^{++} \cdot (H_2PO_4^-)_x(H_2O)_y$ can be written, where $x + y = 6$ for octahedrally coordinated manganese. The most feasible value of x would be 2, because such an ionic association would result in stabilization of the divalent cation with a neutral species: $Mn^{++} \cdot (H_2PO_4^-)_2(H_2O)_4$.

It should be pointed out that this technic of ESR analysis of microsamples taken along the course of a reaction can be advantageous in certain experimental situations. When ion concentrations can be accurately calculated from the equilibrium or rate constants of well-controlled systems, ESR microsample measurements can be a quantitative method which does not disturb the experimental system. This procedure would of course be limited to compounds or complexes concerning paramagnetic species.

Dissociation constants of manganese complexes (22,75) have been determined by room-temperature ESR analysis. For example, the six-line room-temperature spectrum of manganese decreases on addition of 2-phosphoglyceric acid (PGA). From the height of the ESR room-temperature signal, the dissociation constant

$$K_d = \frac{[Mn^{++}][PGA]}{[Mn\text{-}PGA]} \qquad \text{(iii)}$$

could therefore be calculated (75). Dissociation constants of manganous complexes with malonic acid, glycylglycine, histidine, glucose-1-phosphate, ADP, ATP and glucose-6-phosphate were similarly determined by the same principle (22). Cohn and Townsend suggested (22) that the disappearance of the six-line signal in a complex indicates the formation of a covalent bond. However, this was not the case in Malmström's work (75), since the six-line splitting disappears completely in the manganese-PGA complex, which has been shown to involve purely ionic coordination. McGarvey suggested and experimentally demonstrated that the disappearance of the six-line spectrum is due to a line broadening, which would be expected to occur in all complexes except possibly those having a very high degree of symmetry (78). In this thesis, the procedures of low-temperature analysis and microsamples from titration curves are new applications for studying paramagnetic compounds and complexes with ESR spectroscopy.

The study of the environment and function of manganese in this thesis developed from the observation that the manganous ion was always seen in the low-temperature ESR spectra of normal and neoplastic microsomal membranes. Other divalent cations such as calcium, zinc and magnesium, may be present in the microsomes in concentrations more than, or equal to, manganese, but only the manganous ion is detected by ESR. The possibility of oxidation-reduction function of manganese cannot be absolutely ruled out, but the results of this thesis make redox function for manganese very unlikely in the microsomes. There is evi-

dence to suggest a redox function for the manganous ion in the mitochondrial membrane, however (19,20). Manganese is thus postulated to be one of several divalent cations which stabilize protein, and perhaps microsomal membrane protein, surface charge.

From the experimental studies of this thesis, the six-line low-temperature ESR spectrum seen in microsomal fractions appears to be caused by the manganous ion in association with some anion; protein surface is the most likely anion source in microsomes. An example of such a relationship of divalent cation to microsomal protein is illustrated in Figure 28, where manganese, calcium and magnesium all compose a "stabilizing divalent cation layer" on the surface of the particulate membrane. An octahedral configuration of manganese is depicted. The presence of a water shell on protein surfaces (135,144) would support the observation that decreased resolution of the six-line signal was seen when precautions were taken to remove all water from a manganese system.

This structural proximity of the manganous ion to the microsomal membrane is a very attractive hypothesis which explains why manganese may remain at one particular cellular location conveniently available for enzyme catalysis. Numerous enzymes require divalent cations for microsomal reactions. Arginase is an example of a microsomal enzyme requiring manganese (18). Nucleoside phosphatase is a microsomal enzyme activated by magnesium, calcium or manganous ions (90). The apoenzyme of tryptophan pyrrolase is activated from the microsomal particulate to a soluble form which requires manganese or magnesium in

FIGURE 28. A postulated relationship of divalent cation to microsomal protein, where ions such as manganese, calcium and magnesium stabilize electronegative charge of the particulate membrane.

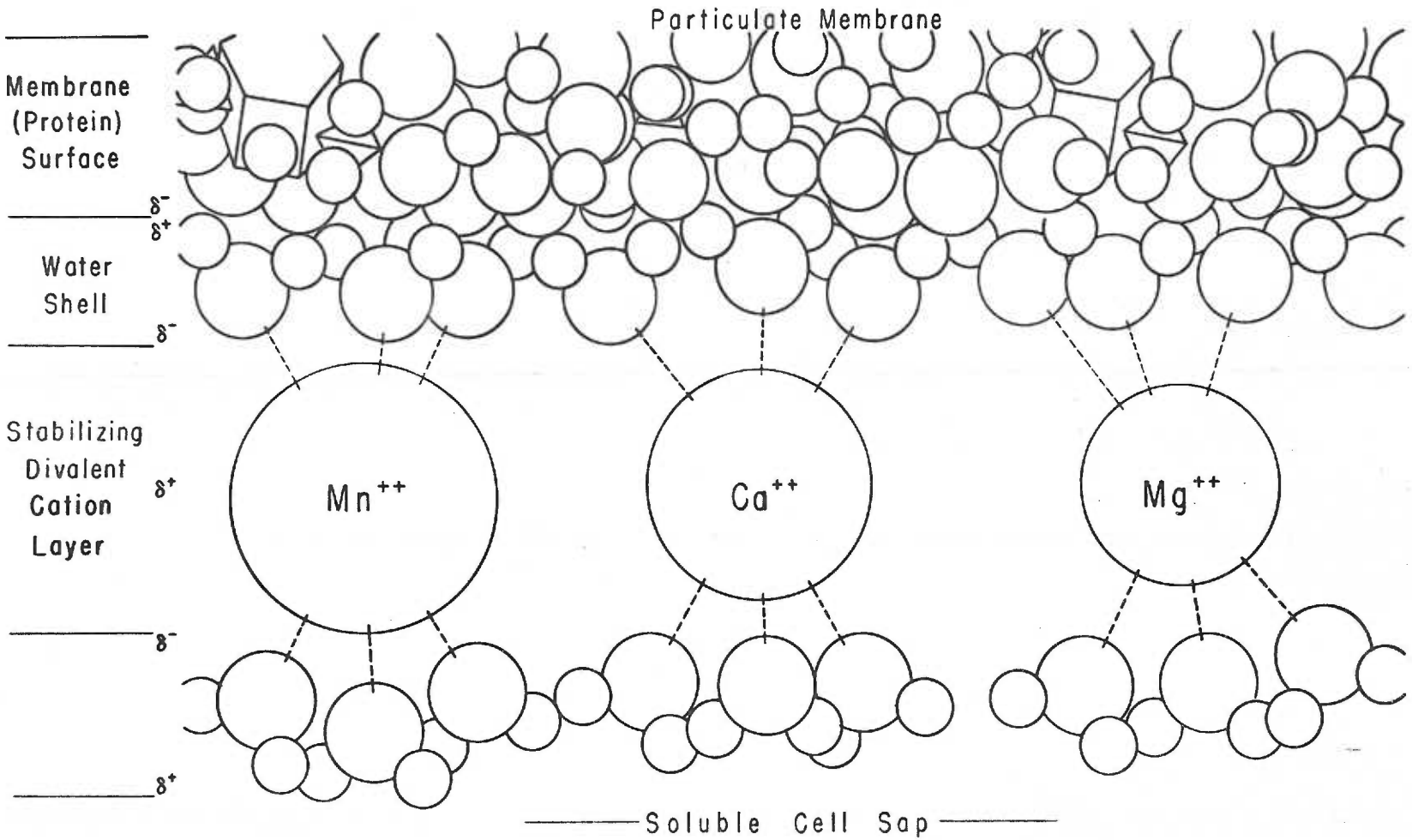
Particulate Membrane
Membrane (Protein) Surface
δ⁻
δ⁺
Water Shell
δ⁻
Stabilizing Divalent Cation Layer
δ⁺
Mn⁺⁺
Ca⁺⁺
Mg⁺⁺
δ⁻
δ⁺
Soluble Cell Sap

breaking down tryptophan (104).

The cell is thus seen as a genetic system capable of forming specific enzymes; this capability may not fully express itself until required to do so for survival of the cell. Selective formation of key enzymes of unique metabolic routes enables the cell to adjust to environmental changes with efficiency and economy. By this same mechanism, "information" of a carcinogenic nature may initiate the steps leading to cancer. Changes in the endoplasmic reticulum early in carcinogenesis suggest that this intracytoplasmic locus might be important in the steps leading to malignancy. Differences between normal liver and hepatoma microsomes, and structural and functional properties of the paramagnetic manganous ion in association with the microsomal membrane, were studied by low-temperature ESR technic. It is hoped these findings in the microsomes may be pertinent in the study of initial events leading to carcinogenesis.

V.

SUMMARY

A new technic, low-temperature ESR spectroscopy, was applied to the problem of the initial events of carcinogenesis.

Twenty-nine types of mouse tumors and two normal mouse tissues were examined in the frozen state; the observation of paramagnetic differences suggested further studies. The major difference between subcellular components of normal mouse liver and mouse hepatoma involved a neoplastic decrease of microsomal Fe_x, a newly-discovered microsomal electron transport substance. Reductive titrations and reduced-direct low-temperature spectrophotometry of mouse liver microsomes raised the question of mitochondrial contamination, which was confirmed by cytochrome oxidase assays and antimycin A inhibition studies. Compared to other tissues, mouse liver was shown to be a tissue from which it was difficult to obtain highly purified subcellular fractions.

Comparisons of rat liver and "minimal deviation" hepatoma 5123-B reaffirmed the fact that very low hepatoma microsomal Fe_x concentration is a constant finding. Microsomal manganese concentration, as detected by low-temperature ESR, was also depressed in the "minimal deviation" hepatoma. No correlation could be established between (a) the inability of tryptophan pyrrolase induction in hepatoma 5123 and (b) the low

microsomal Fe_x and microsomal manganese concentrations in the hepatoma.

A six-fold purification of microsomal manganese was carried out, but further isolation and characterization has not been done. The possibility of redox function of microsomal manganese was ruled out.

Inorganic studies of the environment of the manganous ion led to a speculation that manganese functions as a divalent cation which stabilizes the charge of the microsomal membrane surface. High anion concentration and low pH seemed to be two factors which cause the characteristic low-temperature ESR manganese spectrum. The ESR spectrum of the manganous ion in the frozen state may be explained in terms of a spin hamiltonian utilizing the occurrence of forbidden transitions.

These observations, developed around low-temperature ESR spectroscopy, were discussed as possibly being important in the study of initial events leading to carcinogenesis.

* * *

REFERENCES

1. Adamson, R. H. & Fouts, J. R. The metabolism of drugs by hepatic tumors. Cancer Res. 21:667-672 (1961).

2. Aisenberg, A. C. & Morris, H. P. Energy pathways of hepatoma No. 5123. Nature 191:1314-1315 (1961).

3. Alexander, P. The reactions of carcinogens with macromolecules. Adv. Cancer Res. 2:2-72 (1954).

4. Allen, B. T. & Nebert, D. W. Hyperfine structure in the EPR spectrum of the manganous ion in frozen solutions. J. chem. Phys. In press.

5. American Cancer Society. Symposium: the possible role of viruses in cancer. Cancer Res. 20:669-830 (1960).

6. Beinert, H. & Sands, R. H. Studies on succinic and DPNH dehydrogenase preparations by paramagnetic resonance (ESR) spectroscopy. Biochem. Biophys. Res. Comm. 3:41-46 (1960).

7. Beinert, H. & Lee, W. Evidence for a new type of iron-containing electron carrier in mitochondria. Biochem. Biophys. Res. Comm. 5:40-45 (1961).

8. Beinert, H., Griffiths, D. E., Wharton, D. C. & Sands, R. H. Properties of the copper associated with cytochrome oxidase as studied by paramagnetic resonance spectroscopy. J. Biol. Chem. 237:2337-2346 (1962).

9. Beinert, H., Heinen, W. & Palmer, G. Applications of combined low temperature optical and electron paramagnetic resonance spectroscopy to the study of oxidative enzymes. Brookhaven Symp. Biol. 15:229-265 (1962).

10. Bhargava, P. M., Hadler, H. I. & Heidelberger, C. Studies on the structure of the skin protein-bound compounds following topical application of 1,2,5,6-dibenzanthracene-9,10-C^{14}. I. 2-phenylphenanthrene-3,2'-dicarboxylic acid, a degradation product. J. Am. Chem. Soc. 77:2877-2886 (1955).

11. Bhargava, P. M. & Heidelberger, C. Studies on the structure of the skin protein-bound compounds following topical application of 1,2,5,6-dibenzanthracene-9,10-O^{14}. II. Nature of the 2-phenyl-phenanthrene-3,2'-dicarboxylic acid-protein bond. J. Am. Chem. Soc. 78:3671-3677 (1956).

12. Bottomley, R. H., Pitot, H. C. & Morris, H. P. Metabolic adaptations in rat hepatomas. IV. Regulation of threonine and serine dehydrase. Cancer Res. 23:392-399 (1963).

13. Bottomley, R. H., Pitot, H. C., Potter, V. R. & Morris, H. P. Metabolic adaptations in rat hepatomas. V. Reciprocal relationship between threonine dehydrase and glucose-6-phosphate dehydrogenase. Cancer Res. 23:400-409 (1963).

14. Bourne, G. H. The cytoplasm. In: Division of Labor in Cells. Academic Press, New York, 1962. pp. 25-54.

15. Boutwell, R. K. & Baldwin, H. H. A demonstration of threshold and reversibility in tumor promotion. Proc. Am. Assoc. Cancer Res., 1960, Abs. No. 24.

16. Brues, A. M. & Barron, E. S. G. Biochemistry of cancer. Ann. Rev. Biochem. 20:343-366 (1951).

17. Caper, S. P. The morphology of the growth and regression of Shope's fibroma of rabbits. Unpublished master's dissertation, Univ. of California at Los Angeles, 1963.

18. Carruthers, C., Woernley, D. L., Baumler, A. & Davis, B. Atypical distribution of several enzymes in the fractions of Ehrlich Ascites and liver cells prepared from glycerol homogenates. Cancer Res. 19:59-66 (1959).

19. Chappell, J. B., Greville, G. D. & Bicknell, K. E. Stimulation of respiration of isolated mitochondria by manganese ions. Biochem. J. 84:61P (1962).

20. Chappel, J. B. & Greville, G. D. Isolated mitochondria and accumulation of divalent metal ions. Fed. Proc. 22:526 (1963).

21. Cho, Y. S., Pitot, H. C. & Morris, H. P. Metabolic adaptations in rat hepatomas. VI. Substrate-hormone relationships in tryptophan pyrrolase induction. Cancer Res. 24:52-58 (1964).

22. Cohn, M. & Townsend, J. A study of manganous complexes by paramagnetic resonance absorption. Nature 173:1090-1091 (1954).

23. Commoner, B., Townsend, J. & Pake, G. E. Free radicals in biological materials. Nature 174:689-691 (1954).

24. Commoner, B., Heise, J. J., Lippencott, B. B., Norberg, R. E., Passonneau, J. V. & Townsend, J. Biological activities of free radicals. Science 126:57-63 (1957).

25. Commoner, B. & Ternberg, J. L. Free radicals in surviving tissues. Proc. Natl. Acad. Sci. (U.S.) 47:1374-1384 (1961).

26. Conney, A. H., Brown, R. R., Miller, J. A. & Miller, E. C. The metabolism of methylated aminoazo dyes: VI. Intracellular distribution and properties of the demethylase system. Cancer Res. 17:628-633 (1957).

27. Conney, A. H. & Klutch, A. Increased activity of androgen hydroxylases in liver microsomes of rats pretreated with phenobarbital and other drugs. J. Biol. Chem. 238:1611-1617 (1963).

28. Conney, A. H. & Burns, J. J. Induced synthesis of oxidative enzymes in liver microsomes by polycyclic hydrocarbons and drugs. In: G. Weber (Ed.), Advances in Enzyme Regulation. Macmillan Co., New York, 1963. Volume 1, pp. 189-214.

29. Cotzias, G. C. Manganese. In: Mineral Metabolism, an Advanced Treatise, C. L. Comar & F. Bronner (Ed.). Academic Press, New York, 1962. Volume II, part B.

30. Davenport, G. R. & Heidelberger, C. The interaction of polycyclic hydrocarbons with mouse skin constituents. Proc. Am. Assoc. Cancer Research 3:15 (1959) (Abstract)

31. Day, E. D., Planinsek, J. A. & Pressman, D. Specific localization in vivo of antihepatoma antibodies in autochthonous rat hepatomas. J. Nat. Cancer Inst. 27:1107-1114 (1961).

32. Doeg, K. A. & Ziegler, D. M. Simplified methods for the estimation of iron in mitochondria and submitochondrial fractions. Arch. Biochem. Biophys. 97:37-40 (1962).

33. duBuy, H. G., Woods, M. W. & Lackey, M. D. Enzymatic activities of isolated normal and mutant mitochondria and plastids of higher plants. Science 111:572-574 (1950).

34. Dyer, H. M., Gullino, P. M. & Morris, H. P. Tryptophan pyrrolase activity in transplanted "minimal deviation" hepatomas. Cancer Res. 24:97-106 (1964).

35. Ehrenberg, A. Electron spin resonance absorption by some haemoproteins. Arkiv. Kemi 19:119-128 (1962).

36. Elvidge, J. A. & Lever, A. B. P. Manganese phthalocyanine as an oxygen carrier. Proc. chem. Soc., 195 (1959).

37. Elwood, J. C., Lin, Y., Cristofalo, V. J., Weinhouse, S. & Morris, H. P. Glucose utilization in homogenates of the Morris hepatoma 5123 and related tumors. Cancer Res. 23:906-913 (1963).

38. Essner, E. & Novikoff, A. B. Cytological studies on two functional hepatomas. J. Cell. Biol. 15:289-312 (1962).

39. Estabrook, R. W. Spectrophotometric studies of cytochromes cooled in liquid nitrogen. Hematin Enzymes 19:436-460 (1961).

40. Farber, E. Similarities in the sequence of early histological changes induced in the liver of the rat by ethionine, 2-acetylaminofluorene, and 3'-methyl-3-dimethylaminoazobenzene. Cancer Res. 16:142-148 (1956).

41. Feigelson, P. & Greengard, O. A microsomal iron-porphyrin activator of rat liver tryptophan pyrrolase. J. Biol. Chem. 236:153-167 (1961).

42. Feigelson, P. & Greengard, O. Immunochemical evidence for increased titres of liver tryptophan pyrrolase during substrate and hormonal enzyme induction. J. Biol. Chem. 237:3714-3717 (1962).

43. Fiala, S. & Fiala, A. E. Intracellular localization of carcinogen and its relationship to the mechanism of carcinogenesis in rat liver. Brit. J. Cancer 13:236-250 (1959).

44. Fitzhugh, A. F. Malignant tumors and high polymers. Science 118: 783 (1953).

45. Foulds, L. The experimental study of tumor progression: A review. Cancer Res. 14:327-339 (1954).

46. Fouts, J. R. The metabolism of drugs by subfractions of hepatic microsomes. Biochem. Biophys. Res. Comm. 6:373-378 (1961).

47. Furst, E. L. Metal chelation and carcinogenesis. Unpublished Sigma Xi lecture, University of Oregon Medical School, Jan. 31, 1964.

48. Furth, J. A meeting of ways in cancer research: Thoughts on the evolution and nature of neoplasms. Cancer Res. 19:241-258 (1959).

49. Garfinkel, D. Studies on pig liver microsomes. I. Enzymic and pigment composition of different microsomal fractions. Arch. Biochem. Biophys. 77:493-509 (1958).

50. Gerber, P. Studies on a persistently "masked" viral infection in cells of SV_{40}-induced ependymomas. Proc. Amer. Assoc. Cancer Research 4:22 (1963). (Abstract)

51. Gillette, J. R. Factors that affect the stimulation of the microsomal drug enzymes induced by foreign compounds. In: G. Weber (Ed.), Advances in Enzyme Regulation. Macmillan Co., New York, 1963. Volume 1, pp. 215-223.

52. Goldman, R. D. & Kaplan, N. O. Alterations of tissue lactate dehydrogenase in human neoplasms. Biochem. Biophys. Acta 77:515-518 (1963).

53. Gomori, G. Preparation of buffers for use in enzyme studies. In: S. P. Colowick & N. O. Kaplan (Ed.), Methods of Enzymology. Academic Press, New York, 1955. Volume 1, pp. 138-146.

54. Gornall, A. G., Bardawill, C. J. & David, M. M. Determination of serum proteins by means of the biuret reaction. J. Biol. Chem. 177:751-766 (1949)

55. Green, A. A. & Hughes, W. L. Protein fractionation on the basis of solubility in aqueous solutions of salt and organic solvents. In: S. P. Colowick & N. O. Kaplan (Ed.), Methods of Enzymology. Academic Press, New York, 1955. Volume 1, pp. 67-90.

56. Green, H. N. The immunological theory of cancer. Unio Intern. Contra Cancrum Acta 17:215-233 (1961).

57. Greengard, O. The role of coenzymes, cortisone and RNA in the control of liver enzyme levels. In: G. Weber (Ed.), Advances in Enzyme Regulation. Macmillan Co., New York, 1963. Volume 1, pp. 61-76.

58. Griffin, A. C. Metabolism of the cancer cell. In: W. K. Nowinski (Ed.), Fundamental Aspects of Normal and Malignant Growth. Elsevier, London, 1960. pp. 877-925.

59. Grube, G. & Stäsche, M. Das ternäre system manganophosphat-phosphosäure-wasser und die diphosphatomanganosäure. Z. physik. Chem. 130:572-583 (1927).

60. Haguenau, F. The ergastoplasm: Its history, ultrastructure, and biochemistry. In: G. H. Bourne & J. F. Danielli (Ed.), International Review of Cytology 7:425-485. Academic Press, New York, 1958.

61. Hashimoto, Y., Yamano, T. & Mason, H. S. An ESR study of microsomal electron transport. J. Biol. Chem. 237:PC3843-PC3844 (1962).

62. Hauschka, T. S. The chromosomes in ontogeny and oncogeny. Cancer Res. 21:957-974 (1961).

63. Heidelberger, C. & Davenport, G. R. Local functional components of carcinogenesis. Unio Intern. Contra Cancrum Acta 17:55-63 (1961).

64. Hulsmans, H. A. M. Microsomes in heart-muscle homogenates. Biochim. Biophys. Acta 54:1-14 (1961).

65. Ingram, D. J. E. Free Radicals as Studied by Electron Spin Resonance. Butterworths, London, 1958.

66. Jacob, F. Genetic control of viral functions. The Harvey Lectures (series 54):1-39 (1960).

67. Jacob, F. & Monod, J. Genetic regulatory mechanisms in the synthesis of proteins. J. Mol. Biol. 3:318-356 (1961).

68. Jacob, F. & Monod, J. On the regulation of gene activity. Cold Spring Harbor Symp. Quant. Biol. 26:193-211 (1961).

69. Kalmanson, A. E., Lipchina, L. P. & Chetverikov, A. G. Use of electron spin resonance for study of reactions of semiquinone ion-radicals arising from the use of inhibitors of free-radical processes within normal and tumor cells. Biofizika 6 (4):21-29 (1961).

70. Kit, S. & Griffin, A. C. Cellular metabolism and cancer: A review. Cancer Res. 18:621-656 (1958).

71. Knox, W. E. Two mechanisms which increase in vivo the liver tryptophan peroxidase activity: specific enzyme adaptation and stimulation of the pituitary-adrenal system. Brit. J. Exp. Path. 32: 462-469 (1951).

72. Krisch, K. & Staudinger, H. Solubilization of acetanilide hydroxylase from hog liver microsomes. Biochem. Biophys. Res. Comm. 4:118-122 (1961).

73. Loach, P. A. & Calvin, M. Oxidation states of manganese hematoporphyrin IX in aqueous solution. Biochemistry 2:361-371 (1963).

74. Maling, J. E., Taskovich, L. T. & Blois, M. S., Jr. Electron spin resonance in ATP and RNA. Biophys. J. 3:79-95 (1963).

75. Malmström, B. G., Vänngård, T. & Larsson, M. An E-S-R study of the interaction of manganous ions with enolase and its substrate. Biochim. Biophys. Acta 30:1-5 (1958).

76. Mason, H. S., Ingram, D. J. E. & Allen, B. T. The free radical property of melanins. Arch. Biochem. Biophys. 86:225-230 (1960).

77. McClintock, B. Controlling elements and the gene. Cold Spring Harbor Symp. Quant. Biol. 21:197-216 (1956).

78. McGarvey, B. R. Line widths in the paramagnetic resonance of transition ions in solution. J. Phys. Chem. 61:1232-1237 (1957).

79. Michaelis, L. Fundamentals of Oxidation and Reduction. Interscience Publishers, Inc., 1946. pp. 207-228.

80. Miller, J. A. & Miller, E. C. The carcinogenic aminoazo dyes. Adv. Cancer Res. 1:339-396 (1953).

81. Miller, J. A., Miller, E. C. & Finger, G. C. Further studies on the carcinogenicity of dyes related to 4-dimethylaminoazobenzene. The requirement for an unsubstituted 2-position. Cancer Res. 17: 387-398 (1957).

82. Minnaert, K. The kinetics of cytochrome c oxidase. I. The system: cytochrome c-cytochrome oxidase-oxygen. Biochim. Biophys. Acta 50:23-34 (1961).

83. Monod, J. & Jacob, F. General conclusions: Teleonomic mechanisms in cellular metabolism, growth and differentiation. Cold Spring Harbor Symp. Quant. Biol. 26:389-401 (1961).

84. Morris, H. P., Sidranskey, H., Wagner, B. P. & Dyer, H. M. Some characteristics of transplantable rat hepatoma No. 5123 induced by ingestion of N-(2-fluorenyl)phthalamic acid. Cancer Res. 20:

85. Nakahara, W. Critique of carcinogenic mechanism. Progr. exp. Tumor Res. 2:158-202 (1961).

86. Nebert, D. W. & Allen, B. T. Environmental factors influencing the hyperfine structure of the manganous low-temperature EPR spectrum. To be published.

87. Nebert, D. W. & Mason, H. S. An electron spin resonance study of neoplasms. Proc. Amer. Assoc. Cancer Research 4:47 (1963). (Abstract).

88. Nebert, D. W. & Mason, H. S. An electron spin resonance study of neoplasms. Cancer Res. 23:833-840 (1963).

89. Nebert, D. W. & Mason, H. S. A microsomal difference between normal liver and "minimal deviation" hepatoma 5123 detectable by electron spin resonance. Biochim. Biophys. Acta (May, 1964) In press.

90. Novikoff, A. B. & Heus, M. Microsomal nucleoside phosphatase. J. Biol. Chem. 238:710-716 (1963).

91. Omura, T. & Sato, R. New cytochrome in liver microsomes. J. Biol. Chem. 237:PC1375-PC1376 (1962).

92. Ono, T., Blair, D. G. R., Potter, V. R. & Morris, H. P. The comparative enzymology and cell origin of rat hepatomas. IV. Pyrimidine metabolism in minimal-deviation tumors. Cancer Res. 23: 240-249 (1963).

93. Ono, T., Potter, V. R., Pitot, H. C. & Morris, H. P. Metabolic adaptations in rat hepatomas. III. Glucose-6-phosphate dehydrogenase and pyrimidine reductase. Cancer Res. 23:385-391 (1963).

94. Oppenheimer, B. S., Oppenheimer, E. T., Stout, A. P. & Danishefsky, I. Malignant tumors resulting from embedding plastics in rodents. Science 118:305-306 (1953).

95. Oppenheimer, B. S., Oppenheimer, E. T., Stout, A. P., Danishefsky, I. & Eirich, F. R. Comment on malignant tumors and high polymers. Science 118:783-784 (1953).

96. Oppenheimer, B. S., Oppenheimer, E. T., Stout, A. P., Danishefsky, I. & Eirich, F. R. Further studies of polymers as carcinogenic agents in animals. Cancer Res. 15:333-340 (1955).

97. Orgel, L. E. An Introduction to Transition-Metal Chemistry: Ligand Field Theory. John Wiley & Sons, Inc., New York, 1961.

98. Osgood, E. E. A unifying concept of the etiology of the leukemias, lymphomas, and cancers. J. Nat. Cancer Inst. 18:155-166 (1957).

99. Osgood, E. E. Leukemia as a disturbance of growth regulation. Ross Conference on Pediatric Research 34:61-69 (1960).

100. Osgood, E. E., Seaman, A. J., Tivey, H. & Rigas, D. A. Duration of life and of the different stages of maturation of normal and leukemic leukocytes. Revue d' Hematologie 9:543-554 (1954).

101. Park, H. F. The role of the unpaired electron in carcinogenesis. J. Phys. & Coll. Chem. 54:1383-1384 (1950).

102. Paul, K. G., Theorell, H. & Akeson, A. The molar light absorption of pyridine ferroprotoporphyrin (pyridine haemochromogen). Acta Chem. Scand. 7:1284-1287 (1953).

103. Pitot, H. C. The comparative enzymology and cell origin of rat hepatomas. II. Glutamate dehydrogenase, choline oxidase and glucose-6-phosphatase. Cancer Res. 20:1262-1268 (1960).

104. Pitot, H. C. & Cho, Y. S. Studies on the mechanism of enzyme induction in rat liver. Cold Spring Harbor Symp. Quant. Biol. 26:371-377 (1961).

105. Pitot, H. C. & Morris, H. P. Metabolic adaptations in rat hepatomas. II. Tryptophan pyrrolase and tyrosine α-ketoglutarate transaminase. Cancer Res. 21:1009-1014 (1961).

106. Pitot, H. C., Peraino, C., Bottomley, R. H. & Morris, H. P. The comparative enzymology and cell origin of rat hepatomas. III. Some enzymes of amino acid metabolism. Cancer Res. 23:135-142 (1963).

107. Pitot, H. C., Potter, V. R. & Morris, H. P. Metabolic adaptations in rat hepatomas. I. The effect of dietary protein on some inducible enzymes in liver and hepatoma 5123. Cancer Res. 21: 1001-1008 (1961).

108. Ponten, J. Another clue to viral action of cancer. New Scientist 21:200-201 (1964).

109. Porter, K. R. & Bruni, C. Electron microscopic study of early effects of 3'-methyl-diaminoazobenzene on rat liver cells. Cancer Res. 19:997-1009 (1959).

110. Potter, V. R. The biochemical approach to the cancer problem. Fed. Proc. 17:691-697 (1958).

111. Potter, V. R. Deletion of catabolic enzymes in relation to the cause and nature of cancer. Unio Intern. Contra Cancrum Acta 16:27-31 (1960).

112. Potter, V. R. Transplantable animal cancer, the primary standard. Cancer Res. 21:1331-1333 (1961).

113. Potter, V. R. New prospects in cancer biochemistry. In: G. Weber (Ed.), Advances in Enzyme Regulation. Macmillan Co., New York, 1963. Volume 1, pp. 279-308.

114. Potter, V. R. & Ono, T. Enzyme patterns in rat liver and Morris hepatoma 5123 during metabolic transitions. Cold Spring Harbor Symp. Quant. Biol. 26:355-362 (1961).

115. Potter, V. R., Pitot, H. C., Ono, T. & Morris, H. P. The comparative enzymology and cell origin of rat hepatomas. I. Deoxycytidylate deaminase and thymine degradation. Cancer Res. 20: 1255-1261 (1960).

116. Prehn, R. T. A clonal selection theory of chemical carcinogenesis. J. Nat. Cancer Inst. 32:1-17 (1964).

117. Quastel, J. H. & Bickis, I. J. Metabolism of normal tissues and neoplasms in vitro. Nature 183:281-286 (1959).

118. Reid, E. Biochemical effects of hepatocarcinogens in the rat: A review. Cancer Res. 22:398-430 (1962).

119. Rhoades, M. M. Plastid mutations. Cold Spring Harbor Symp. Quant. Biol. 11:202-207 (1946).

120. Richmond, H. G. The carcinogenicity of an iron-dextran complex. In: R. W. Raven (Ed.), Cancer Progress. Butterworths, London, 1960. pp. 24-33.

121. Roth, J. S., Hilton, S. & Morris, H. P. Ribonuclease activity in some transplantable rat hepatomas. Cancer Res. 24:294-301 (1964).

122. Rous, P. Opening remarks (on tumors in relation to viruses). Cancer Res. 20:672-676 (1960).

123. Sager, R. Genetic systems in Chlamydomonas. Science 132:1459-1465 (1960).

124. Sager, R. The particulate nature of nonchromosomal genes in Chlamydomonas. Proc. Natl. Acad. Sci. (U.S.) 50:260-268 (1963).

125. Sager, R. & Ryan, F. J. Cell Heredity. John Wiley & Sons, Inc., New York, 1961. pp. 234-270.

126. Sands, R. H. Paramagnetic resonance absorption in glass. Phys. Rev. 99:1222-1226 (1955).

127. Schneider, W. C. Intracellular distribution of enzymes. III. The oxidation of octanoic acid by rat liver fractions. J. Biol. Chem. 176:259-266 (1948).

128. Sonneborn, T. M. Recent advances in the genetics of Paramecium and Euplotes. Adv. Genet. 1:264-358 (1947).

129. Sorof, S. & Cohen, P. P. Electrophoretic and ultracentrifugal studies on the soluble proteins of various tumors and of liver from rats fed 4-dimethylaminoazobenzene. Cancer Res. 11:378-382 (1951).

130. Sorof, S., Young, E. M. & Ott, M. G. Soluble liver h proteins during hepatocarcinogenesis by aminoazodyes and 2-acetylaminofluorene in the rat. Cancer Res. 18:33-46 (1958).

131. Southam, C. M. The complex etiology of cancer. Cancer Res. 23: 1105-1115 (1963).

132. Strittmatter, C. F. Differentiation of electron transport systems in mitochondria and microsomes during embryonic development. Arch. Biochem. Biophys. 102:293-305 (1963).

133. Sweeney, M. J., Ashmore, J., Morris, H. P. & Weber, G. Comparative biochemistry of hepatomas. IV. Isotope studies of glucose and fructose metabolism in liver tumors of different growth rates. Cancer Res. 23:995-1002 (1963).

134. Syverton, J. T., Wells, E., Koomen, J., Jr., Dascomb, H. E. & Berry, G. P. The virus-induced rabbit papilloma-to-carcinoma sequence. III. Immunological tests for papilloma virus in cottontail carcinomas. Cancer Res. 10:474-482 (1950).

135. Szent-Gyorgyi, A. Introduction to a Submolecular Biology. Academic Press, New York, 1960. pp. 27-98.

136. Szent-Gyorgyi, A., Hegyeli, A. & McLaughlin, J. A. Cancer therapy: A possible new approach. Science 140:1391-1392 (1963).

137. Treharne, R. W., Brown, T. E., Eyster, H. C. & Tanner, H. A. Electron spin resonance studies of manganese in Chlorella pyrenoidosa. Biochem. Biophys. Res. Comm. 3:119-122 (1960).

138. Treharne, R. W. & Eyster, H. C. An electron spin resonance study of manganese and iron in Chlorella pyrenoidosa. Biochem. Biophys. Res. Comm. 8:477-480 (1962).

139. Vogt, M. E. & Dulbecco, R. Studies on cells rendered neoplastic by polyoma virus: The problem of the presence of virus-related materials. Virology 16:41-51 (1962).

140. Wagle, S. R., Morris, H. P. & Weber, G. Comparative biochemistry of hepatomas. V. Studies on amino acid incorporation in liver tumors of different growth rates. Cancer Res. 23:1003-1007 (1963).

141. Wakonig-Vaartija, R. Search for the essential factors of carcinogenesis. Ann. N. Y. Acad. Sci. 105:3-24 (1963).

142. Warburg, O. On the origin of cancer cells. Science 123:309-314 (1956).

143. Warburg, O. On respiratory impairment in cancer cells. Science 124:269-270 (1956).

144. Warner, D. T. Proposed molecular models: II. conformations of staphylomycin and other polypeptides and a possible relation to the structure of water. J. Theoret. Biol. 1:514-528 (1961).

145. Weber, G. & Morris, H. P. Comparative biochemistry of hepatomas. III. Carbohydrate enzymes in liver tumors of different growth rates. Cancer Res. 23:987-994 (1963).

146. Weinhouse, S. Oxidative metabolism of neoplastic tissues. Adv. Cancer Res. 3:269-325 (1955).

147. Weinhouse, S. On respiratory impairment in cancer cells. Science 124:267-269 (1956)

148. Weinhouse, S. Metabolism of respiratory fuels in cancer cells. Unio Intern. Contra Cancrum Acta 16:32-35 (1960).

149. Woods, M. W. & duBuy, H. G. Hereditary and pathogenic nature of mutant mitochondria in Nepeta. J. Nat. Cancer Inst. 11:1105-1151 (1951).

150. Yamano, T. & Mason, H. S. An ESR study of microsomal electron transport. To be published.

151. Yonetani, T. Studies on cytochrome oxidase. III. Improved preparation and some properties. J. Biol. Chem. 236:1680-1688 (1961).

* * *